

MASS SPECTROMETRY OF  
FLUORINATED METAL  $\beta$ -DIKETONATES  
AND  
MONOTHIO- $\beta$ -DIKETONATES

by

Mark Lindsay John Reimer

B.Sc.(Hons.), University of Manitoba, 1981

A Thesis

Submitted to the Faculty of Graduate Studies  
in partial fulfillment of the requirements  
for the degree of  
Doctor of Philosophy

University of Manitoba

Winnipeg, Manitoba

February, 1988.

Permission has been granted to the National Library of Canada to microfilm this thesis and to lend or sell copies of the film.

The author (copyright owner) has reserved other publication rights, and neither the thesis nor extensive extracts from it may be printed or otherwise reproduced without his/her written permission.

L'autorisation a été accordée à la Bibliothèque nationale du Canada de microfilmer cette thèse et de prêter ou de vendre des exemplaires du film.

L'auteur (titulaire du droit d'auteur) se réserve les autres droits de publication; ni la thèse ni de longs extraits de celle-ci ne doivent être imprimés ou autrement reproduits sans son autorisation écrite.

ISBN 0-315-44206-9

**MASS SPECTROMETRY OF FLUORINATED METAL B-DIKETONATES  
AND MONOTHIO-B-DIKETONATES**

**BY**

**MARK LINDSAY JOHN REIMER**

A thesis submitted to the Faculty of Graduate Studies of  
the University of Manitoba in partial fulfillment of the requirements  
of the degree of

**DOCTOR OF PHILOSOPHY**

© 1988

Permission has been granted to the LIBRARY OF THE UNIVER-  
SITY OF MANITOBA to lend or sell copies of this thesis, to  
the NATIONAL LIBRARY OF CANADA to microfilm this  
thesis and to lend or sell copies of the film, and UNIVERSITY  
MICROFILMS to publish an abstract of this thesis.

The author reserves other publication rights, and neither the  
thesis nor extensive extracts from it may be printed or other-  
wise reproduced without the author's written permission.

PREFACE

"The ultimate goal of science is to make order out of chaos, that is, to find the underlying coherent patterns which exist in the bewildering multitude of events which occur in nature."

Author unknown.

This thesis is composed of two distinct parts. The first chapter (steroid mass spectra) pertains to research conducted during my brief tenure as a Master's student while under the supervision of Professor J.B. Westmore, Department of Chemistry, University of Manitoba. Later in my Ph.D program when the VG7070E-HF double-focusing mass spectrometer became available, I was able to complement the existing data by performing linked-scanning, metastable analyses on several of the steroids. The remainder of the thesis is devoted to my primary doctoral research project, namely the mass spectrometry of metal  $\beta$ -diketonates and monothio- $\beta$ -diketonates. The thesis title reflects the greater depth and emphasis placed on this aspect of the work.

M.L.J.R.

ABSTRACT

Positive-ion electron ionization mass spectra of the four isomeric 17 $\xi$ -hydroxy-17 $\xi$ -methyl-5 $\xi$ -androstane C(3) ketones and eight isomeric C(3 $\xi$ ) alcohols are reported. Linked-scanning, metastable analyses are used to confirm postulated fragmentation pathways. The ratios of the intensity of several fragment ions to that of the molecular ion differentiate between the 5 $\alpha$ - and 5 $\beta$ -isomers in both C(3) ketones and alcohols, the extent of fragmentation being greater for 5 $\beta$ -steroids. However, contrary to earlier reports, no definitive correlations are evident between fragment ion intensities and the configuration at C(17).

Positive-ion electron ionization mass spectra are presented for Al(III), Ga(III), Co(III), Ni(II), Pd(II), Cu(II) and Zn(II)  $\beta$ -diketonates and Co(III), Ni(II), Pd(II), Cu(II) and Zn(II) monothio- $\beta$ -diketonates of the general form  $\text{Met}^{n+}(\text{RCXCHCOR}')_n$ , where Met = metal, R = aryl or substituted-aryl group, X = O ( $\beta$ -diketonates) or S (monothio- $\beta$ -diketonates), R' = difluoromethyl, trifluoromethyl, pentafluoroethyl or heptafluoropropyl group, and n = 2 or 3. Mechanisms of ion decomposition are proposed with the aid of linked-scanning metastable results. Trends in observed ion abundances are interpreted in light of several different concepts, including the metal's ability to undergo a change in valency, the principle of Hard and Soft Acids and Bases (HSAB) and the inductive capabilities of the ligand donor atoms and the R and R' groups.

ACKNOWLEDGEMENTS

I should like to express my appreciation to Professor John B. Westmore who served as the major advisor for this study. I should also like to thank the other members of my advisory committee, Professors A.F. Janzen, D.M. McKinnon and K.G. Standing.

I am grateful to the Natural Sciences and Engineering Research Council of Canada for financial assistance in the form of a scholarship (1984-85) and to the Faculty of Graduate Studies for the award of a University of Manitoba Graduate Fellowship (1983-84, 1985-86).

I wish to thank Professor J.F. Templeton and Dr. C.C. Jackson for providing the steroids used in this study. I am also grateful to Drs. M. Das and D.T. Haworth for the kind donation of several of the metal chelates.

I wish to express my appreciation to Mr. Gary Stern for his helpful advice and to Mr. Wayne Buchannon for the sharing of his expertise in the operation and maintenance of the mass spectrometer.

Finally, I must recognize the love and support of friends and family, and especially the understanding and encouragement of my wife Shauna, to whom this work is dedicated.

TABLE OF CONTENTS

	Page
Preface .....	i-1
Abstract .....	i-2
Acknowledgements .....	i-3
List of Tables .....	i-6
List of Figures .....	i-10
List of Schemes .....	i-24
Abbreviations, Symbols and Definition of Terms .....	i-34

Chapter

I. MASS SPECTRA OF 17 $\xi$ -HYDROXY-17 $\xi$ -METHYL-5 $\xi$ -ANDROSTANE C(3) KETONE AND C(3 $\xi$ ) ALCOHOL ISOMERS .....	1
A. Introduction .....	2
B. Experimental .....	13
C. Results and Discussion .....	14
1. 3-Keto-17-hydroxysteroids .....	14
2. 3,17-Dihydroxysteroids .....	46
D. Summary .....	51

Chapter	Page
II. MASS SPECTRA OF FLUORINATED METAL $\beta$ -DIKETONATES AND MONOTHIO- $\beta$ -DIKETONATES .....	52
A. Introduction .....	53
1. General Chemistry .....	54
2. X-ray Structural Studies .....	63
3. Nuclear Magnetic Resonance Studies .....	75
4. Dipole Moments .....	82
5. Mass Spectrometry Studies .....	86
6. Hard and Soft Acids and Bases .....	118
B. Experimental .....	131
1. Mass Spectra .....	131
2. Ligand Synthesis .....	134
3. Metal Chelate Synthesis .....	138
C. Results and Discussion .....	150
1. General Remarks .....	150
2. Mass Spectra of $\beta$ -diketonates .....	155
3. Mass Spectra of Monothio- $\beta$ -diketonates .....	405
D. Summary .....	558
APPENDIX .....	564
REFERENCES .....	593



LIST OF TABLES

Table	Page
1. Mass spectra of 17 $\xi$ -hydroxy-17 $\xi$ -methyl-5 $\xi$ -androstane-3-ones .....	15
2. Mass spectra of 17 $\alpha$ -methyl-5 $\xi$ -androstane-3 $\xi$ ,17 $\beta$ -diols .	16
3. Mass spectra of 17 $\beta$ -methyl-5 $\xi$ -androstane-3 $\xi$ ,17 $\alpha$ -diols .	17
4. Classification of hard and soft acids .....	122
5. Classification of hard and soft bases .....	124
6. Numbering system and IUPAC names of ligands .....	151
7. Listing of metal $\beta$ -diketonates and monothio- $\beta$ -diketonates	153
8. 70 eV-EI mass spectra of compounds <b>Al-3a</b> , <b>Al-4a</b> and <b>Al-5a</b> .	160
9. 70 eV-EI mass spectra of compounds <b>Al-8a</b> and <b>Al-9a</b> .....	161
10. 70 eV-EI mass spectra of compounds <b>Al-1a</b> and <b>Al-2a</b> .....	162
11. 70 eV-EI mass spectra of compounds <b>Ga-1a</b> and <b>Ga-2a</b> .....	190
12. 70 eV-EI mass spectra of compounds <b>Ga-3a</b> , <b>Ga-4a</b> and <b>Ga-5a</b> .	191
13. 70 eV-EI mass spectra of compounds <b>Ga-8a</b> and <b>Ga-12a</b> .....	192
14. 70 eV-EI mass spectra of compounds <b>Co-1a</b> and <b>Co-2a</b> .....	220

Table	Page
15. 70 eV-EI mass spectra of compounds <b>Co-3a</b> , <b>Co-4a</b> and <b>Co-6a</b> .	221
16. 70 eV-EI mass spectra of compounds <b>Co-8a</b> and <b>Co-10a</b> .....	222
17. 70 eV-EI mass spectra of compounds <b>Co-11a</b> and <b>Co-12a</b> .....	224
18. 70 eV-EI mass spectra of compounds <b>Co-13a</b> and <b>Co-14a</b> .....	226
19. 70 eV-EI mass spectra of compounds <b>Co-16a</b> and <b>Co-17a</b> .....	228
20. 70 eV-EI mass spectra of compounds <b>Ni-1a</b> and <b>Ni-2a</b> .....	270
21. 70 eV-EI mass spectra of compounds <b>Ni-3a</b> , <b>Ni-8a</b> and <b>Ni-9a</b> .	272
22. 70 eV-EI mass spectra of compounds <b>Ni-13a</b> and <b>Ni-14a</b> .....	273
23. 70 eV-EI mass spectra of compounds <b>Ni-16a</b> and <b>Ni-17a</b> .....	274
24. 70 eV-EI mass spectra of compounds <b>Pd-3a</b> and <b>Pd-8a</b> .....	306
25. 70 eV-EI mass spectra of compounds <b>Pd-13a</b> and <b>Pd-14a</b> .....	308
26. 70 eV-EI mass spectra of compounds <b>Pd-16a</b> and <b>Pd-17a</b> .....	310
27. 70, 20 and 12 eV-EI mass spectra of compound <b>Cu-1a</b> .....	336
28. 70, 20 and 12 eV-EI mass spectra of compound <b>Cu-2a</b> .....	337
29. 70, 20 and 12 eV-EI mass spectra of compound <b>Cu-3a</b> .....	338
30. 70, 20 and 12 eV-EI mass spectra of compound <b>Cu-8a</b> .....	339

Table	Page
31. 70, 20 and 12 eV-EI mass spectra of compound <b>Cu-9a</b> .....	340
32. 70, 20 and 12 eV-EI mass spectra of compound <b>Cu-11a</b> .....	341
33. 70, 20 and 12 eV-EI mass spectra of compound <b>Cu-12a</b> .....	342
34. 70, 20 and 12 eV-EI mass spectra of compound <b>Cu-13a</b> .....	343
35. 70, 20 and 12 eV-EI mass spectra of compound <b>Cu-14a</b> .....	345
36. 70, 20 and 12 eV-EI mass spectra of compound <b>Cu-16a</b> .....	346
37. 70, 20 and 12 eV-EI mass spectra of compound <b>Cu-17a</b> .....	347
38. 70 eV-EI mass spectra of compounds <b>Zn-1a</b> and <b>Zn-2a</b> .....	380
39. 70 eV-EI mass spectra of compounds <b>Zn-3a</b> , <b>Zn-8a</b> and <b>Zn-9a</b> .	381
40. 70 eV-EI mass spectra of compounds <b>Zn-13a</b> and <b>Zn-14a</b> .....	382
41. 70 eV-EI mass spectra of compounds <b>Zn-16a</b> and <b>Zn-17a</b> .....	383
42. 70 eV-EI mass spectra of compounds <b>Co-13b</b> , <b>Co-14b</b> and <b>Co-15b</b> .....	408
43. 70 eV-EI mass spectra of compounds <b>Co-16b</b> , <b>Co-17b</b> and <b>Co-18b</b> .....	410
44. 70 eV-EI mass spectra of compounds <b>Ni-3b</b> , <b>Ni-5b</b> and <b>Ni-7b</b> .	435
45. 70 eV-EI mass spectra of compounds <b>Ni-8b</b> and <b>Ni-9b</b> .....	437

Table	Page
46. 70 eV-EI mass spectra of compounds <b>Ni-13b</b> , <b>Ni-14b</b> and <b>Ni-15b</b> .....	439
47. 70 eV-EI mass spectra of compounds <b>Ni-16b</b> , <b>Ni-17b</b> and <b>Ni-18b</b> .....	441
48. 70 eV-EI mass spectra of compounds <b>Pd-3b</b> , <b>Pd-7b</b> and <b>Pd-8b</b> .	482
49. 70 eV-EI mass spectra of compounds <b>Pd-13b</b> , <b>Pd-14b</b> and <b>Pd-15b</b> .....	484
50. 70 eV-EI mass spectra of compounds <b>Pd-16b</b> , <b>Pd-17b</b> and <b>Pd-18b</b> .....	486
51. 70 eV-EI mass spectra of compounds <b>Cu-3b</b> and <b>Cu-4b</b> .....	514
52. 70 eV-EI mass spectra of compounds <b>Cu-5b</b> and <b>Cu-8b</b> .....	516
53. 70 eV-EI mass spectra of compounds <b>Cu-13b</b> and <b>Cu-16b</b> .....	518
54. 70 eV-EI mass spectra of compounds <b>Zn-3b</b> , <b>Zn-5b</b> and <b>Zn-7b</b> .	538
55. 70 eV-EI mass spectra of compounds <b>Zn-8b</b> and <b>Zn-9b</b> .....	540

LIST OF FIGURES

Figure	Page
1. 17 $\xi$ -hydroxy-17 $\xi$ -methyl-5 $\xi$ -androstane C(3) ketone and C(3 $\xi$ ) alcohol isomers .....	3
2. 3-methoxy-17 $\xi$ -alkyl- $\Delta^{1,3,5(10),8-D}$ - homoestratetraen-17 $\xi$ -ol isomers .....	5
3. Isomers of (a) 3-methoxy-17 $\xi$ -alkyl- $\Delta^{1,3,5(10)}$ - estratrien-17 $\xi$ -ol and (b) 17 $\xi$ -alkyl-19-nortestosterone ..	7
4. Isomers of (a) 17 $\xi$ -R-5 $\alpha$ -androstane-17 $\xi$ -ol and (b) 17 $\xi$ -R-5 $\alpha$ ,14 $\beta$ -androstane-14,17 $\xi$ -diol .....	9
5. Isomers of (a) 5 $\xi$ -androstane-3-one-17 $\xi$ -ols and (b) 5 $\xi$ -androstane-3 $\xi$ ,17 $\xi$ -diols .....	11
6. Normalized 70 eV-EI mass spectrum of 17 $\beta$ -hydroxy-17 $\alpha$ -methyl-5 $\alpha$ -androstane-3-one .....	19
7. Normalized 70 eV-EI mass spectrum of 17 $\beta$ -hydroxy-17 $\alpha$ -methyl-5 $\beta$ -androstane-3-one .....	21
8. Normalized 70 eV-EI mass spectrum of 17 $\alpha$ -hydroxy-17 $\beta$ -methyl-5 $\alpha$ -androstane-3-one .....	23
9. Normalized 70 eV-EI mass spectrum of 17 $\alpha$ -hydroxy-17 $\beta$ -methyl-5 $\beta$ -androstane-3-one .....	25

Figure	Page
10. Normalized 70 eV-EI mass spectrum of 17 $\alpha$ -methyl-5 $\alpha$ -androstan-3 $\alpha$ ,17 $\beta$ -diol .....	27
11. Normalized 70 eV-EI mass spectrum of 17 $\alpha$ -methyl-5 $\alpha$ -androstan-3 $\beta$ ,17 $\beta$ -diol .....	29
12. Normalized 70 eV-EI mass spectrum of 17 $\alpha$ -methyl-5 $\beta$ -androstan-3 $\alpha$ ,17 $\beta$ -diol .....	31
13. Normalized 70 eV-EI mass spectrum of 17 $\alpha$ -methyl-5 $\beta$ -androstan-3 $\beta$ ,17 $\beta$ -diol .....	33
14. Normalized 70 eV-EI mass spectrum of 17 $\beta$ -methyl-5 $\alpha$ -androstan-3 $\alpha$ ,17 $\alpha$ -diol .....	35
15. Normalized 70 eV-EI mass spectrum of 17 $\beta$ -methyl-5 $\alpha$ -androstan-3 $\beta$ ,17 $\alpha$ -diol .....	37
16. Normalized 70 eV-EI mass spectrum of 17 $\beta$ -methyl-5 $\beta$ -androstan-3 $\alpha$ ,17 $\alpha$ -diol .....	39
17. Normalized 70 eV-EI mass spectrum of 17 $\beta$ -methyl-5 $\beta$ -androstan-3 $\beta$ ,17 $\alpha$ -diol .....	41
18. Tautomerism of $\beta$ -diketones .....	55
19. Tautomerism of monothio- $\beta$ -diketones .....	60
20. Trimeric structure of Ni(II) acetylacetonate .....	65

Figure	Page
21. Molecular structure of bis(2,2,6,6-tetramethyl-3,5-heptanedionato)Ni(II) .....	67
22. Molecular structure of bis(4-mercapto-pent-3-en-2-onato)Ni(II) .....	68
23. Molecular structure of bis(1,1,1-trifluoro-4-mercapto-pent-3-en-2-onato)Ni(II) .....	70
24. Molecular structure of bis(1-phenyl-1,3-butanedionato)Pd(II)	71
25. Molecular structure of bis(2,2,6,6-tetramethyl-3,5-heptanedionato)Zn(II) .....	74
26. Molecular structure of tris(1,1,1-trifluoro-4-mercapto-4-phenyl-but-3-en-2-onato)Co(III) .....	76
27. Configurations of cis and trans isomers in Co(III) $\beta$ -diketonates .....	78
28. Geometrical isomerism in (a) square-planar Ni(II) and (b) octahedral Co(III) monothio- $\beta$ -diketonates .....	81
29. Normalized 70 eV-EI mass spectrum of tris[1,1,1-trifluoro-4-phenyl-2,4-butanedionato]Al(III) .....	164
30. Normalized 70 eV-EI mass spectrum of tris[1,1,1-trifluoro-4-(4'-methylphenyl)-2,4-butanedionato]Al(III) .....	166

Figure	Page
31. Normalized 70 eV-EI mass spectrum of tris[1,1,1-trifluoro-4-(4'-fluorophenyl)-2,4-butanedionato]Al(III) .....	168
32. Normalized 70 eV-EI mass spectrum of tris[1,1,1-trifluoro-4-(2'-thienyl)-2,4-butanedionato]Al(III) .....	170
33. Normalized 70 eV-EI mass spectrum of tris[1,1,1-trifluoro-4-(5'-methyl-2'-thienyl)-2,4-butanedionato]Al(III) .....	172
34. Normalized 70 eV-EI mass spectrum of tris[1,1,-difluoro-4-phenyl-2,4-butanedionato]Al(III) .....	174
35. Normalized 70 eV-EI mass spectrum of tris[1,1,-difluoro-4-(2'-thienyl)-2,4-butanedionato]Al(III) .....	176
36. Normalized 70 eV-EI mass spectrum of tris[1,1,-difluoro-4-phenyl-2,4-butanedionato]Ga(III) .....	194
37. Normalized 70 eV-EI mass spectrum of tris[1,1,-difluoro-4-(2'-thienyl)-2,4-butanedionato]Ga(III) .....	196
38. Normalized 70 eV-EI mass spectrum of tris[1,1,1-trifluoro-4-phenyl-2,4-butanedionato]Ga(III) .....	198
39. Normalized 70 eV-EI mass spectrum of tris[1,1,1-trifluoro-4-(4'-methylphenyl)-2,4-butanedionato]Ga(III) .....	200
40. Normalized 70 eV-EI mass spectrum of tris[1,1,1-trifluoro-4-(4'-fluorophenyl)-2,4-butanedionato]Ga(III) .....	202



Figure	Page
41. Normalized 70 eV-EI mass spectrum of tris[1,1,1-trifluoro-4-(2'-thienyl)-2,4-butanedionato]Ga(III) .....	204
42. Normalized 70 eV-EI mass spectrum of tris[1,1,1-trifluoro-4-(2'-naphthyl)-2,4-butanedionato]Ga(III) .....	206
43. Normalized 70 eV-EI mass spectrum of tris[1,1-difluoro-4-phenyl-2,4-butanedionato]Co(III) .....	230
44. Normalized 70 eV-EI mass spectrum of tris[1,1,-difluoro-4-(2'-thienyl)-2,4-butanedionato]Co(III) .....	232
45. Normalized 70 eV-EI mass spectrum of tris[1,1,1-trifluoro-4-phenyl-2,4-butanedionato]Co(III) .....	234
46. Normalized 70 eV-EI mass spectrum of tris[1,1,1-trifluoro-4-(4'-methylphenyl)-2,4-butanedionato]Co(III) .....	236
47. Normalized 70 eV-EI mass spectrum of tris[1,1,1-trifluoro-4-(4'-chlorophenyl)-2,4-butanedionato]Co(III) .....	238
48. Normalized 70 eV-EI mass spectrum of tris[1,1,1-trifluoro-4-(2'-thienyl)-2,4-butanedionato]Co(III) .....	240
49. Normalized 70 eV-EI mass spectrum of tris[1,1,1-trifluoro-4-(5'-chloro-2'-thienyl)-2,4-butanedionato]Co(III) .....	242
50. Normalized 70 eV-EI mass spectrum of tris[1,1,1-trifluoro-4-(2'-furyl)-2,4-butanedionato]Co(III) .....	244

Figure	Page
51. Normalized 70 eV-EI mass spectrum of tris[1,1,1-trifluoro-4-(2'-naphthyl)-2,4-butanedionato]Co(III) .....	246
52. Normalized 70 eV-EI mass spectrum of tris[1,1,1,2,2-pentafluoro-5-phenyl-3,5-pentanedionato]Co(III) .....	248
53. Normalized 70 eV-EI mass spectrum of tris[1,1,1,2,2-pentafluoro-5-(2'-thienyl)-3,5-pentanedionato]Co(III) .....	250
54. Normalized 70 eV-EI mass spectrum of tris[1,1,1,2,2,3,3-heptafluoro-6-phenyl-4,6-hexanedionato]Co(III) .....	252
55. Normalized 70 eV-EI mass spectrum of tris[1,1,1,2,2,3,3-heptafluoro-6-(2'-thienyl)-4,6-hexanedionato]Co(III) .....	254
56. Normalized 70 eV-EI mass spectrum of bis[1,1-difluoro-4-phenyl-2,4-butanedionato]Ni(II) .....	276
57. Normalized 70 eV-EI mass spectrum of bis[1,1-difluoro-4-(2'-thienyl)-2,4-butanedionato]Ni(II) .....	278
58. Normalized 70 eV-EI mass spectrum of bis[1,1,1-trifluoro-4-phenyl-2,4-butanedionato]Ni(II) .....	280
59. Normalized 70 eV-EI mass spectrum of bis[1,1,1-trifluoro-4-(2'-thienyl)-2,4-butanedionato]Ni(II) .....	282
60. Normalized 70 eV-EI mass spectrum of bis[1,1,1-trifluoro-4-(5'-methyl-2'-thienyl)-2,4-butanedionato]Ni(II) .....	284

Figure	Page
61. Normalized 70 eV-EI mass spectrum of bis[1,1,1,2,2-pentafluoro-5-phenyl-3,5-pentanedionato]Ni(II) .....	286
62. Normalized 70 eV-EI mass spectrum of bis[1,1,1,2,2-pentafluoro-5-(2'-thienyl)-3,5-pentanedionato]Ni(II) .....	288
63. Normalized 70 eV-EI mass spectrum of bis[1,1,1,2,2,3,3-heptafluoro-6-phenyl-4,6-hexanedionato]Ni(II) .....	290
64. Normalized 70 eV-EI mass spectrum of bis[1,1,1,2,2,3,3-heptafluoro-6-(2'-thienyl)-4,6-hexanedionato]Ni(II) .....	292
65. Normalized 70 eV-EI mass spectrum of bis[1,1,1-trifluoro-4-phenyl-2,4-butanedionato]Pd(II) .....	313
66. Normalized 70 eV-EI mass spectrum of bis[1,1,1-trifluoro-4-(2'-thienyl)-2,4-butanedionato]Pd(II) .....	315
67. Normalized 70 eV-EI mass spectrum of bis[1,1,1,2,2-pentafluoro-5-phenyl-3,5-pentanedionato]Pd(II) .....	317
68. Normalized 70 eV-EI mass spectrum of bis[1,1,1,2,2-pentafluoro-5-(2'-thienyl)-3,5-pentanedionato]Pd(II) .....	319
69. Normalized 70 eV-EI mass spectrum of bis[1,1,1,2,2,3,3-heptafluoro-6-phenyl-4,6-hexanedionato]Pd(II) .....	321
70. Normalized 70 eV-EI mass spectrum of bis[1,1,1,2,2,3,3-heptafluoro-6-(2'-thienyl)-4,6-hexanedionato]Pd(II) .....	323

Figure	Page
71. Normalized 70 eV-EI mass spectrum of bis[1,1-difluoro-4-phenyl-2,4-butanedionato]Cu(II) .....	350
72. Normalized 70 eV-EI mass spectrum of bis[1,1-difluoro-4-(2'-thienyl)-2,4-butanedionato]Cu(II) .....	352
73. Normalized 70 eV-EI mass spectrum of bis[1,1,1-trifluoro-4-phenyl-2,4-butanedionato]Cu(II) .....	354
74. Normalized 70 eV-EI mass spectrum of bis[1,1,1-trifluoro-4-(2'-thienyl)-2,4-butanedionato]Cu(II) .....	356
75. Normalized 70 eV-EI mass spectrum of bis[1,1,1-trifluoro-4-(5'-methyl-2'-thienyl)-2,4-butanedionato]Cu(II) .....	358
76. Normalized 70 eV-EI mass spectrum of bis[1,1,1-trifluoro-4-(2'-furyl)-2,4-butanedionato]Cu(II) .....	360
77. Normalized 70 eV-EI mass spectrum of bis[1,1,1-trifluoro-4-(2'-naphthyl)-2,4-butanedionato]Cu(II) .....	362
78. Normalized 70 eV-EI mass spectrum of bis[1,1,1,2,2-pentafluoro-5-phenyl-3,5-pentanedionato]Cu(II) .....	364
79. Normalized 70 eV-EI mass spectrum of bis[1,1,1,2,2-pentafluoro-5-(2'-thienyl)-3,5-pentanedionato]Cu(II) .....	366
80. Normalized 70 eV-EI mass spectrum of bis[1,1,1,2,2,3,3-heptafluoro-6-phenyl-4,6-hexanedionato]Cu(II) .....	368

Figure	Page
81. Normalized 70 eV-EI mass spectrum of bis[1,1,1,2,2,3,3-heptafluoro-6-(2'-thienyl)-4,6-hexanedionato]Cu(II) .....	370
82. Normalized 70 eV-EI mass spectrum of bis[1,1-difluoro-4-phenyl-2,4-butanedionato]Zn(II) .....	385
83. Normalized 70 eV-EI mass spectrum of bis[1,1-difluoro-4-(2'-thienyl)-2,4-butanedionato]Zn(II) .....	387
84. Normalized 70 eV-EI mass spectrum of bis[1,1,1-trifluoro-4-phenyl-2,4-butanedionato]Zn(II) .....	389
85. Normalized 70 eV-EI mass spectrum of bis[1,1,1-trifluoro-4-(2'-thienyl)-2,4-butanedionato]Zn(II) .....	391
86. Normalized 70 eV-EI mass spectrum of bis[1,1,1-trifluoro-4-(5'-methyl-2'-thienyl)-2,4-butanedionato]Zn(II) .....	393
87. Normalized 70 eV-EI mass spectrum of bis[1,1,1,2,2-pentafluoro-5-phenyl-3,5-pentanedionato]Zn(II) .....	395
88. Normalized 70 eV-EI mass spectrum of bis[1,1,1,2,2-pentafluoro-5-(2'-thienyl)-3,5-pentanedionato]Zn(II) .....	397
89. Normalized 70 eV-EI mass spectrum of bis[1,1,1,2,2,3,3-heptafluoro-6-phenyl-4,6-hexanedionato]Zn(II) .....	399
90. Normalized 70 eV-EI mass spectrum of bis[1,1,1,2,2,3,3-heptafluoro-6-(2'-thienyl)-4,6-hexanedionato]Zn(II) .....	401

Figure	Page
91. Normalized 70 eV-EI mass spectrum of tris[1,1,1,2,2-pentafluoro-5-mercapto-5-phenyl-pent-4-en-3-onato]Co(III) .	413
92. Normalized 70 eV-EI mass spectrum of tris[1,1,1,2,2-pentafluoro-5-mercapto-5-(2'-thienyl)-pent-4-en-3-onato]Co(III) .....	415
93. Normalized 70 eV-EI mass spectrum of tris[1,1,1,2,2-pentafluoro-5-mercapto-5-(2'-naphthyl)-pent-4-en-3-onato]Co(III) .....	417
94. Normalized 70 eV-EI mass spectrum of tris[1,1,1,2,2,3,3-heptafluoro-6-mercapto-6-phenyl-hex-5-en-4-onato]Co(III) ..	419
95. Normalized 70 eV-EI mass spectrum of tris[1,1,1,2,2,3,3-heptafluoro-6-mercapto-6-(2'-thienyl)-hex-5-en-4-onato]Co(III) .....	421
96. Normalized 70 eV-EI mass spectrum of tris[1,1,1,2,2,3,3-heptafluoro-6-mercapto-6-(2'-naphthyl)-hex-5-en-4-onato]Co(III) .....	423
97. Normalized 70eV-EI mass spectrum of bis[1,1,1-trifluoro-4-mercapto-4-phenyl-but-3-en-2-onato]Ni(II) .....	444
98. Normalized 70 eV-EI mass spectrum of bis[1,1,1-trifluoro-4-mercapto-4-(4'-fluorophenyl)-but-3-en-2-onato]Ni(II) ....	446

Figure	Page
99. Normalized 70 eV-EI mass spectrum of bis[1,1,1-trifluoro-4-mercapto-4-(4'-methoxyphenyl)-but-3-en-2-onato]Ni(II) ...	448
100. Normalized 70 eV-EI mass spectrum of bis[1,1,1-trifluoro-4-mercapto-4-(2'-thienyl)-but-3-en-2-onato]Ni(II) .....	450
101. Normalized 70 eV-EI mass spectrum of bis[1,1,1-trifluoro-4-mercapto-4-(5'-methyl-2'-thienyl)-but-3-en-2-onato]Ni(II)	452
102. Normalized 70 eV-EI mass spectrum of bis[1,1,1,2,2-pentafluoro-5-mercapto-5-phenyl-pent-4-en-3-onato]Ni(II) ..	454
103. Normalized 70 eV-EI mass spectrum of bis[1,1,1,2,2-pentafluoro-5-mercapto-5-(2'-thienyl)-pent-4-en-3-onato]Ni(II) .....	456
104. Normalized 70 eV-EI mass spectrum of bis[1,1,1,2,2-pentafluoro-5-mercapto-5-(2'-naphthyl)-pent-4-en-3-onato]Ni(II) .....	458
105. Normalized 70 eV-EI mass spectrum of bis[1,1,1,2,2,3,3-heptafluoro-6-mercapto-6-phenyl-hex-5-en-4-onato]Ni(II) ...	460
106. Normalized 70 eV-EI mass spectrum of bis[1,1,1,2,2,3,3-heptafluoro-6-mercapto-6-(2'-thienyl)-hex-5-en-4-onato]Ni(II) .....	462

Figure	Page
107. Normalized 70 eV-EI mass spectrum of bis[1,1,1,2,2,3,3-heptafluoro-6-mercapto-6-(2'-naphthyl)-hex-5-en-4-onato]Ni(II) .....	464
108. Normalized 70 eV-EI mass spectrum of bis[1,1,1-trifluoro-4-mercapto-4-phenyl-but-3-en-2-onato]Pd(II) .....	489
109. Normalized 70 eV-EI mass spectrum of bis[1,1,1-trifluoro-4-mercapto-4-(4'-methoxyphenyl)-but-3-en-2-onato]Pd(II) ...	491
110. Normalized 70 eV-Ei mass spectrum of bis[1,1,1-trifluoro-4-mercapto-4-(2'-thienyl)-but-3-en-2-onato]Pd(II) .....	493
111. Normalized 70 eV-EI mass spectrum of bis[1,1,1,2,2-pentafluoro-5-mercapto-5-phenyl-pent-4-en-3-onato]Pd(II) ..	495
112. Normalized 70 eV-EI mass spectrum of bis[1,1,1,2,2-pentafluoro-5-mercapto-5-(2'-thienyl)-pent-4-en-3-onato]Pd(II) .....	497
113. Normalized 70 eV-EI mass spectrum of bis[1,1,1,2,2-pentafluoro-5-mercapto-5-(2'-naphthyl)-pent-4-en-3-onato]Pd(II) .....	499
114. Normalized 70 eV-EI mass spectrum of bis[1,1,1,2,2,3,3-heptafluoro-6-mercapto-6-phenyl-hex-5-en-4-onato]Pd(II) ...	501



Figure	Page
115. Normalized 70 eV-EI mass spectrum of bis[1,1,1,2,2,3,3-heptafluoro-6-mercapto-6-(2'-thienyl)-hex-5-en-4-onato]Pd(II) .....	503
116. Normalized 70 eV-EI mass spectrum of bis[1,1,1,2,2,3,3-heptafluoro-6-mercapto-6-(2'-naphthyl)-hex-5-en-4-onato]Pd(II) .....	505
117. Normalized 70 eV-EI mass spectrum of bis[1,1,1-trifluoro-4-mercapto-4-phenyl-but-3-en-2-onato]Cu(II) .....	521
118. Normalized 70 eV-EI mass spectrum of bis[1,1,1-trifluoro-4-mercapto-4-(4'-methylphenyl)-but-3-en-2-onato]Cu(II) ....	523
119. Normalized 70 eV-EI mass spectrum of bis[1,1,1-trifluoro-4-mercapto-4-(4'-fluorophenyl)-but-3-en-2-onato]Cu(II) ....	525
120. Normalized 70 eV-EI mass spectrum of bis[1,1,1-trifluoro-4-mercapto-4-(2'-thienyl)-but-3-en-2-onato]Cu(II) .....	527
121. Normalized 70 eV-EI mass spectrum of bis[1,1,1,2,2-pentafluoro-5-mercapto-5-phenyl-pent-4-en-3-onato]Cu(II) ..	529
122. Normalized 70 eV-EI mass spectrum of bis[1,1,1,2,2,3,3-heptafluoro-6-mercapto-6-phenyl-hex-5-en-4-onato]Cu(II) ...	531
123. Normalized 70 eV-EI mass spectrum of bis[1,1,1-trifluoro-4-mercapto-4-phenyl-but-3-en-2-onato]Zn(II) .....	542

Figure	Page
124. Normalized 70 eV-EI mass spectrum of bis[1,1,1-trifluoro-4-mercapto-4-(4'-fluorophenyl)-but-3-en-2-onato]Zn(II) ....	544
125. Normalized 70 eV-Ei mass spectrum of bis[1,1,1-trifluoro-4-mercapto-4-(4'-methoxyphenyl)-but-3-en-2-onato]Zn(II) ...	546
126. Normalized 70 eV-EI mass spectrum of bis[1,1,1-trifluoro-4-mercapto-4-(2'-thienyl)-but-3-en-2-onato]Zn(II) .....	548
127. Normalized 70 eV-EI mass spectrum of bis[1,1,1-trifluoro-4-mercapto-4-(5'-methyl-2'-thienyl)-but-3-en-2-onato]Zn(II)	550
128. Comparison of experimental and calculated isotopic envelope distribution for the cluster ion $[\text{Zn(II)}_2\text{L}_3]^+$ .....	551
129. Comparison of experimental and calculated isotopic envelope distribution for the cluster ion $[\text{Zn(II)}_2\text{FL}_2]^+$ .....	552

LIST OF SCHEMES

Scheme	Page
1. Suggested fragmentation pathways for the 3-keto- 17-hydroxysteroids .....	42
2. Fragmentation mechanisms for the formation of ions [M - 73] <sup>+</sup> , [M - 58] <sup>+</sup> and [M - 57] <sup>+</sup> .....	43
3. Suggested fragmentation pathways for the 3,17-diols .....	47
4. Chair-to-boat isomerization of ring A in 3 $\alpha$ -hydroxy- 5 $\beta$ -steroids .....	49
5. Principal fragmentation pathways of the Al(III) and Fe(III) complexes of 2,4-pentanedione .....	89
6. Fragmentation pathways for metal chelates of 2,4-pentane- dione involving no change of metal oxidation state .....	92
7. Fragmentation pathways for metal chelates of 2,4-pentane- dione involving a reduction of metal oxidation state .....	93
8. Fragmentation routes for tris metal complexes of 1,1,1-trifluoro-2,4-pentanedione and 1,1,1,5,5,5-hexafluoro-2,4-pentanedione .....	100

Scheme	Page
9. Fragmentation routes for bis metal complexes of 1,1,1-trifluoro-2,4-pentanedione and 1,1,1,5,5,5-hexafluoro-2,4-pentanedione .....	101
10. Fragmentation pathway involving loss of CO <sub>2</sub> from some fluorinated Fe(III) and Co(III) β-diketonates .....	107
11. Fragmentation pathways for (a) Zn(II) and (b) Ni(II) chelates Met(RCSCHCOF <sub>3</sub> ) <sub>2</sub> .....	110
12. Fragmentation pathways for (a) Pd(II) and (b) Pt(II) chelates Met(RCSCHCOF <sub>3</sub> ) <sub>2</sub> .....	112
13. Fragmentation pathways for the cobalt(III) chelates Co(RCSCHCOF <sub>3</sub> ) <sub>3</sub> .....	113
14. Fragmentation pathways for (a) Ni(II), Zn(II), Pd(II), Pt(II) and Rh(III) chelates Met <sup>n</sup> (RCSCHCOF <sub>3</sub> ) <sub>n</sub> and (b) Fe(III), Ru(III) and Co(III) chelates Met(RCSCHCOF <sub>3</sub> ) <sub>3</sub> .....	115
15. Fragmentation pathways involving loss of MetS from chelates of 1,1,1-trifluoro-4-mercapto- 4-(2'-naphthyl)-but-3-en-2-one .....	117
16. Proposed fragmentation pathways for Al(III) β-diketonates where R' = CF <sub>3</sub> .....	177

Scheme	Page
17. Suggested mechanisms for the formation of [Al(III)FL(L-R')] <sup>+</sup> and [Al(III)FL] <sup>+</sup> .....	178
18. Suggested mechanism for the formation of [Al(III)F <sub>2</sub> (L-R')] <sup>+</sup> from [Al(III)FL(L-R')] <sup>+</sup> .....	179
19. Suggested mechanism for the formation of [Al(III)F <sub>2</sub> (L-R')] <sup>+</sup> .....	180
20. Proposed fragmentation pathways for Al(III) β-diketonates where R' = CHF <sub>2</sub> .....	181
21. Suggested mechanism for the formation of [Al(III)FL(L-COF)] <sup>+</sup> .....	182
22. Suggested mechanisms for the formation of [Al(III)FL] <sup>+</sup> ....	183
23. Suggested mechanism for the elimination of Al(III)F <sub>3</sub> .....	184
24. Proposed fragmentation pathways for Ga(III) β-diketonates where R' = CHF <sub>2</sub> .....	207
25. Suggested mechanism for the formation of [Ga(III)L <sub>2</sub> ] <sup>+</sup> and [Ga(I)] <sup>+</sup> .....	208
26. Suggested mechanism for the formation of [Ga(III)RL] <sup>+</sup> .....	209
27. Suggested mechanism for the elimination of Ga(III)F <sub>3</sub> from [Ga(III)FL] <sup>+</sup> .....	210

Scheme	Page
28. Proposed fragmentation pathways for Ga(III) $\beta$ -diketonates where $R' = CF_3$ .....	211
29. Proposed fragmentation pathways for Co(III) $\beta$ -diketonates where $R' = CHF_2$ .....	255
30. Suggested mechanism for the formation of $[Co(II)L(L-R')]^+$ and $[Co(II)L]^+$ .....	256
31. Suggested mechanism for the formation of $[Co(II)F(L-COF)]^+$ and $[L-COF_2]^+$ .....	257
32. Suggested mechanism for the elimination of $Co(II)F_2$ from $[Co(II)L]^+$ .....	258
33. Suggested mechanism for the formation of $[Co(II)F(L-R')]^+$ and $[Co(I)]^+$ .....	259
34. Proposed fragmentation pathways for Co(III) $\beta$ -diketonates where $R' = CF_3$ .....	260
35. Suggested mechanism for the formation of $[Co(II)LCHCR]^+$ , $[Co(II)L]^+$ , $[Co(II)F(L-R')]^+$ and $[Co(II)FCHCR]^+$ .....	261
36. Suggested mechanism for the formation of $[Co(II)(L-CF_2-HF)]^+$ and $[Co(II)R]^+$ .....	262

Scheme	Page
37. Proposed fragmentation pathways for Co(III) $\beta$ -diketonates where $R' = C_2F_5$ or $C_3F_7$ .....	263
38. Proposed fragmentation pathways for Ni(II) $\beta$ -diketonates where $R' = CHF_2$ .....	293
39. Proposed fragmentation pathways for Ni(II) $\beta$ -diketonates where $R' = CF_3$ .....	294
40. Proposed fragmentation pathways for Ni(II) $\beta$ -diketonates where $R' = C_2F_5$ or $C_3F_7$ .....	295
41. Suggested mechanism for the formation of $[Ni(II)L(L-COF)]^+$ .....	296
42. Suggested mechanism for the formation of $[Ni(III)FL(L-CF_3)]^+$ .....	297
43. Suggested mechanism for the formation of $[Ni(L-H)]^+$ .....	298
44. Suggested mechanism for the formation of $[Ni(II)HL]^+$ .....	299
45. Suggested mechanism for the formation of $[Ni(I)HL]^+$ .....	300
46. Suggested mechanism for the formation of $[Ni(II)HL]^+$ .....	301
47. Proposed fragmentation pathways for Pd(II) $\beta$ -diketonates where $R' = CF_3$ .....	324

Scheme	Page
48. Suggested mechanism for the formation of [Pd(II)(L-H)] <sup>+</sup> and [Pd(II)(L-H-R')] <sup>+</sup> .....	325
49. Suggested mechanism for the formation of [Pd(III)FR(L-COF)] <sup>+</sup> .....	326
50. Proposed fragmentation pathways for Pd(II) β-diketonates where R' = C <sub>2</sub> F <sub>5</sub> or C <sub>3</sub> F <sub>7</sub> .....	327
51. Suggested mechanism for the formation of [Pd(II)R(L-R'CO)] <sup>+</sup> .....	328
52. Suggested mechanism for the formation of [Pd(II)R'CHCR] <sup>+</sup> ..	329
53. Suggested mechanisms for the formation of [Pd(II)(L-O)] <sup>+</sup> ..	330
54. Proposed fragmentation pathways for Cu(II) β-diketonates where R' = CHF <sub>2</sub> , CF <sub>3</sub> , C <sub>2</sub> F <sub>5</sub> or C <sub>3</sub> F <sub>7</sub> .....	371
55. (a) Suggested mechanism for the formation of [L] <sup>+</sup> . (b) Proposed resonance-stabilized forms of [L] <sup>+</sup> .....	372
56. Suggested mechanism for the formation of [Cu(I)L <sub>2</sub> -2R'] <sup>+</sup> ...	373
57. Suggested mechanism for the formation of [Cu(I)(L-R')] <sup>+</sup> from (a) [Cu(I)L(L-R')] <sup>+</sup> and (b) [Cu(I)L <sub>2</sub> -2R'] <sup>+</sup> .....	374
58. Suggested mechanism for the formation of [Cu(I)(L-R')] <sup>+</sup> from [Cu(II)L] <sup>+</sup> .....	375



Scheme	Page
59. Proposed fragmentation pathways for Zn(II) $\beta$ -diketonates where $R' = CHF_2$ .....	402
60. Proposed fragmentation pathways for Zn(II) $\beta$ -diketonates where $R' = CF_3$ .....	403
61. Proposed fragmentation pathways for Zn(II) $\beta$ -diketonates where $R' = C_2F_5$ or $C_3F_7$ .....	404
62. Proposed fragmentation pathways for Co(III) monothio- $\beta$ -diketonates where $R' = C_2F_5$ or $C_3F_7$ .....	424
63. Suggested mechanism for the formation of $[Co(III)FL(L-CF_3)]^+$ and $[Co(III)FL(L-R')]^+$ .....	425
64. Suggested mechanism for the formation of $[Co(II)L(L-R')]^+$ , $[Co(II)L(L-R'CO)]^+$ and $[Co(II)L]^+$ .....	426
65. Suggested mechanism for the formation of $[Co(I)L]^+$ , $[Co(I)SC(R)CH]^+$ and $[Co(I)CHCR]^+$ .....	427
66. Suggested mechanism for the formation of $[Co(II)LCHCR]^+$ ...	428
67. Suggested mechanism for the formation of $[2L-S-R'CO]^+$ and $[2L-2S-R'CO]^+$ .....	429
68. Proposed fragmentation pathways for Ni(II) monothio- $\beta$ -diketonates where $R' = CF_3$ .....	465

Scheme	Page
69. (a) Suggested mechanism for the formation of $[L]^+$ from $[Ni(II)L_2]^+$ : (b) Proposed resonance-stabilized forms of $[L]^+$ .....	466
70. Suggested mechanism for the formation of $[Ni(II)L(L-S)]^+$ ..	467
71. Suggested mechanism for the formation of $[Ni(II)SL]^+$ .....	468
72. Suggested mechanism for the formation of $[Ni(L-H)]^+$ .....	469
73. Suggested mechanism for the formation of $[Ni(I)SC(R)CH]^+$ , $[Ni(I)SCR]^+$ and $[Ni(I)]^+$ .....	470
74. Proposed fragmentation pathways for Ni(II) monothio- $\beta$ -diketonates where $R' = C_2F_5$ or $C_3F_7$ .....	471
75. Suggested mechanism for the formation of $[Ni(II)L(L-F)]^+$ and $[Ni(II)L(L-F-HF)]^+$ .....	472
76. Suggested mechanism for the formation of $[Ni(III)FL(L-CF_3)]^+$ and $[Ni(III)FL(L-C_2F_5)]^+$ .....	473
77. Suggested mechanism for the formation of $[Ni(II)HL]^+$ .....	474
78. Suggested mechanism for the formation of $[Ni(I)HL]^+$ .....	475
79. Suggested mechanism for the formation of $[Ni(II)HL]^+$ .....	476
80. Proposed fragmentation pathways for Pd(II) monothio- $\beta$ -diketonates where $R' = CF_3$ .....	506

Scheme	Page
81. Suggested mechanism for the formation of [Pd(II)SC(R)CH] <sup>+</sup> and [Pd(II)CHCR] <sup>+</sup> .....	507
82. Suggested mechanism for the formation of [Pd(II)(L-H-R')] <sup>+</sup>	508
83. Suggested mechanism for the formation of [Pd(II)L] <sup>+</sup> and [Pd(II)R] <sup>+</sup> .....	509
84. Proposed fragmentation pathways for Pd(II) monothio- $\beta$ -diketonates where R' = C <sub>2</sub> F <sub>5</sub> or C <sub>3</sub> F <sub>7</sub> .....	510
85. Suggested mechanism for the formation of [2L-S] <sup>+</sup> , [2L-S-R'] <sup>+</sup> , [2L-S-R'CO] <sup>+</sup> and [2L-S-2R'CO] <sup>+</sup> .....	511
86. Proposed fragmentation pathways for Cu(II) monothio- $\beta$ -diketonates where R' = CF <sub>3</sub> .....	532
87. Suggested mechanism for the formation of [Cu(I)] <sup>+</sup> .....	533
88. Proposed fragmentation pathways for Cu(II) monothio- $\beta$ -diketonates where R' = C <sub>2</sub> F <sub>5</sub> or C <sub>3</sub> F <sub>7</sub> .....	534
89. Proposed fragmentation pathways for Zn(II) monothio- $\beta$ -diketonates where R' = CF <sub>3</sub> .....	553
90. Suggested mechanism for the formation of [Zn(II)F(L-R')] <sup>+</sup> and [Zn(II)FCHCR] <sup>+</sup> .....	554

Scheme	Page
91. Suggested mechanism for the formation of [Zn(II)(L-CF <sub>2</sub> -HF)] <sup>+</sup> .....	555
92. Suggested mechanism for the formation of [Zn(II)F(L-R')] <sup>+</sup> .	556
93. Suggested mechanism for the formation of [Zn(II) <sub>2</sub> FL <sub>2</sub> ] <sup>+</sup> from [Zn(II) <sub>2</sub> L <sub>3</sub> ] <sup>+</sup> .....	557

ABBREVIATIONS, SYMBOLS AND DEFINITION OF TERMS

Mass spectrometric literature contains a confusingly large number of acronyms, abbreviations and symbols, many of which are misunderstood simply because of their redundant nature. Researchers working in closely-related fields of mass spectrometry often perceive distinctions (be they real or imagined) between their work and that of their colleagues and therefore affix labels according to their own limited view and preference (1). In recent years, the International Union of Pure and Applied Chemistry (IUPAC) (2,3) and the Editorial Board of the journal Organic Mass Spectrometry (4,5) have made attempts at standardizing the symbolism and nomenclature for mass spectrometry. Many of their recommendations pertaining to topics covered in this thesis are given below. When necessary, more recent sources (6-10) have also been consulted.

(i) Abbreviations

EIMS	electron ionization mass spectrometry
FIMS	field ionization mass spectrometry
FDMS	field desorption mass spectrometry
CIMS	chemical ionization mass spectrometry
CAMS	collisional activation mass spectrometry
PIMS	photoionization mass spectrometry
SIMS	secondary ion mass spectrometry
FTMS	Fourier transform mass spectrometry

GC/MS	gas chromatography and mass spectrometry (linked)
LC/MS	liquid chromatography and mass spectrometry (linked)
ICR	ion cyclotron resonance
	The letters preceding MS can also be used separately. However, the initials MS can have several different connotations when used on their own.
u	dalton or mass unit ( $^{12}\text{C} = 12$ daltons), formerly "amu"
e	magnitude of the electronic charge
m	the mass number of an ion
z	the charge number of an ion
$\% \Sigma_n$	percentage of total ionization (see Definitions)
m/z	the mass-to-charge ratio, formerly "m/e"
IE	ionization energy, formerly "ionization potential"
AE	appearance energy, formerly "appearance potential"
Rel.int.	the relative intensity of a peak as a percentage of the intensity of a base peak (% Rel.int.)
Mol.mass	relative molecular mass

(ii) Symbols

$\text{M}^{\cdot+}$ or $[\text{M}]^{\cdot+}$	molecular radical cation
$\text{F}^+$ or $[\text{F}]^+$	positive even electron fragment ion
$\text{F}^{\cdot+}$ or $[\text{F}]^{\cdot+}$	positive odd electron fragment ion
$m^*$	apparent m/z value of a metastable peak
$m^{2+}, m^{3-}$	multiply charged ions, preferable to $m^{++}, m^{-3}$
$\xrightarrow{*}$	process confirmed by the observation of a metastable peak
$\xrightarrow{\cdot}$	indication of a one electron shift
$\xrightarrow{\cdot\cdot}$	indication of a two electron shift

- B                    magnetic field (or magnetic sector)
- E                    electric field (or electric sector)

(iii) Definitions

Mass Spectrograph. An instrument used for the simultaneous recording of focused ion beams on a photographic plate; used primarily for the accurate determination of atomic masses.

Mass Spectrometer. An instrument used for the recording of separated ion beams by means of dedicated electronic devices; more suited for the measurement of isotopic abundances.

Molecular ion. The ion formed by the removal of one electron from a molecule (positive) or the addition of one electron to a molecule (negative). Represents the ionized molecule containing only the isotopes of greatest natural abundance.

Fragment ion. An ion formed by the cleavage of one or more bonds in the molecular ion. It may be an even electron ion (ion produced by removing an electron from a radical) or an odd electron ion (ion produced by removing an electron from a molecule).

Rearrangement ion. An ion formed by the rearrangement process of some ion species, including the molecular ion.

Parent ion. The precursor to a given fragment ion, not necessarily the molecular ion.

$\alpha$ -Cleavage. The cleavage of a bond adjacent to an electron deficient group.

$\beta$ -Cleavage. The cleavage of a bond  $\beta$  (one removed) to a given atom.

Allylic cleavage. The cleavage of a bond one removed from a double bond.

Benzylic cleavage. The cleavage of a bond one removed from an aromatic ring.

McLafferty rearrangement.  $\beta$ -cleavage with concomitant specific transfer of a  $\gamma$ -hydrogen atom in a six-membered transition state in mono-unsaturated systems, irrespective of whether the rearrangement is formulated by a radical or ionic mechanism and irrespective of the position of the charge.

Resolution: 10 per cent valley definition. Let two peaks of equal height in a mass spectrum at masses  $m$  and  $m+\Delta m$  be separated by a valley which at its lowest point is just 10 per cent of the height of

either peak. The resolution can then be described as  $m/\Delta m$  at a 10% valley definition. For example, when two masses (100.000, 100.005) are separated by a 10 per cent valley, the resolution of the instrument is  $100.000/0.005$ , i.e. 20,000.

Percentage Total Ionization. The abundance of an individual ion compared with the sum of the abundances of all the ions in a specified mass range or of a specified ion type.



## CHAPTER I.

## MASS SPECTRA OF

17 $\xi$  -HYDROXY-17 $\xi$  -METHYL-5 $\xi$  -ANDROSTANE C(3) KETONE

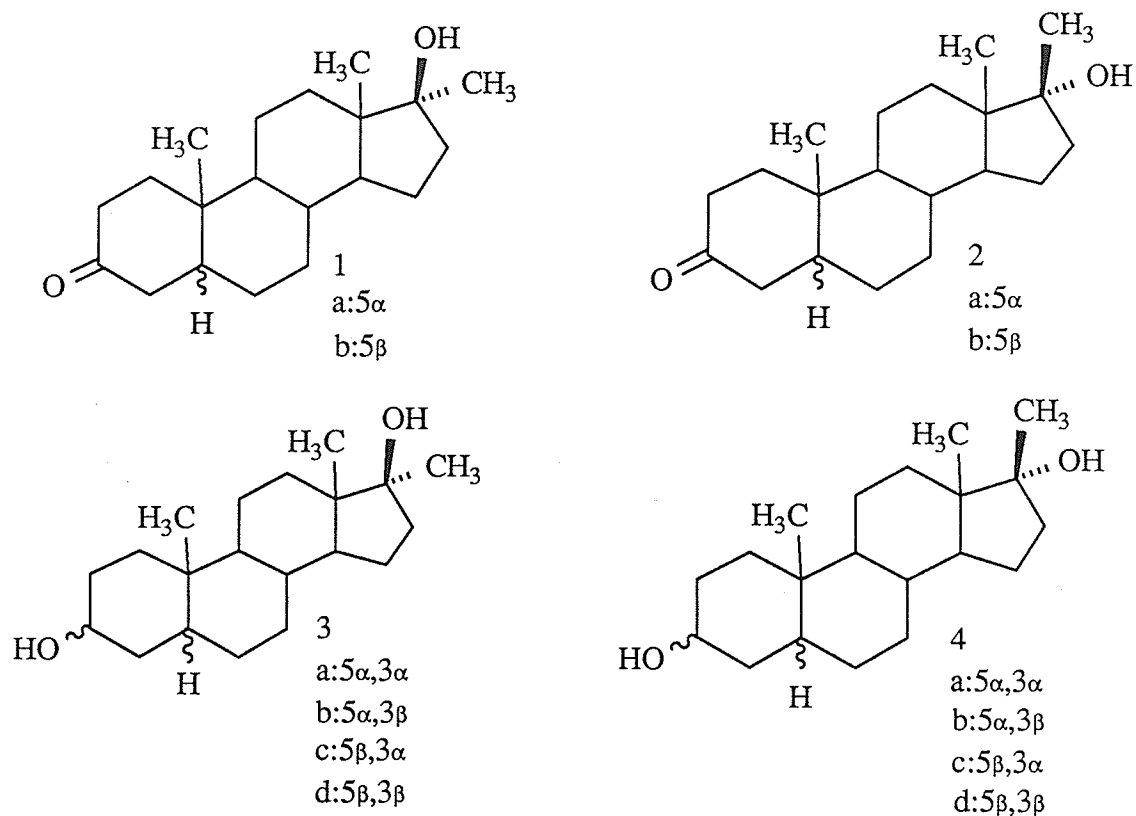
AND

C(3 $\xi$ ) ALCOHOL ISOMERS

## A. INTRODUCTION

Establishing a correlation between the stereochemistry of a molecule and its mass spectrum has been the goal of countless studies in organic mass spectrometry. Included among them is the application of mass spectrometry to the structural and stereochemical problems encountered in the analysis of naturally-occurring steroids. Steroids were among the first natural products to be examined in a mass spectrometer and immediately exemplified the potential of the technique for organic analysis (11,12). Since that time, the biological and medical importance of these compounds has made them the subject of many studies relating structure to fragmentation processes. In fact, the complexity of steroid fragmentation patterns and the difficulties encountered in their interpretation have led to two important developments in organic mass spectrometry: the routine incorporation of stable isotopes into molecules for the purposes of elucidating decomposition pathways (such as the studies by Djerassi and co-workers of hydrogen migration in steroids using  $^2\text{H}$ -labelled analogs (13)), and secondly, the use of derivatives (primarily silyl ether) to aid in the structural characterization of steroids by combined GC/MS (14).

The present work describes the positive-ion, electron ionization (EI) mass spectra of the four isomeric  $17\xi$ -hydroxy- $17\xi$ -methyl- $5\xi$ -androsterane C(3) ketones and the eight corresponding C(3 $\xi$ ) alcohols (see Figure 1). The impetus behind this study, besides the continuing interest in the mass spectrometry of steroids in general, was the



- 1a: 17 $\beta$ -hydroxy-17 $\alpha$ -methyl-5 $\alpha$ -androstane-3-one  
 1b: 17 $\beta$ -hydroxy-17 $\alpha$ -methyl-5 $\beta$ -androstane-3-one  
 2a: 17 $\alpha$ -hydroxy-17 $\beta$ -methyl-5 $\alpha$ -androstane-3-one  
 2b: 17 $\alpha$ -hydroxy-17 $\beta$ -methyl-5 $\beta$ -androstane-3-one  
 3a: 17 $\alpha$ -methyl-5 $\alpha$ -androstane-3 $\alpha$ ,17 $\beta$ -diol  
 3b: 17 $\alpha$ -methyl-5 $\alpha$ -androstane-3 $\beta$ ,17 $\beta$ -diol  
 3c: 17 $\alpha$ -methyl-5 $\beta$ -androstane-3 $\alpha$ ,17 $\beta$ -diol  
 3d: 17 $\alpha$ -methyl-5 $\beta$ -androstane-3 $\beta$ ,17 $\beta$ -diol  
 4a: 17 $\beta$ -methyl-5 $\alpha$ -androstane-3 $\alpha$ ,17 $\alpha$ -diol  
 4b: 17 $\beta$ -methyl-5 $\alpha$ -androstane-3 $\beta$ ,17 $\alpha$ -diol  
 4c: 17 $\beta$ -methyl-5 $\beta$ -androstane-3 $\alpha$ ,17 $\alpha$ -diol  
 4d: 17 $\beta$ -methyl-5 $\beta$ -androstane-3 $\beta$ ,17 $\alpha$ -diol

**Figure 1.** 17 $\xi$ -hydroxy-17 $\xi$ -methyl-5 $\xi$ -androstane C(3) ketone and C(3 $\xi$ ) alcohol isomers.

availability of the complete sets of epimeric ketones (**1a,b**; **2a,b**) and diols (**3a-d**; **4a-d**) and the opportunity to evaluate the stereochemical factors influencing their mass spectra. Of particular interest were the effects of the tertiary hydroxyl group orientation at C(17), for reasons to be discussed presently.

Although direct comparative evidence is lacking, some parallels to the present work can be drawn from published data on steroids of similar structure (both electron and chemical ionization studies have been performed, so each will receive consideration). Z.V. Zaretskii and co-workers (15-17) reported the EI mass spectra of a series of epimeric tertiary alcohols, derivatives of 3-methoxy-17 $\xi$ -alkyl- $\Delta$ 1,3,5(10),8-D-homoestratetraen-17 $\xi$ -ol (see Figure 2). The most striking mass spectral feature of these steroids is the large difference in intensities for the  $[M - 18]^+$  peaks (loss of water from molecular ion) between C(17) epimers. A comparison of the  $[M - H_2O]^+ / [M]^+$  ratios reveals much larger values for the 17 $\alpha$ -OH compounds as compared to their 17 $\beta$ -OH isomers. Trideutero-methyl analogs at C(17) were used to elucidate the mechanism of dehydration, indicating an axial arrangement of the 17 $\alpha$ -OH group (equatorial configuration for 17 $\beta$ -OH). Significant correlations were also made between the relative abundances of the  $[M - H_2O - (17\text{-alkyl})]^+$  and  $[M - H_2O]^+$  ions; the former species is greatly favored over the latter in epimers with an axial-OH group (i.e. 17 $\alpha$ -OH), while the opposite trend exists for isomers with an equatorial hydroxyl. Again, deuterated analogs were used to clarify decomposition pathways. Minor

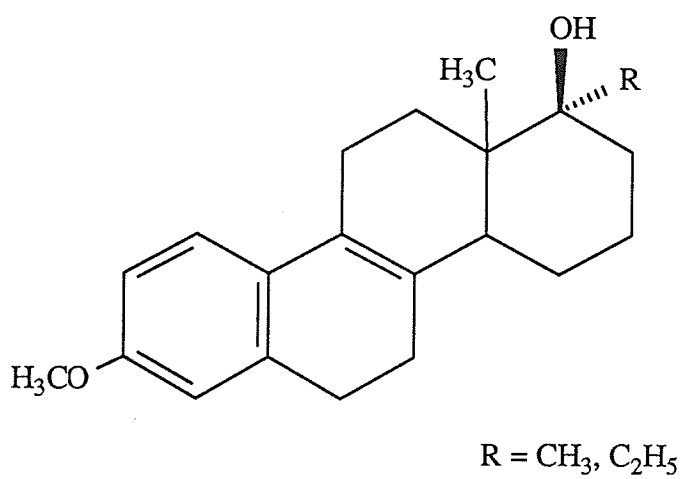
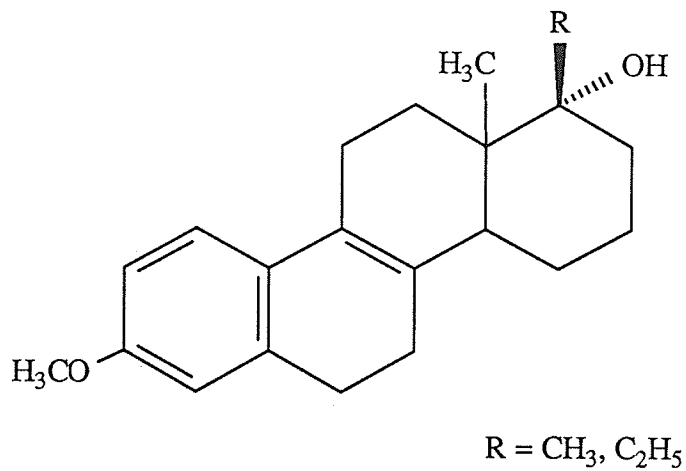
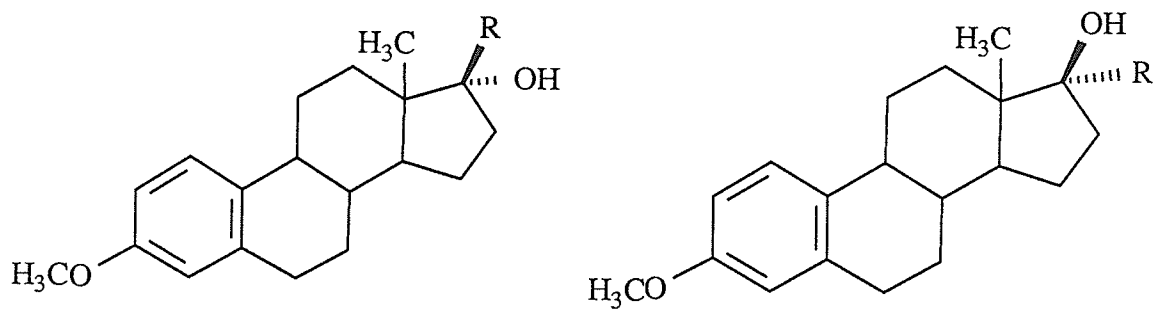


**Figure 2.** 3-methoxy-17 $\xi$ -alkyl- $\Delta^{1,3,5(10),8}$ -D-homoestratetraen-17 $\xi$ -ol isomers (16).

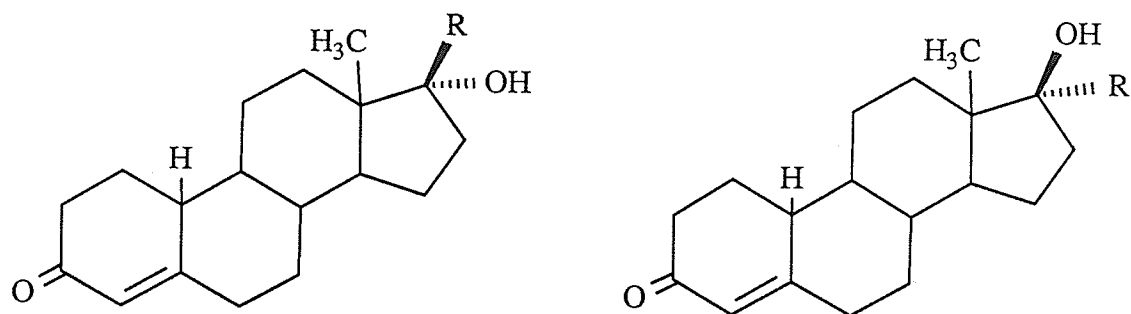
peaks arising from ring D fragmentation processes were deemed to be dependent upon the configuration at C(17) as well.

In order to determine if the trends in the mass spectral behavior observed in the D-homo series would be retained in alcohols possessing a 5-membered ring D, Zaretskii (18,19) examined the isomers of 3-methoxy-17 $\xi$ -alkyl- $\Delta^{1,3,5(10)}$ -estratrien-17 $\xi$ -ol and 17 $\xi$ -alkyl-19-nortestosterone (see Figure 3). The mass spectra of the 17-alkylestradiol derivatives differ only in the values of the  $[M - H_2O]^{+\cdot}/[M]^{+\cdot}$  ratios; as with the D-homo series, the ratios are higher in alcohols having a 17 $\alpha$ -OH as compared to a 17 $\beta$ -OH group, lending support to the view that the  $\alpha$ - and  $\beta$ -bonds at C(17) are axial and equatorial respectively (in relation to ring C). No other correlations between ion abundances and C(17) stereochemistry are observed for these epimers. The dehydration of the 17 $\xi$ -alkyl-19-nortestosterones also proceeds more readily in the 17 $\alpha$ -hydroxy isomers. However, it is in the  $[M - H_2O - (17\text{-alkyl})]^{+\cdot}/[M - H_2O]^{+\cdot}$  ratio that noticeable differences are reported. The considerable decrease in the value of this ratio for the 17 $\beta$ -OH epimers is attributed to different dehydration mechanisms at work in the corresponding molecular ions. The ring D fragmentations so prevalent in the alcohols of the D-homo series are either non-existent (for the 17-alkyl-estradiols) or no longer dependent upon the stereochemistry at the 17-center (for the 17-alkyl-19-nortestosterones).

The identification of stereoisomers by electron ionization is often complicated by extensive fragmentation, which occurs as a result of the



(a)  $R = \text{CH}_3, \text{C}_2\text{H}_5, \text{C}_4\text{H}_7$



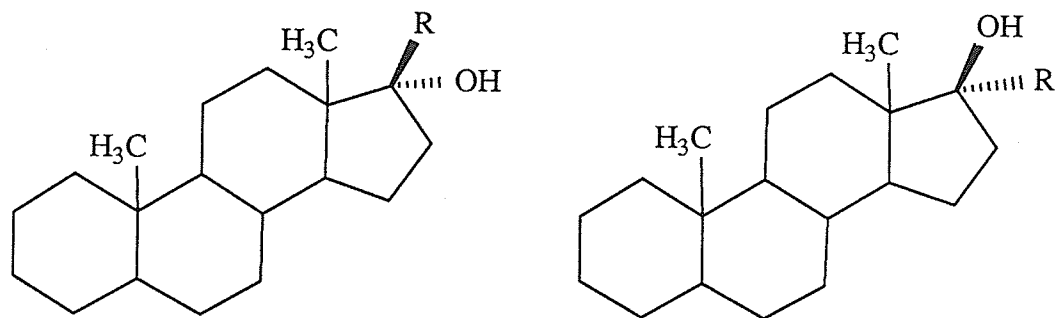
(b)  $R = \text{CH}_3, \text{C}_2\text{H}_5$

**Figure 3.** Isomers of (a) 3-methoxy-17 $\xi$ -alkyl- $\Delta^{1,3,5(10)}$ -estratrien-17 $\xi$ -ol and (b) 17 $\xi$ -alkyl-19-nortestosterone (19).

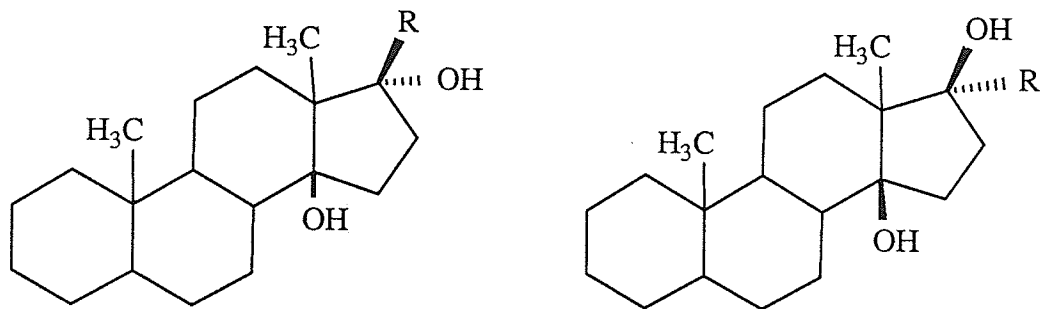
high internal energy imparted to the molecular ion. Since the variations in the fragmentation patterns among stereoisomers are due to only minor steric or energetic differences, the probability of their detection will be enhanced if the internal energies of the nascent ions are minimized (20). Not surprisingly, attention has recently shifted to the use of softer ionization methods, in particular chemical ionization (CI). Chemical ionization allows for the regulation of the internal energy by selection of the appropriate reagent gas mixture as well as suitable source temperatures and pressures. The result is a simpler mass spectrum (as compared to EI), unencumbered by fragmentations arising from complex rearrangements.

The  $\text{OH}^-$  negative chemical ionization (NCI) mass spectra of  $17\xi$ -R- $5\alpha$ -androstane- $17\xi$ -ol (R = H,  $\text{C}_2\text{H}_3$ ,  $\text{C}_2\text{H}$ ) and  $17\xi$ -R- $5\alpha$ , $14\beta$ -androstane- $14,17\xi$ -diols (R =  $\text{CH}_3$ ,  $\text{C}_2\text{H}_5$ ,  $\text{C}_2\text{H}_3$ ,  $\text{C}_2\text{H}$ ) were recently published by Beloeil et al (21) (see Figure 4). All spectra are characterized by abundant pseudomolecular anions  $[\text{M} - \text{H}]^-$  and the competitive losses of water and either (i) an exocyclic hydrocarbon (RH) for tertiary alcohols, or (ii) molecular hydrogen ( $\text{H}_2$ ) for secondary alcohols. Results for the 17-androstanols show no stereochemical effect for hydroxyl groups in position 17. The diols, however, exhibit very strong preferences in the spectra of their stereoisomers: only the trans diols ( $14\beta, 17\alpha$ ) eliminate a hydrocarbon molecule to a significant extent. Mechanistic work based upon isotopic (deuterium) labelling of the alcohol groups reveals that a bifunctional  $14,17$  interaction plays a major role in stabilizing the resulting  $[\text{M} - \text{H} - \text{RH}]^-$  fragment.





(a)  $R = H, C_2H_3, C_2H$



(b)  $R = H, CH_3, C_2H_5, C_2H_3, C_2H$

**Figure 4.** Isomers of (a)  $17\xi-R-5\alpha$ -androstane- $17\xi$ -ol and  
(b)  $17\xi-R-5\alpha,14\beta$ -androstane- $14,17\xi$ -diol (21).

Prome and co-workers (22) have examined the methane and ammonia positive CI and  $\text{OH}^-/\text{NCI}$  mass spectra of a series of four stereoisomeric  $5\xi$ -androstan-3-one-17 $\xi$ -ols and eight  $5\xi$ -androstan-3 $\xi$ ,17 $\xi$ -diols (see Figure 5) using a reversed-geometry, double-focusing instrument. Under  $\text{CH}_4/\text{CI}$  conditions, the spectra of the diols are dominated by  $[\text{M}+\text{H}-\text{H}_2\text{O}]^+$  and  $[\text{M}+\text{H}-2\text{H}_2\text{O}]^+$  ions. The abundance ratio of these two species is greatly dependent upon the stereochemistry at C(17); the value of  $[\text{M}+\text{H}-2\text{H}_2\text{O}]^+ / [\text{M}+\text{H}-\text{H}_2\text{O}]^+$  is much larger for the 17 $\alpha$ -epimers. Similar behavior is observed under  $\text{NH}_3/\text{CI}$  conditions. The authors attribute the higher abundance of  $[\text{M}+\text{H}-2\text{H}_2\text{O}]^+$  ions in the 17 $\alpha$ -series to a closer proximity of the axial hydroxyl group to other ring D hydrogen atoms as compared to its equatorial epimer. A second stereochemical effect is observed in the mass-analyzed ion kinetic energy (MIKE) spectra of the  $[\text{M}+\text{NH}_4]^+$  ions formed from the diols under  $\text{NH}_3/\text{CI}$  conditions. The competitive losses of  $\text{H}_2\text{O}$  and  $\text{NH}_3$ , as monitored by the ratio  $[\text{M}+\text{NH}_4-\text{H}_2\text{O}]^+ / [\text{M}+\text{NH}_4-\text{NH}_3]^+$ , are highly dependent upon the configuration at C(17), with dehydration the major process in the 17 $\alpha$ -series. A slight hindrance of the  $\alpha$ -face is believed responsible for the reaction preference. In contrast, the 3-keto-17-hydroxysteroids appear insensitive to the configuration at C(17) in their methane and ammonia CI spectra. Under  $\text{OH}^-/\text{NCI}$  conditions, however, the loss of water is once again favored in the 17 $\alpha$ -series (yielding  $[\text{M}-\text{H}-\text{H}_2\text{O}]^-$  ions). Fragmentation trends in terms of the stereochemistry at C(3) and C(5) could not be unequivocally established for the compounds examined.

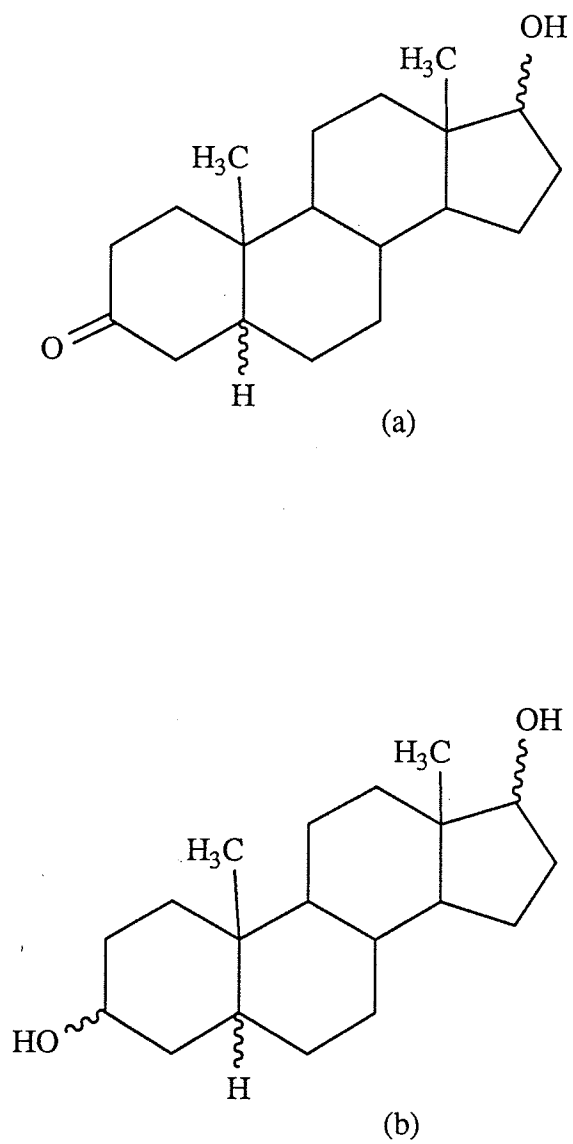


**Figure 5.** Isomers of (a) 5 $\xi$ -androstane-3-one-17 $\xi$ -ols and (b) 5 $\xi$ -androstane-3 $\xi$ ,17 $\xi$ -diols (22).

To this point, the body of evidence presented for C(17) epimeric steroidal alcohols suggests that the rates of certain fragmentation processes, in particular those involving the loss of water from the molecular ion (or  $[\dot{M}+H]^+$  ion), are dependent upon the stereochemistry at C(17). In sharp contrast to these reports, no general correlation could be established between the  $[M - H_2O]^+$  abundances and the configuration at C(17) for the steroids shown in Figure 1. The only relationship which was found concerned the increased abundances of several fragment ions in the mass spectra of the  $5\beta$  - versus  $5\alpha$  -ketone and alcohol isomers.

## B. EXPERIMENTAL

Positive-ion electron ionization mass spectra were recorded on an Hitachi RMU-6D single-focusing magnetic sector instrument at an ion accelerating voltage of 1800 V. The ionization chamber temperature was left to equilibrate without external heating (ca. 180 °C). Electron beam energies of 70, 20 and 12 eV (nominal) were used, and all samples were introduced via a direct-inlet probe.

Linked-scanning experiments were performed on a VG7070E-HF double-focusing mass spectrometer. Constant B/E scans of  $[M]^{+\bullet}$  and  $[M - 18]^{+\bullet}$ , constant  $B^2/E$  scans of  $[M - 33]^+$  and  $[M - 75]^+$ , and constant neutral loss scans of 15 and 18 were obtained for selected steroids (**1a/2a, 3d/4d**). Mass assignments in the parent ion scans (constant  $B^2/E$ ) were made with some uncertainty due to the inherent broadening of peaks by kinetic energy release. The daughter ion and mass loss scans were of greater interpretive use. Collision-induced dissociation (CID) was implemented to increase the abundance of metastable ions; helium gas was introduced into a collision cell located in the first field-free region (FFR) of the spectrometer. The pressure in the collision cell was adjusted so that approximately 50% attenuation of the molecular ion beam was achieved.

The synthesis and proton NMR spectra of the steroids have been described elsewhere (23).

### C. RESULTS AND DISCUSSION

The mass spectra of the 3-keto-17-hydroxysteroids (Table 1) and 3,17-dihydroxysteroids (Tables 2 and 3) are given in the form of peak heights relative to that of the molecular ion. This mode of tabulation permits easy comparison with results of the type cited above. Data are shown for electron beam energies of 70 eV (to which the 20 eV results are very similar) and 12 eV. Normalized monoisotopic plots of the major ions above  $m/z$  150 are presented in Figures 6-17 (70 eV data).

#### 1. 3-Keto-17-hydroxysteroids

The proposed fragmentation pathways and documented metastable transitions for these compounds are summarized in Scheme 1. Several of the more prominent ions resulting from ring D fragmentation processes ( $[M - 73]^+$ ,  $[M - 58]^+$  and  $[M - 57]^+$ ) are believed to arise according to the documented mechanisms (24-26) illustrated in Scheme 2. None of these fragment abundances seem sensitive to the configuration at C(17), but two of the peaks, namely  $[M - 57]^+$  and  $[M - 58]^+$ , appear suppressed in the  $5\alpha$ - versus the  $5\beta$ -steroid mass spectra (compare (1,2)a with (1,2)b). The mechanistic implications of such "long-range" conformational effects are not clear, but do imply that the avenues of decomposition available to the molecular ions of the isomers differ.

Of considerable diagnostic value is the observation that  $[M - 57]^+$  is the parent of  $[M - 75]^+$  through the loss of water, a decomposition

**Table 1.** Mass spectra of 17 $\xi$  -hydroxy-17 $\xi$  -methyl-5 $\xi$  -androstan-3-ones.  
Peak heights relative to [M]<sup>+</sup>=1.00.

m/z	Compound <b>1a</b>		Compound <b>1b</b>		Compound <b>2a</b>		Compound <b>2b</b>	
	70eV	12eV	70eV	12eV	70ev	12eV	70eV	12eV
304	1.00	1.00	1.00	1.00	1.00	1.00	1.00	1.00
289	0.80	0.86	0.39	0.41	0.74	0.76	0.29	0.32
286	0.54	0.64	0.19	0.63	0.67	0.66	0.57	0.65
271	0.57	0.99	0.58	0.47	1.18 <sup>a</sup>	0.83	1.17	1.05
253	0.07	0.05	0.33	0.19	0.04	0.02	0.38	0.22
247	1.10 <sup>a</sup>	0.99	2.78 <sup>a</sup>	3.13	0.87	0.83	2.36	2.62
246	0.53	0.50	2.31	2.78	0.46	0.44	2.00	2.38
244	0.33	0.32	2.58	3.00	0.32	0.24	2.38 <sup>a</sup>	2.70
231	0.84	0.56	0.72	0.56	0.80	0.48	0.64	0.46
229	0.29	0.16	2.50	0.56	0.29	0.14	2.17	1.43
215	0.29	0.15	0.97	0.53	0.29	0.12	0.86	0.46
163	0.68	0.37	0.72	0.25	0.79	0.34	0.67	0.24
	← 5 $\alpha$ →		← 5 $\beta$ →		← 5 $\alpha$ →		← 5 $\beta$ →	
	← 17 $\beta$ -o1 →				← 17 $\alpha$ -o1 →			

<sup>a</sup> Base peak at 70 eV.

**Table 2.** Mass spectra of  $17\alpha$ -methyl- $5\xi$ -androstane- $3\xi,17\beta$ -diols.  
Peak heights relative to  $[M]^{++}=1.00$ .

m/z	Compound 3a		Compound 3b		Compound 3c		Compound 3d	
	70eV	12eV	70eV	12eV	70eV	12eV	70eV	12eV
306	1.00	1.00	1.00 <sup>a</sup>	1.00	1.00	1.00	1.00	1.00
291	0.95	0.92	0.83	0.81	0.83	0.92	1.33	1.49
288	0.56	0.58	0.35	0.36	2.83	3.17	2.08 <sup>a</sup>	2.44
273	0.59	0.51	0.41	0.33	1.00	0.92	1.04	0.90
270	0.35	0.38	0.07	0.08	1.67	2.08	1.19	1.39
255	0.36	0.23	0.18	0.11	1.50	1.08	0.85	0.54
248	0.52	0.53	0.35	0.34	1.83	1.92	0.63	0.59
246	0.11	0.09	0.20	0.12	0.67	0.45	0.52	0.44
233	0.84	0.60	0.59	0.46	0.67	0.58	0.96	0.80
231	1.00	0.78	0.41	0.33	4.75	4.25	1.17	1.10
230	1.33 <sup>a</sup>	1.28	0.24	0.19	8.65 <sup>a</sup>	8.67	1.65	1.78
217	1.09	0.58	0.59	0.35	3.92	2.83	1.79	1.22
215	0.85	0.31	0.44	0.18	3.83	2.00	1.38	0.73
165	0.97	0.47	0.60	0.30	0.83	0.50	0.65	0.34
149	0.89	0.24	0.30	0.10	2.08	0.75	1.77	0.73

$\leftarrow 3\alpha \quad \leftarrow 3\beta \quad \leftarrow 3\alpha \quad \leftarrow 3\beta \rightarrow$   
 $\leftarrow 5\alpha \quad \leftarrow 5\beta \rightarrow$

<sup>a</sup> Base peak at 70 eV.



**Table 3.** Mass spectra of  $17\beta$ -methyl- $5\xi$ -androstane- $3\xi$ ,  $17\alpha$ -diols.  
Peak heights relative to  $[M]^+ = 1.00$ .

m/z	Compound 4a		Compound 4b		Compound 4c		Compound 4d	
	70eV	12eV	70eV	12eV	70eV	12eV	70eV	12eV
306	1.00	1.00	1.00 <sup>a</sup>	1.00	1.00	1.00	1.00	1.00
291	1.11	1.11	0.76	0.74	0.83	1.00	1.22	1.31
288	0.78	0.80	0.39	0.39	3.08	3.46	2.17 <sup>a</sup>	2.38
273	1.59 <sup>a</sup>	1.27	0.60	0.53	2.17	2.00	1.59	1.36
270	0.41	0.41	0.07	0.08	2.17	2.23	1.13	1.29
255	0.75	0.37	0.23	0.13	2.50	1.38	1.07	0.62
248	0.59	0.53	0.32	0.31	1.98	1.97	0.54	0.48
246	0.08	0.04	0.17	0.10	0.67	0.46	0.39	0.33
233	0.94	0.64	0.53	0.42	0.83	0.54	0.85	0.64
231	1.14	0.81	0.42	0.34	4.83	3.85	1.11	0.86
230	1.51	1.43	0.20	0.16	8.33 <sup>a</sup>	7.69	1.57	1.45
217	1.22	0.63	0.54	0.34	4.17	2.92	1.54	0.93
215	0.92	0.27	0.42	0.17	4.17	1.77	1.17	0.55
165	1.06	0.51	0.47	0.27	0.83	0.46	0.46	0.29
149	0.83	0.21	0.27	0.09	2.25	0.69	1.39	0.55
	← 3 $\alpha$ →		← 3 $\beta$ →		← 3 $\alpha$ →		← 3 $\beta$ →	
	← 5 $\alpha$ →				← 5 $\beta$ →			

<sup>a</sup> Base peak at 70 eV.

**Figure 6.**

Normalized 70 eV-EI mass spectrum of  
17 $\beta$ -hydroxy-17 $\alpha$ -methyl-5 $\alpha$ -androstane-3-one

STEROID 1A 70EV.

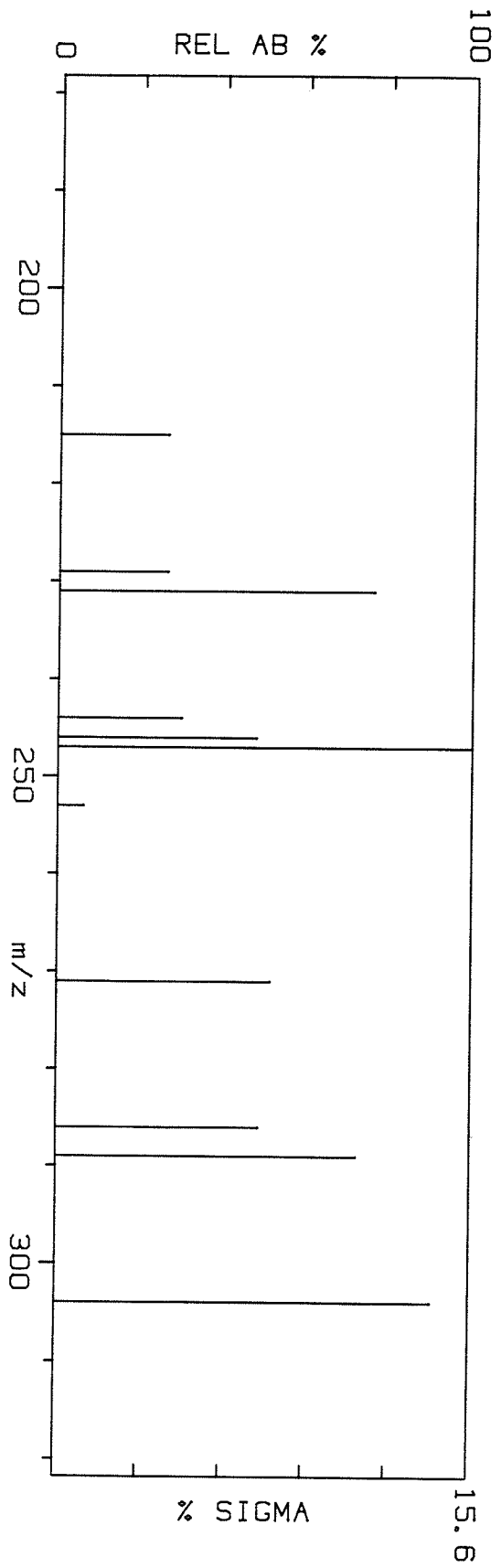
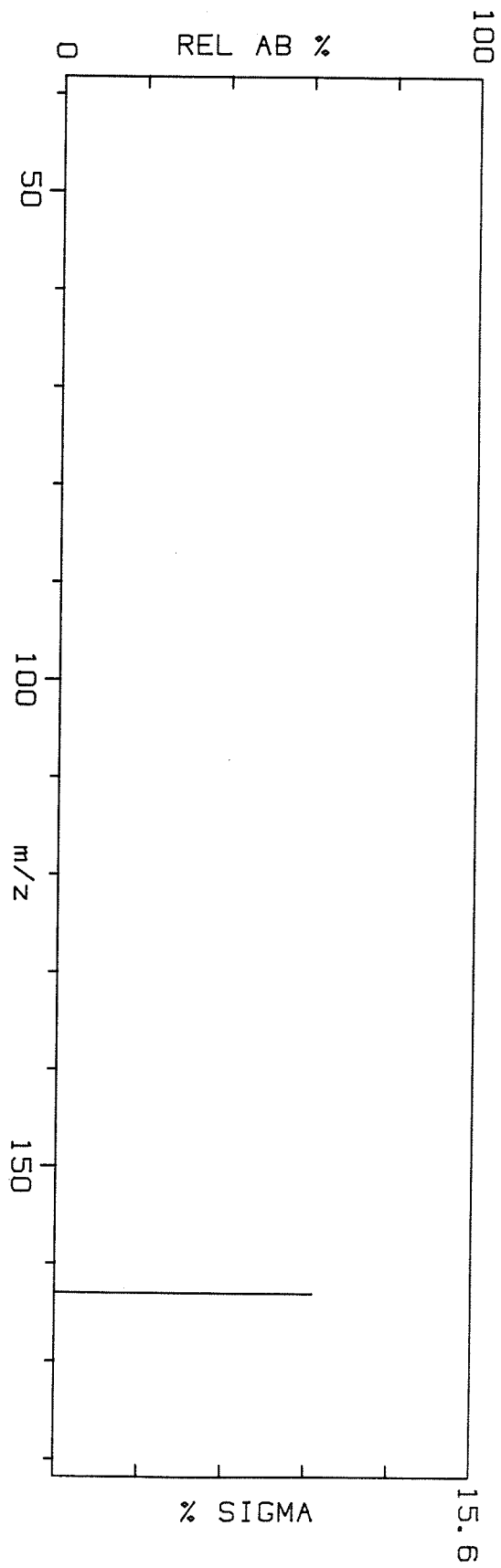


**Figure 7.**

Normalized 70 eV-EI mass spectrum of  
 $17\beta$ -hydroxy- $17\alpha$ -methyl- $5\beta$ -androstane-3-one

STEROID 1B 70EV.

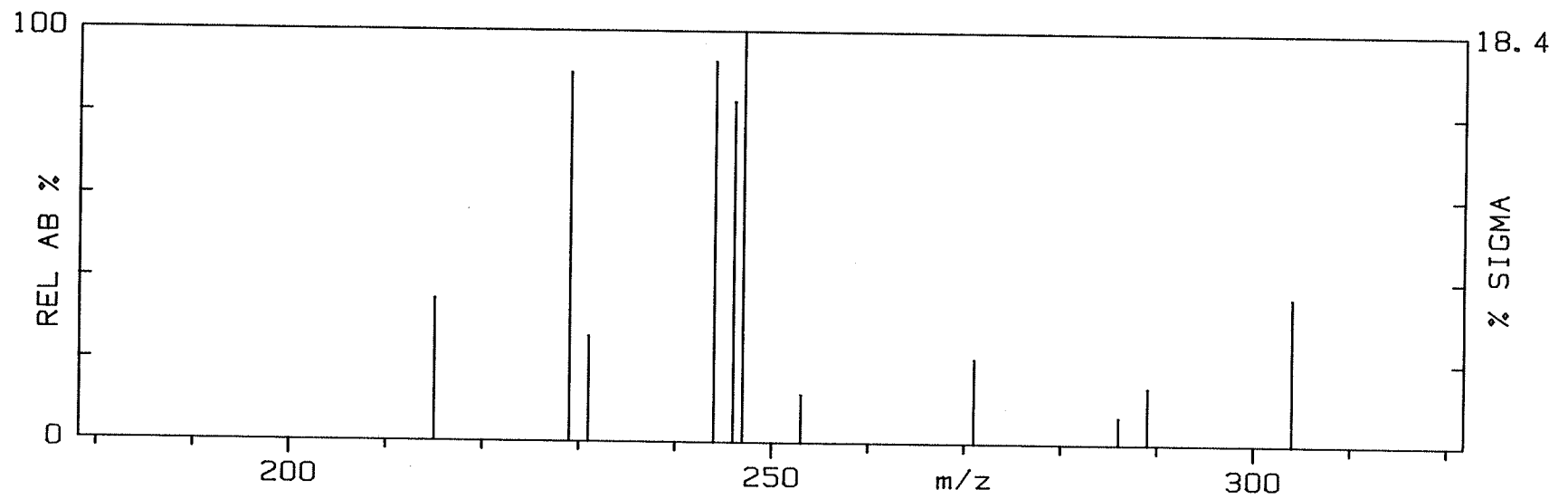
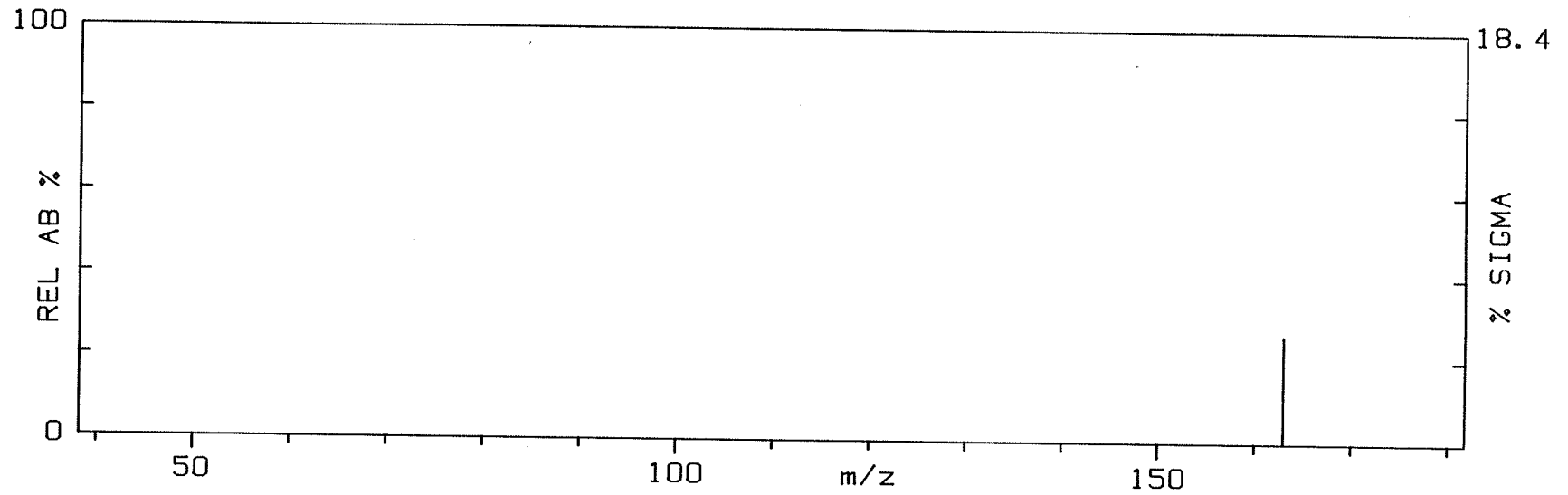


**Figure 8.**

Normalized 70 eV-EI mass spectrum of  
 $17\alpha$ -hydroxy- $17\beta$ -methyl- $5\alpha$ -androstane-3-one

STEROID 2A 70EV.

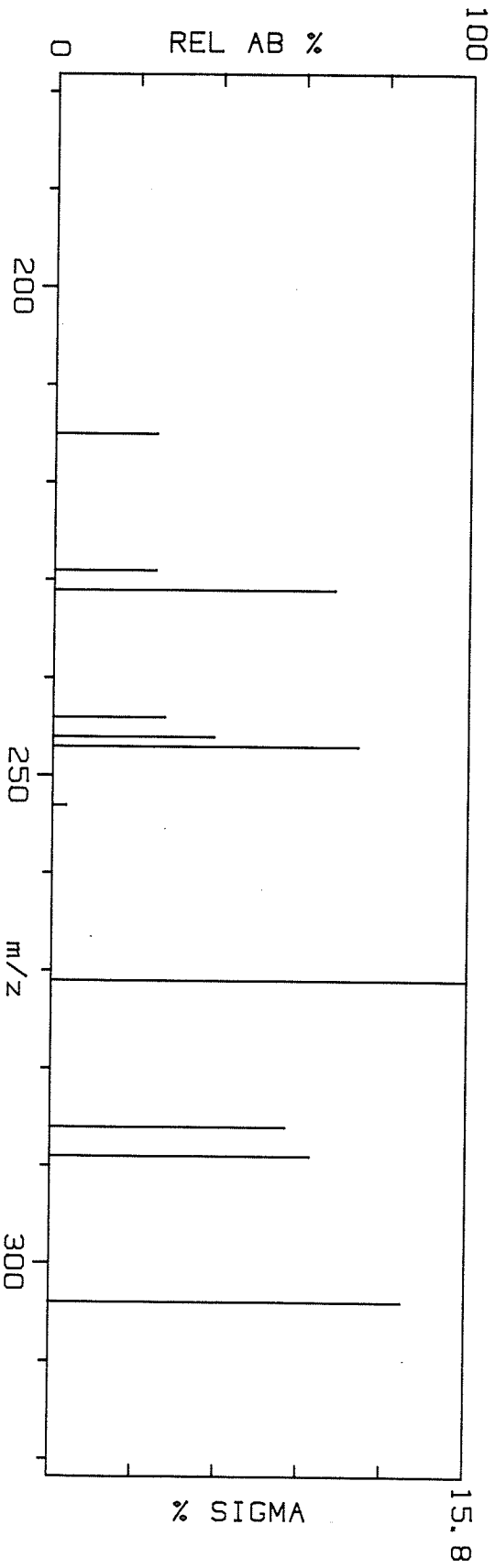
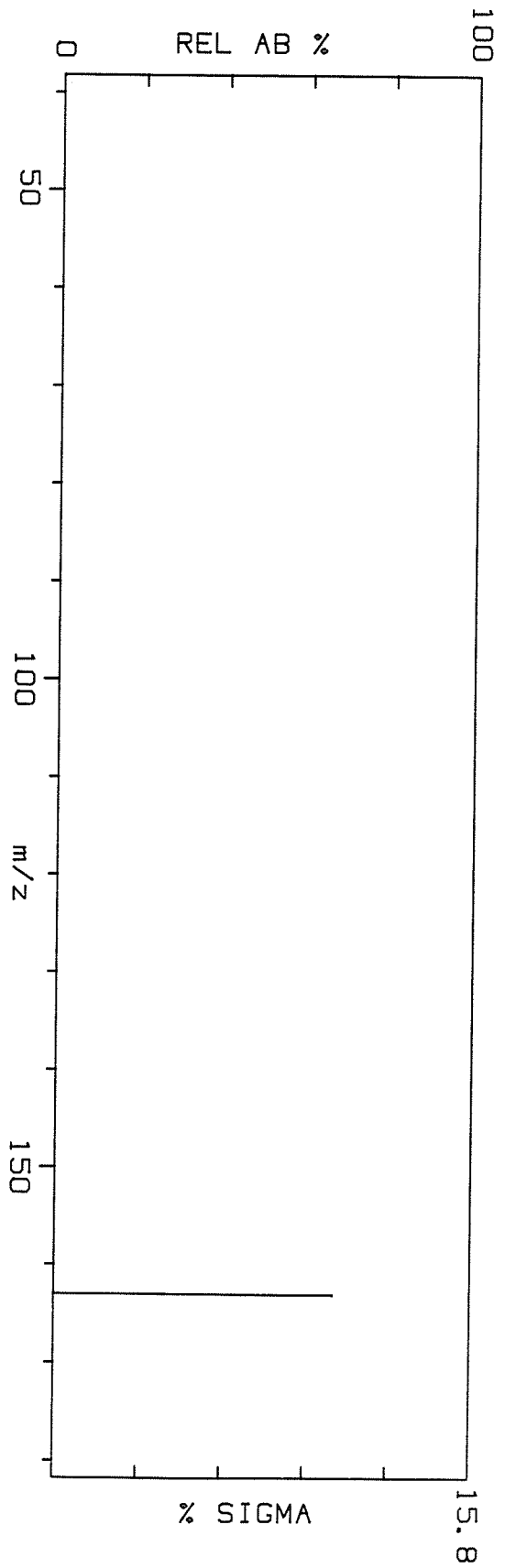


**Figure 9.**

Normalized 70 eV-EI mass spectrum of  
17 $\alpha$ -hydroxy-17 $\beta$ -methyl-5 $\beta$ -androsterone-3-one



STEROID 2B 70EV.

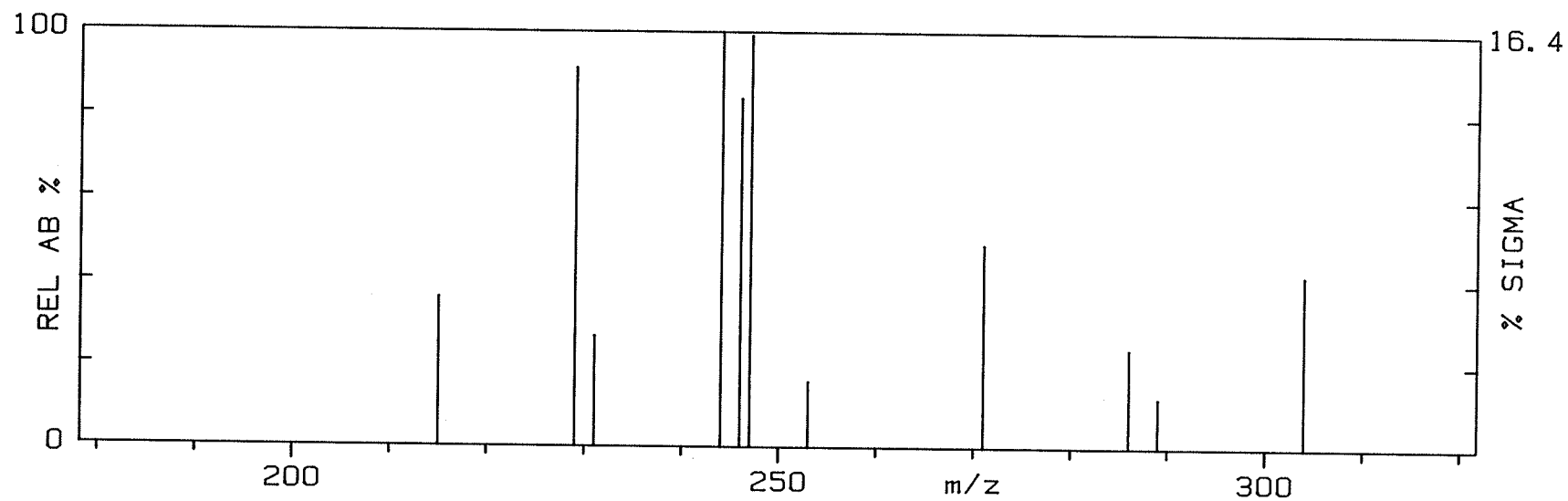
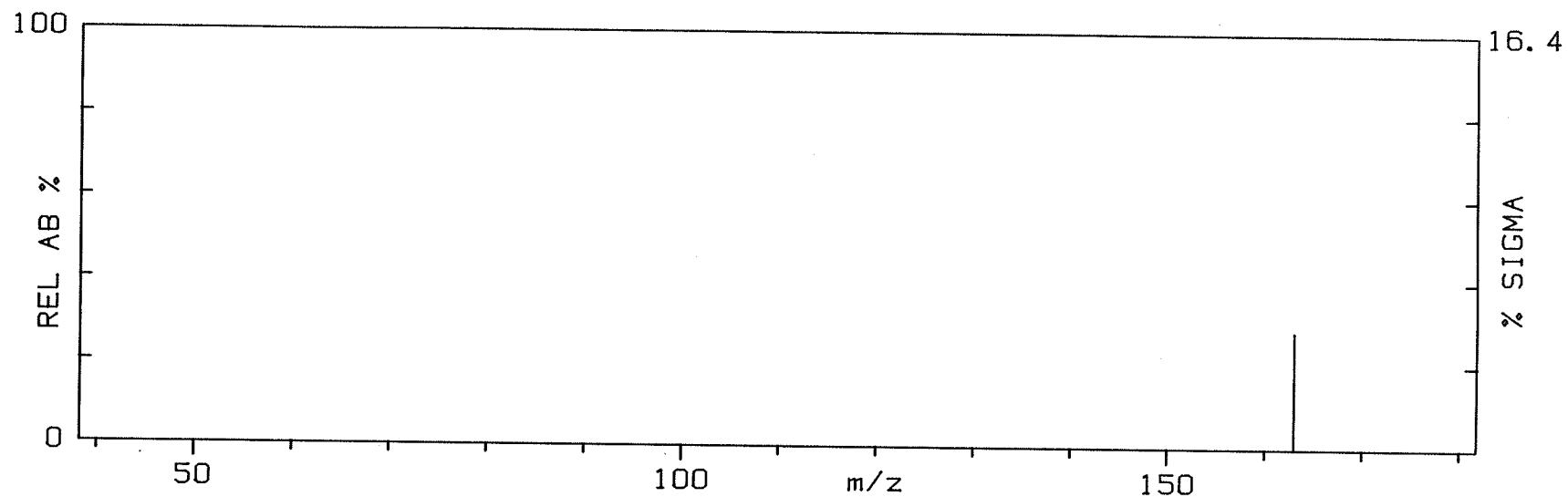


Figure 10.

Normalized 70 eV-EI mass spectrum of  
17 $\alpha$ -methyl-5 $\alpha$ -androstane-3 $\alpha$ ,17 $\beta$ -diol

STEROID 3A 70EV.

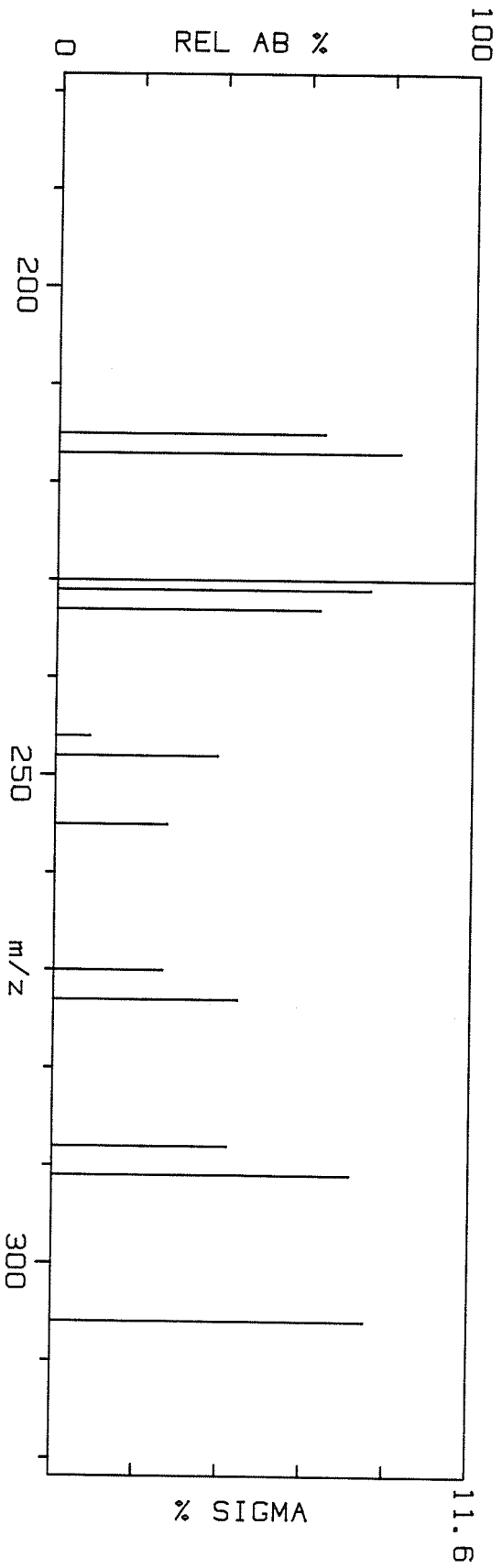
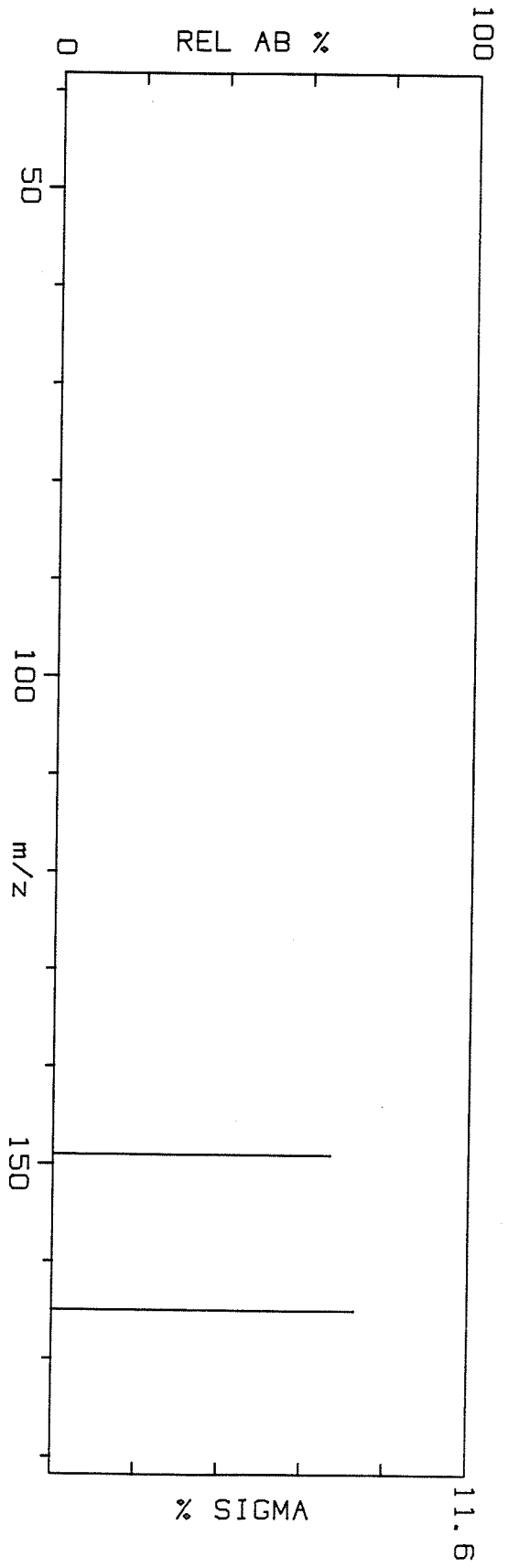
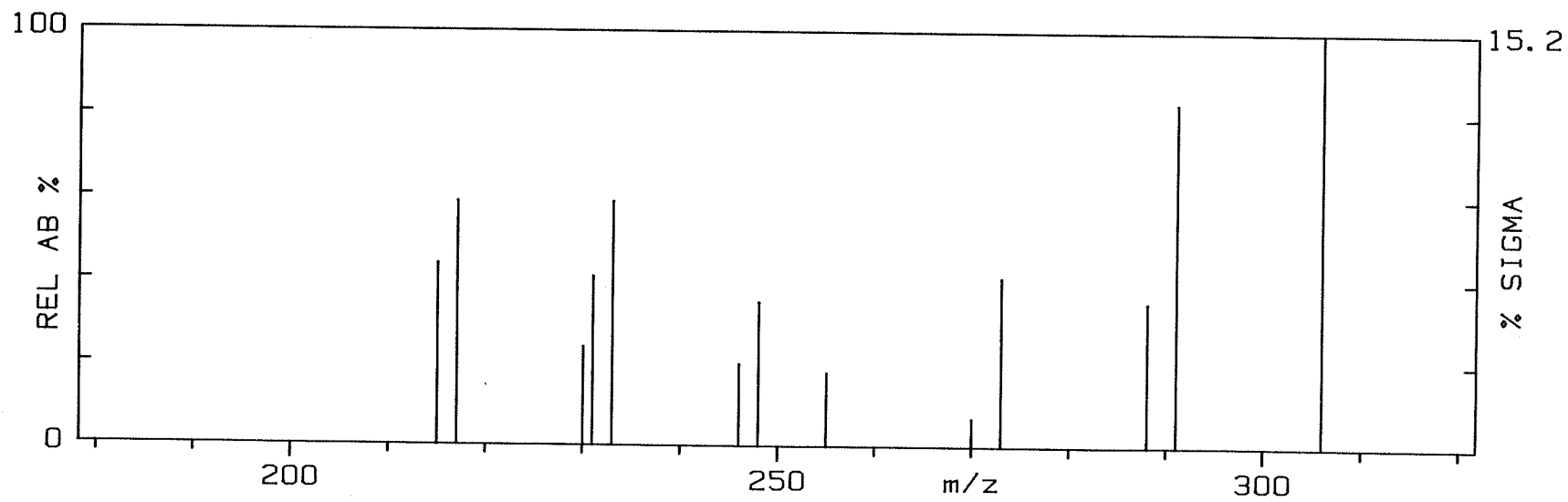
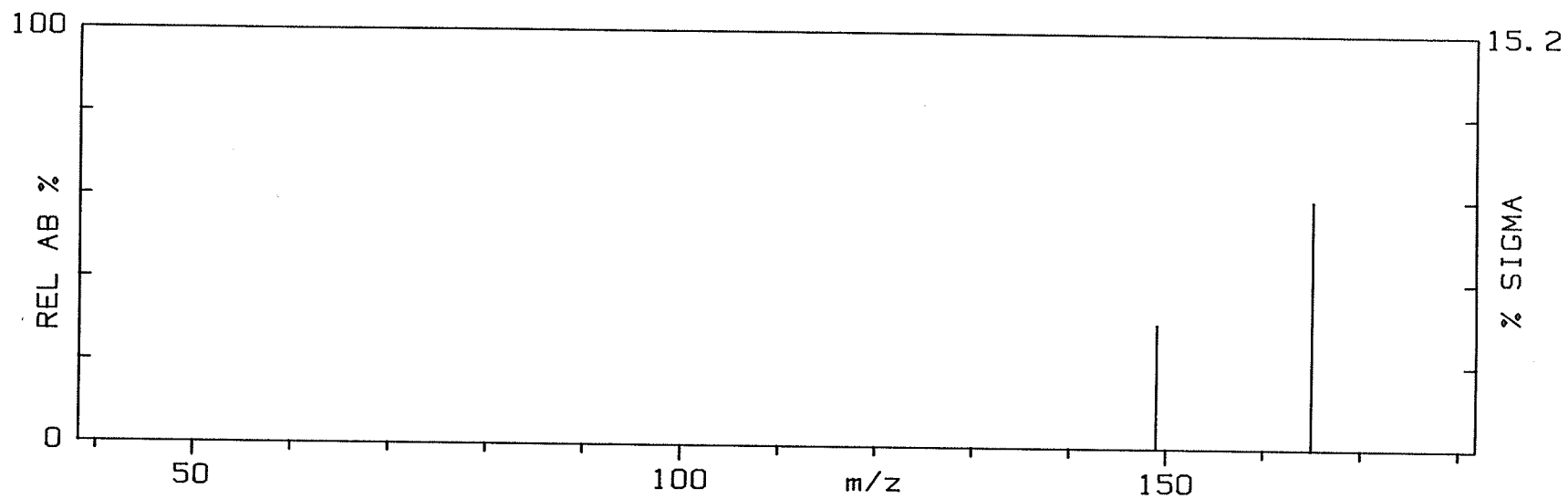


Figure 11.

Normalized 70 eV-EI mass spectrum of  
17 $\alpha$ -methyl-5 $\alpha$ -androstane-3 $\beta$ ,17 $\beta$ -diol

STEROID 3B 70EV.



**Figure 12.**

Normalized 70 eV-EI mass spectrum of  
17 $\alpha$ -methyl-5 $\beta$ -androstane-3 $\alpha$ ,17 $\beta$ -diol

STEROID 3C 70EV.

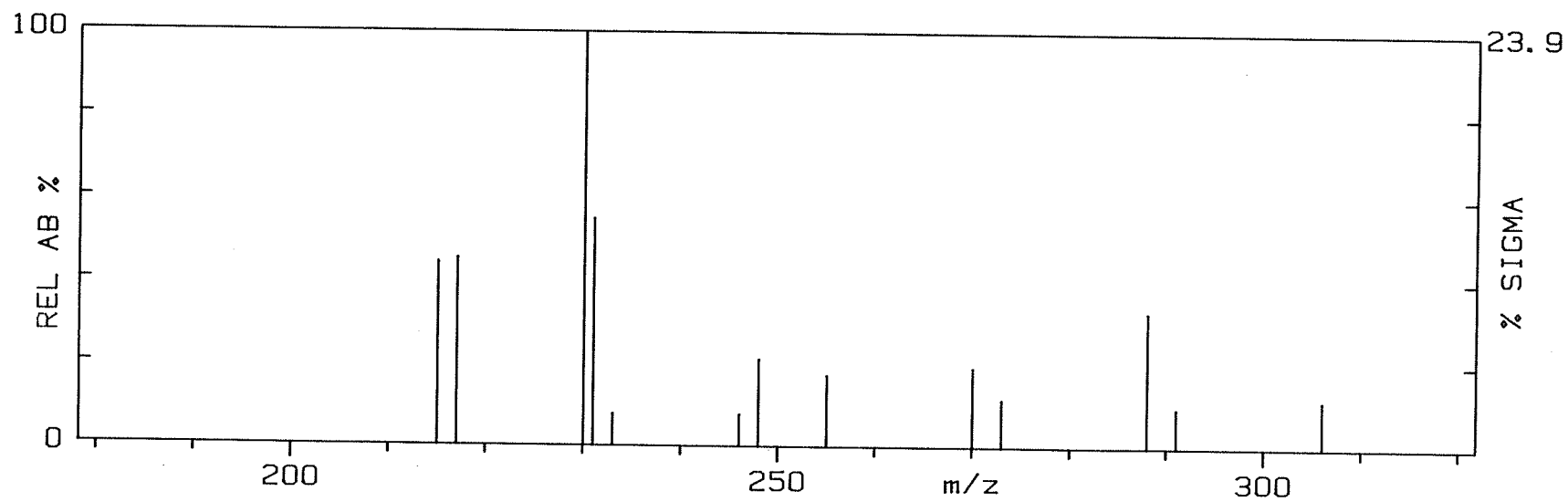
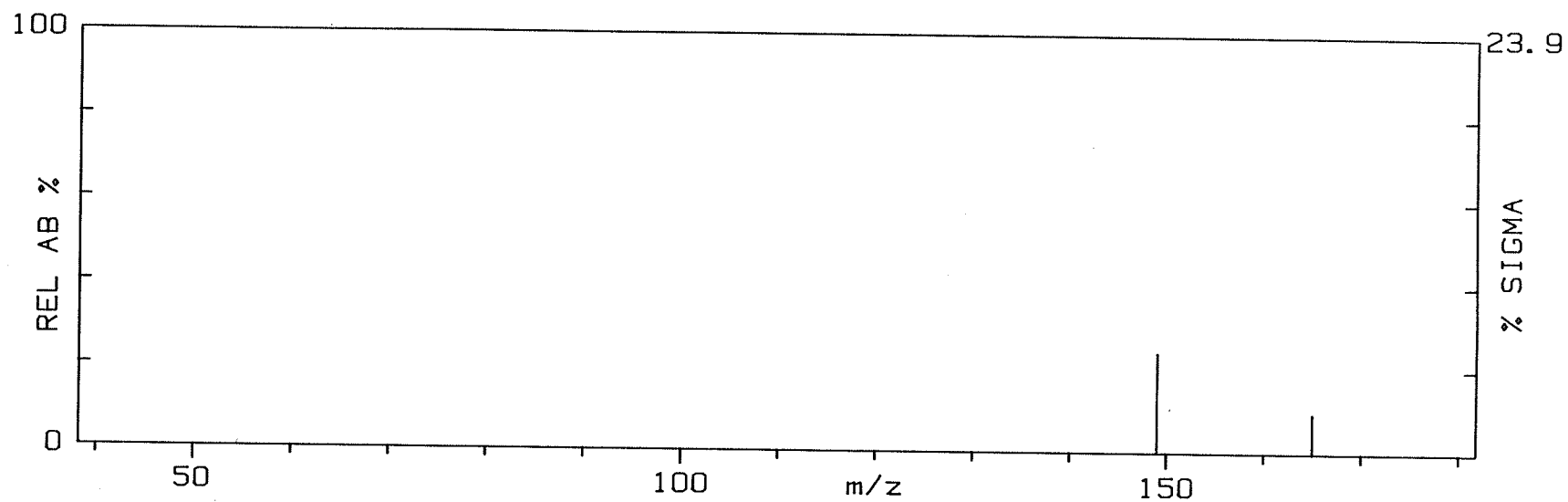


**Figure 13.**

Normalized 70 eV-EI mass spectrum of  
17 $\alpha$ -methyl-5 $\beta$ -androstane-3 $\beta$ ,17 $\beta$ -diol



STEROID 3D 70EV.

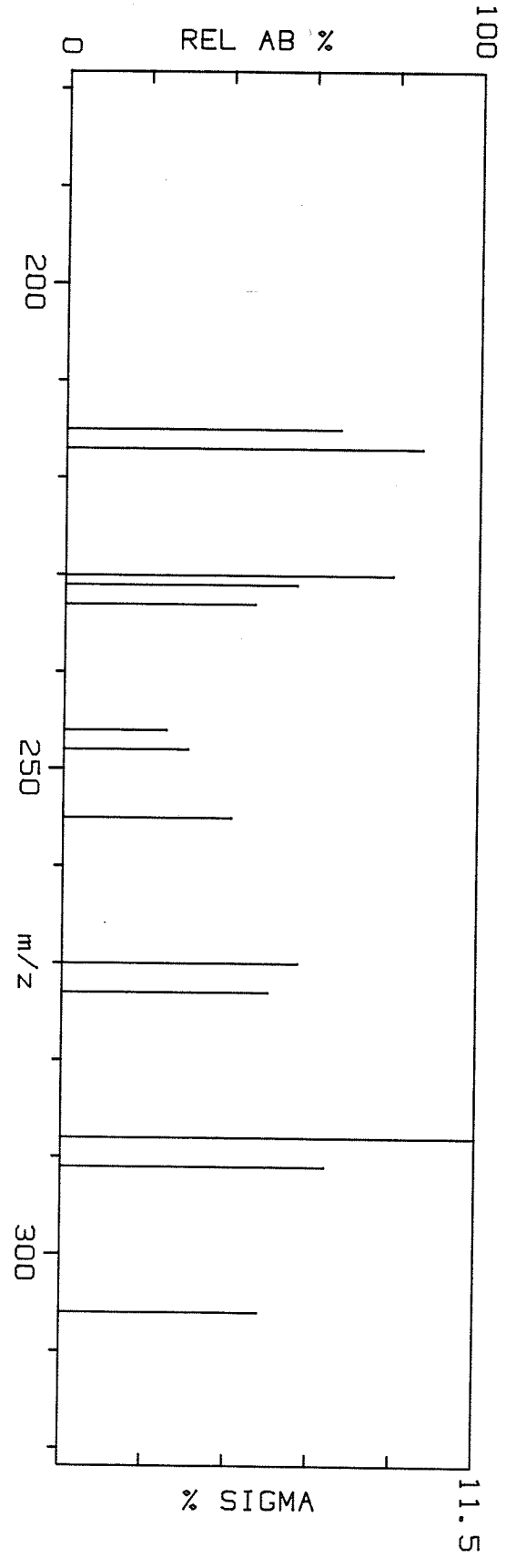
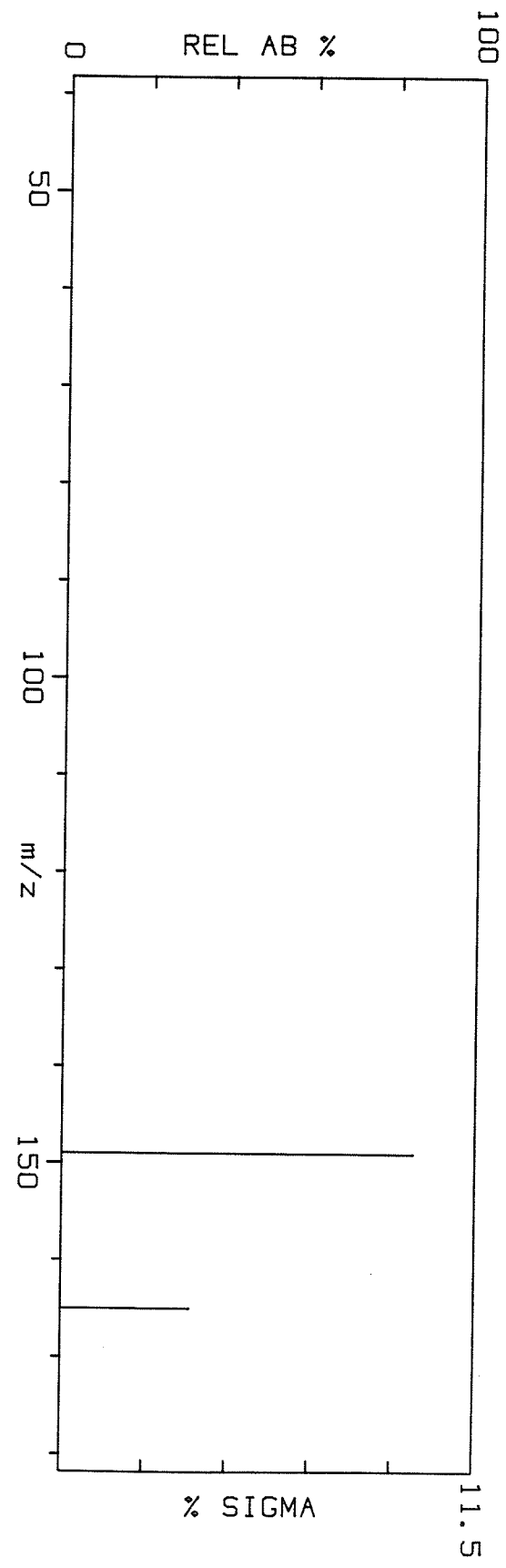


**Figure 14.**

Normalized 70 eV-EI mass spectrum of  
 $17\beta$ -methyl- $5\alpha$ -androstane- $3\alpha$ , $17\alpha$ -diol

STEROID 4A 70EV.

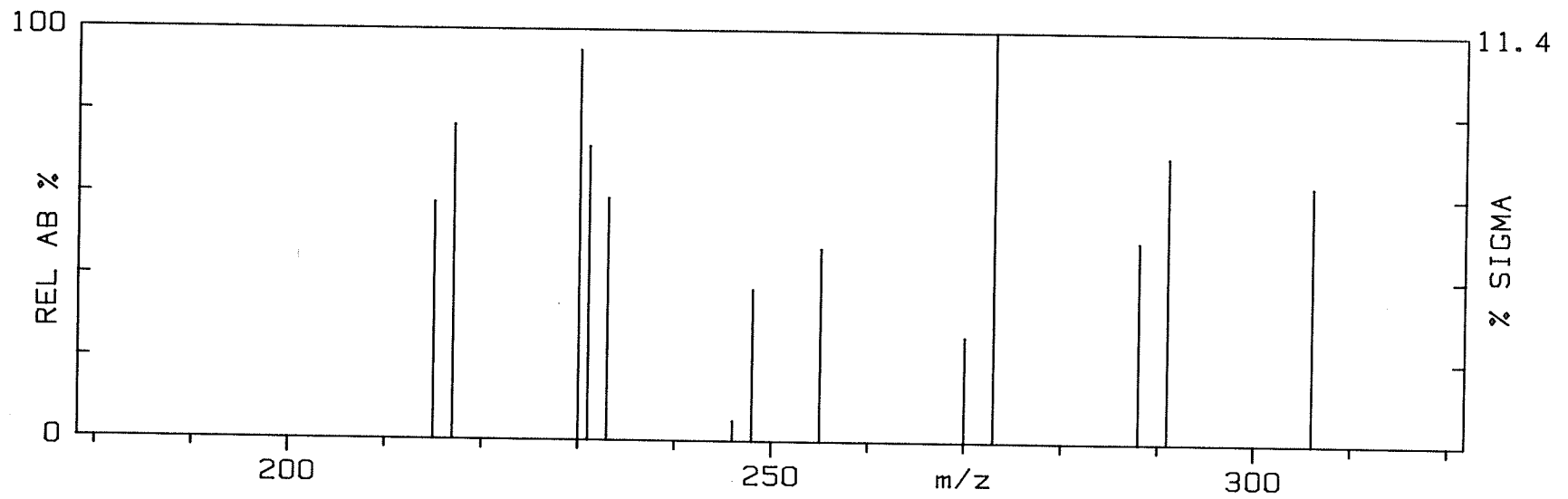
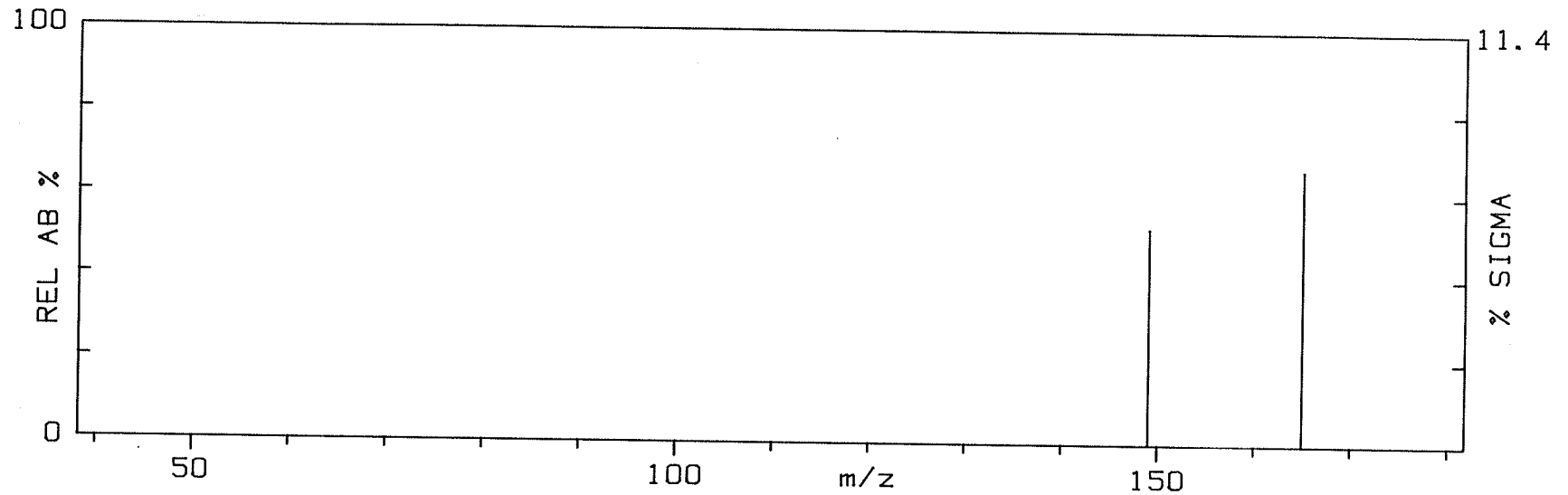
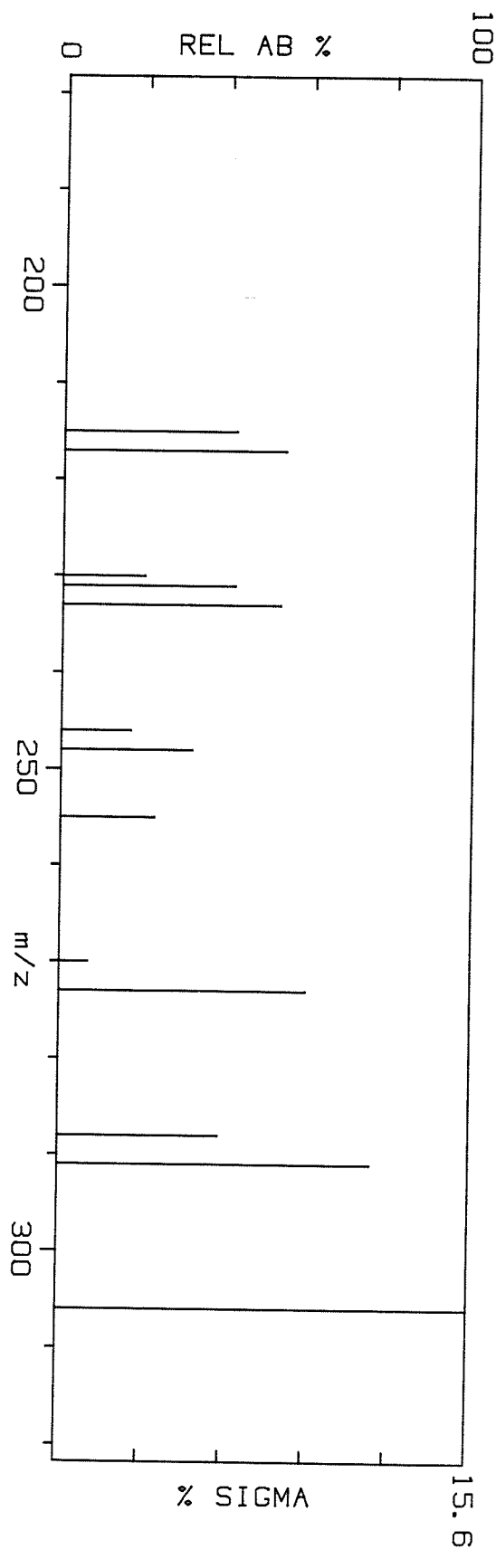
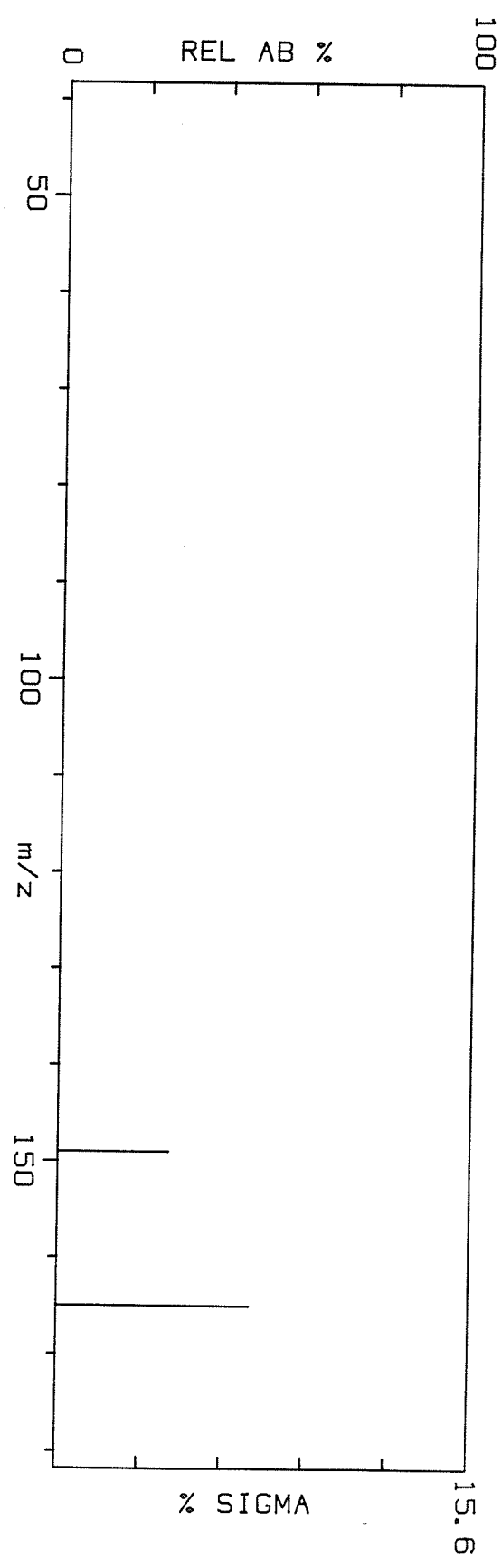


Figure 15.

Normalized 70 eV-EI mass spectrum of  
17 $\beta$ -methyl-5 $\alpha$ -androstane-3 $\beta$ ,17 $\alpha$ -diol

STEROID 4B 70EV.



**Figure 16.**

Normalized 70 eV-EI mass spectrum of  
17 $\beta$ -methyl-5 $\beta$ -androsterane-3 $\alpha$ ,17 $\alpha$ -diol

STEROID 4C 70EV.

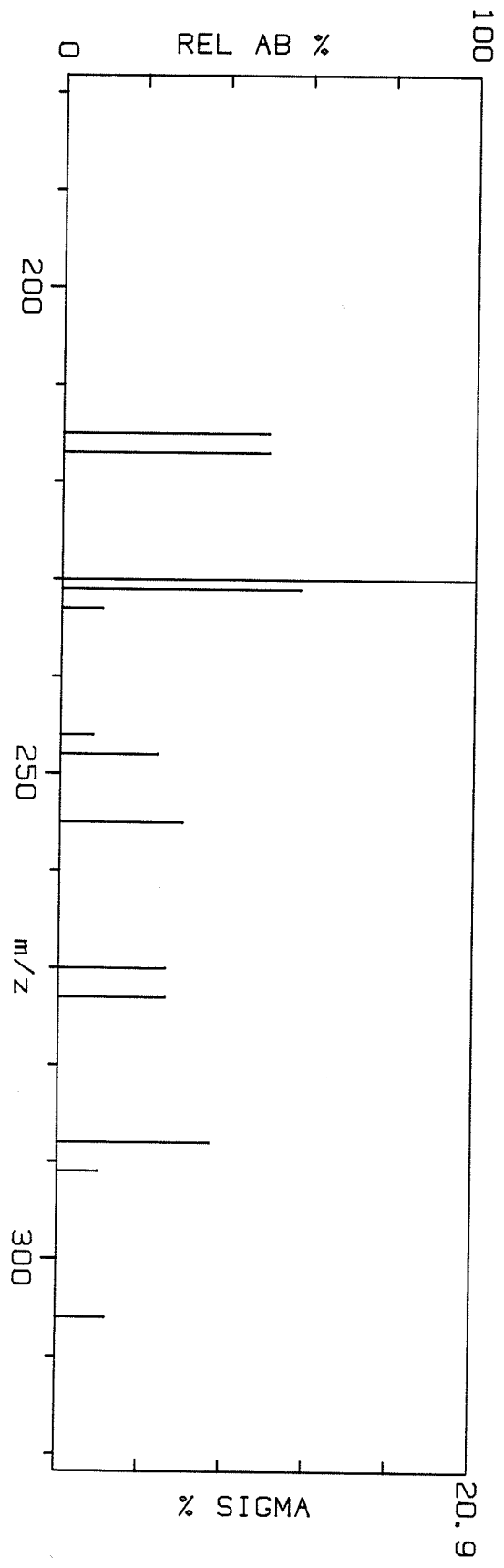
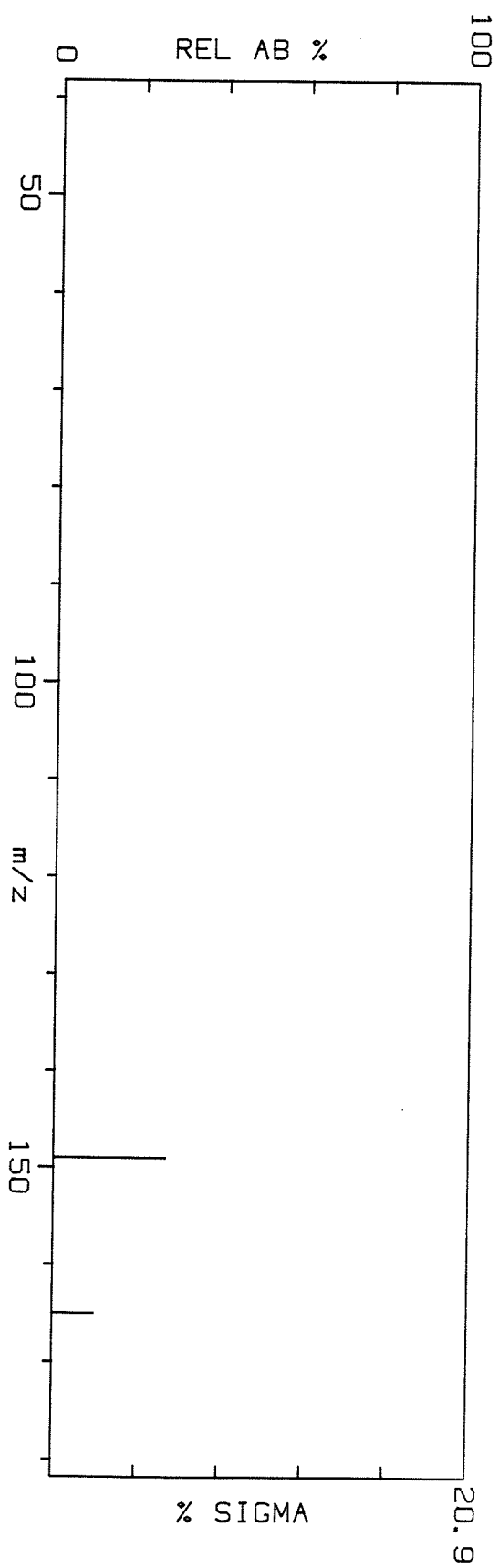
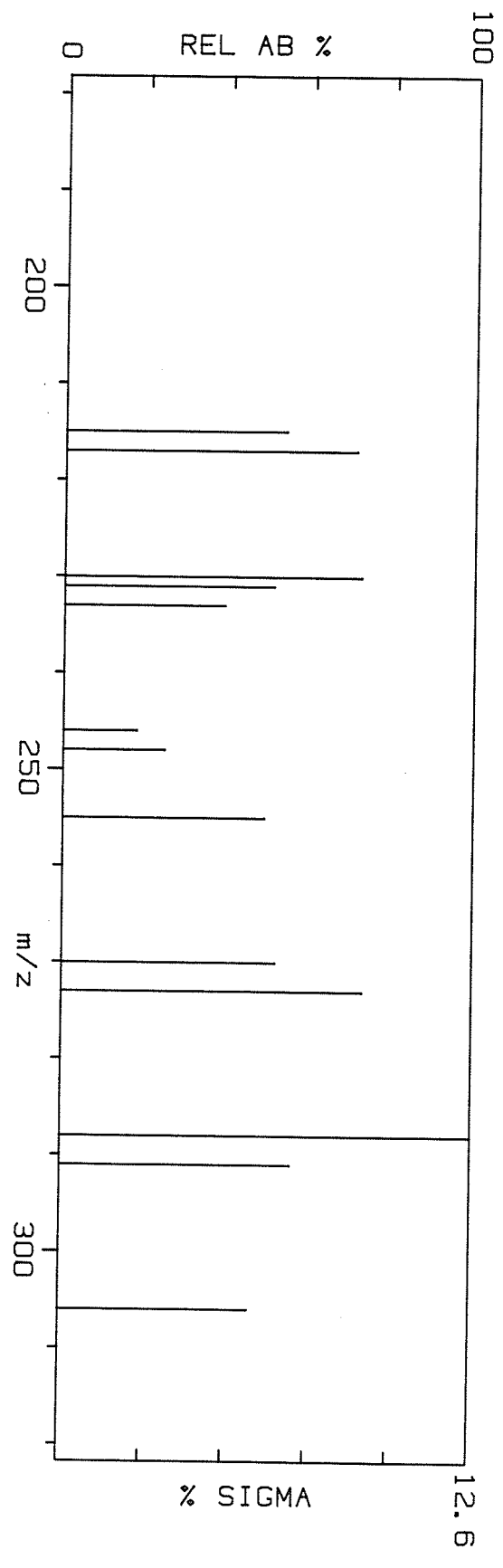
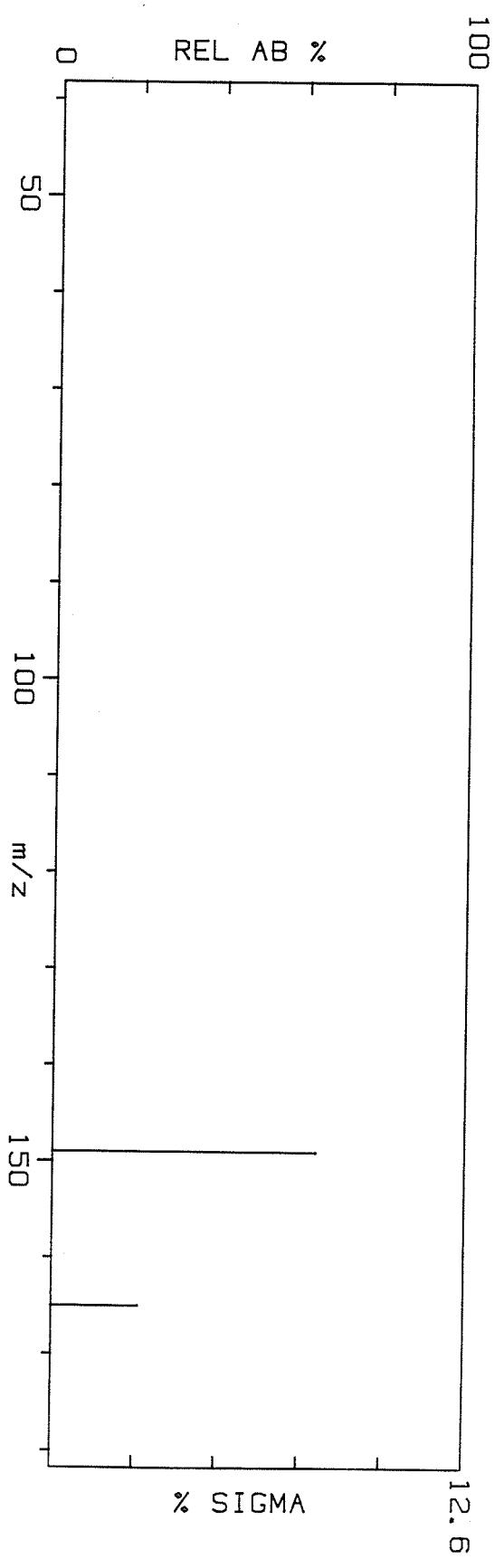


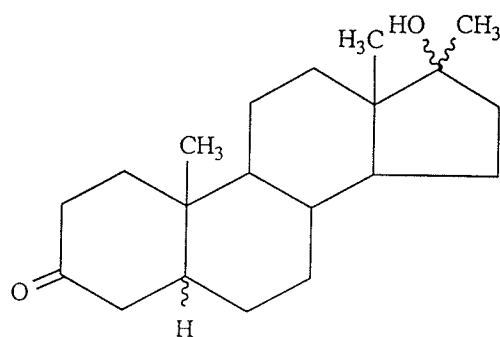
**Figure 17.**

Normalized 70 eV-EI mass spectrum of  
 $17\beta$ -methyl- $5\beta$ -androstane- $3\beta$ , $17\alpha$ -diol



STEROID 40 70EV.

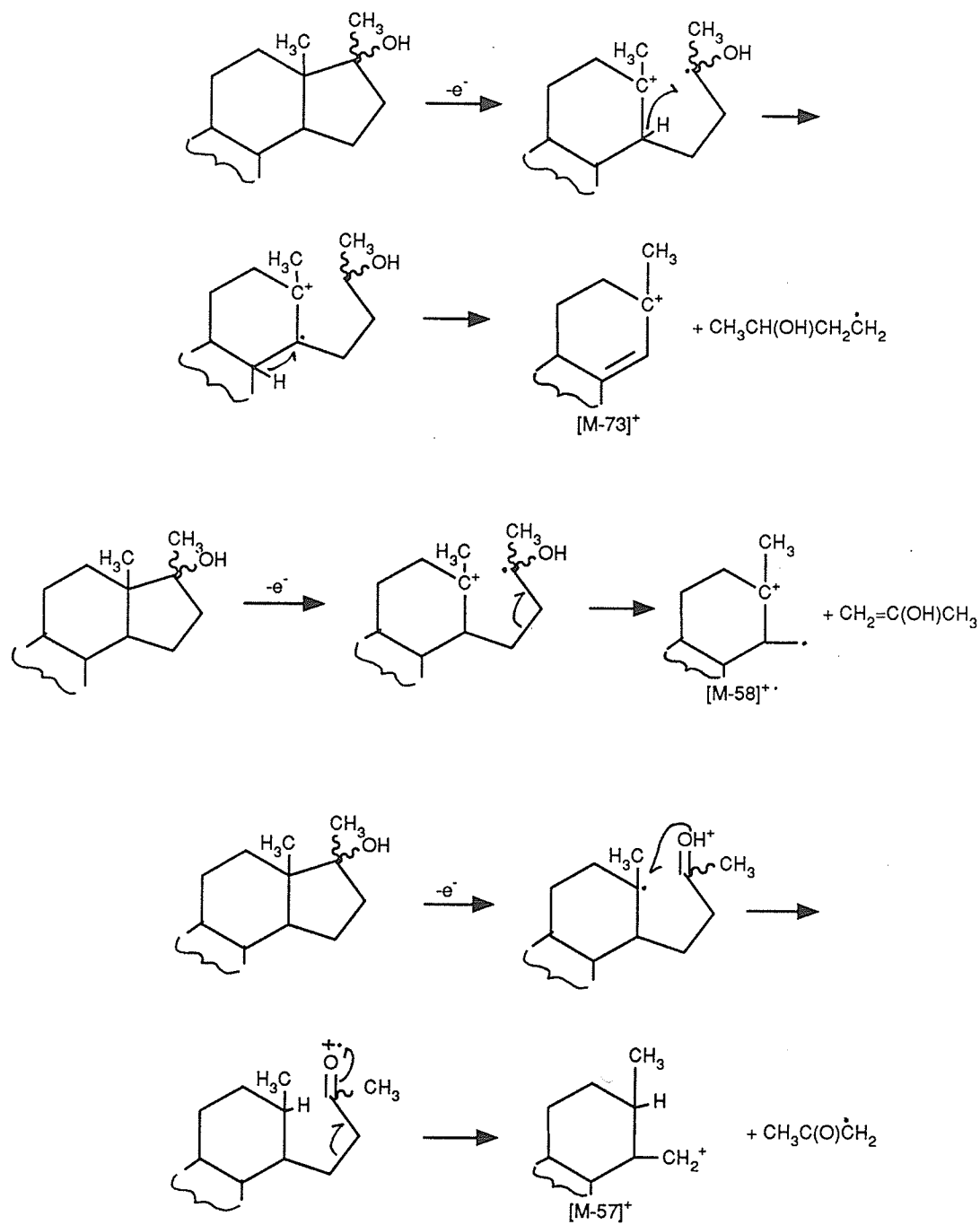




<u>m/z</u>	<u>Ion</u>
304	[M] <sup>+</sup>
289	[M-15] <sup>+</sup>
286	[M-18] <sup>+</sup>
271	[M-33] <sup>+</sup>
253	[M-51] <sup>+</sup>
247	[M-57] <sup>+</sup>
246	[M-58] <sup>+</sup>
244	[M-60] <sup>+</sup>
231	[M-73] <sup>+</sup>
229	[M-75] <sup>+</sup>
215	[M-89] <sup>+</sup>
163	[M-141] <sup>+</sup>

—▶ process confirmed by the observation of a metastable transition in at least one of the complexes.

**Scheme 1.** Suggested fragmentation pathways for the 3-keto-17-hydroxysteroids.



**Scheme 2.** Fragmentation mechanisms for the formation of ions  $[M-73]^+$ ,  $[M-58]^+$  and  $[M-57]^+$  (24-26).

supported by metastable evidence in the spectra of all four ketones. This loss occurs much more readily from cis A/B fused  $5\beta$ -steroids than from the more stable (less strained) trans A/B fused  $5\alpha$ -steroids. No preference is shown between C(17) epimeric pairs **1a/2a** or **1b/2b**, which is not unexpected since their stereochemical integrities have already been lost. The source of the two hydrogens transferring to the ketonic oxygen is not known, but the reaction probably occurs via ring opening. Without ring opening, O-H bond formation is unlikely, since molecular models indicate that the closest O to H approach in the intact skeleton is about 2.5 Å (between O and H(9) in the  $5\beta$ -isomer), which is considerably larger than normal O-H bonding distances (0.96 Å in H<sub>2</sub>O). Additional support for this view can be seen in the 12 eV data, where the relative intensity of the  $[M - 75]^+$  peak decreases significantly compared to most of the other high mass peaks in these spectra (see Table 1), indicating a relatively high activation energy for the process.

The  $[M - H_2O]^+ / [M]^+$  ratios shown in Table 1 (where water loss is presumably from ring D) do not distinguish between C(17) epimeric pairs, despite the implications of earlier reports (15-19). The only major structural differences between the 17-alkylestradiols/17-alkyl-19-nortestosterones studied by Zaretskii et al (18,19) and the 3-keto-17-hydroxysteroids (**1a,b;2a,b**) of this study are confined to the vicinity of ring A (specifically, the C(10) methyl group, C(3) substituent and/or the degree of ring A unsaturation; compare Figures 1 and 3). Compare as well the NCI results of Prome (22) and Beloeil (21): while Prome reports that water loss from the  $[M - H]^-$  ions of

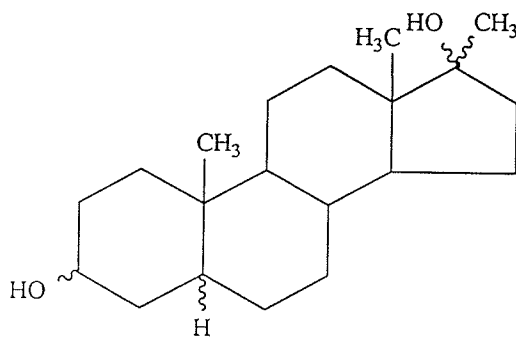
androstane-3-one-17 $\xi$ -ols is markedly dependent upon the stereochemistry at position 17, Beloeil observes no difference in the dehydration of  $[M - H]^-$  ions for androstane-17 $\xi$ -ols, which lack a C(3) substituent. In the end, one can only surmise that the functional group character of ring A in some way influences the rate of water loss from C(17). The nature of the interaction is evidently quite complex; it may involve the transfer of conformational modifications from ring A to ring D (22).

The only influence attributable to the stereochemistry of the C(17) position is the approximate doubling of the  $[M - H_2O - CH_3]^+ / [M]^+$  ratio for a 17 $\alpha$ -compared to a 17 $\beta$ -OH isomer. Unfortunately, the enhancement is too small to be of significant diagnostic value. Metastable evidence indicates that  $[M - 33]^+$  arises from the molecular ion in two ways: either by successive abstractions of  $H_2O$  and a Me $\cdot$  radical, or as a result of elimination of these groups in the opposite sequence (see Scheme 1). The competition between these two fragmentation pathways may partially conceal the stereochemical effects at C(17). Evidence of this type of behavior has been provided by Zaretskii (18,19) in the mass spectra of 17-ethyltestosterones.  $[M - 33]^+$  is also the precursor of  $[M - 51]^+$  (via water loss; confirmed through linked-scanning) with the latter ion undergoing a definite enhancement for 5 $\beta$ - over 5 $\alpha$ -steroids. The ketonic oxygen is necessarily lost in this step, in a decomposition which presumably parallels the formation of  $[M - 75]^+$  from  $[M - 57]^+$  described above.

Common ring A fragmentation products  $[M - 70]^{+\cdot}$ ,  $[M - 71]^+$  and  $[M - 72]^{+\cdot}$  are absent from the spectra of the steroidal ketones.  $[M - 70]^{+\cdot}$  is a characteristic fragment for 3-ketosteroids having a cis-fused A/B ring junction (24,27). The suppression of  $[M - 71]^+$  and  $[M - 72]^{+\cdot}$  is not surprising considering that they are only reported for 3-keto-5 $\alpha$ -steroids lacking a C(17) substituent (24,28).

## 2. 3,17-Dihydroxysteroids

The proposed fragmentation pathways and metastable transitions for the diols are shown in Scheme 3. Many of the observed fragmentations parallel those discussed for the ketones, thereby supporting suggested assignments (compare  $[M - 33]^+$ ,  $[M - 51]^+$ ,  $[M - 58]^{+\cdot}$  and  $[M - 73]^+$ ). However, the  $[M - 57]^+$  fragment, characteristic of 17-hydroxysteroids, is absent in the diol spectra. At the same time, the new fragments  $[M - 36]^{+\cdot}$ ,  $[M - 76]^{+\cdot}$  and  $[M - 91]^+$  are now prominent. Metastable peaks indicate that these ions are formed from  $[M - 18]^{+\cdot}$ ,  $[M - 58]^{+\cdot}$  and  $[M - 73]^+$ ; respectively, by loss of water. Linked-scanning confirms that  $[M - 18]^{+\cdot}$  is the precursor of both  $[M - 76]^{+\cdot}$  and  $[M - 91]^+$ .  $[M - 76]^{+\cdot}$  also eliminates a methyl radical to give  $[M - 91]^+$  as evidenced by a metastable transition.  $[M - 58]^{+\cdot}$  and  $[M - 73]^+$  arise from ring D decompositions (see Scheme 2), so the dehydration of these species must involve the -OH group from ring A (and another hydrogen of undetermined origin). As evidenced in the steroidal ketones, this process is highly sensitive to the stereochemistry of the A/B ring junction;  $[M - 76]^{+\cdot}$  and  $[M - 91]^+$  are



<u>m/z</u>	<u>Ion</u>
306	[M] <sup>+</sup>
291	[M-15] <sup>+</sup>
288	[M-18] <sup>+</sup>
273	[M-33] <sup>+</sup>
270	[M-36] <sup>+</sup>
255	[M-51] <sup>+</sup>
248	[M-58] <sup>+</sup>
246	[M-60] <sup>+</sup>
233	[M-73] <sup>+</sup>
231	[M-75] <sup>+</sup>
230	[M-76] <sup>+</sup>
217	[M-89] <sup>+</sup>
215	[M-91] <sup>+</sup>
165	[M-141] <sup>+</sup>

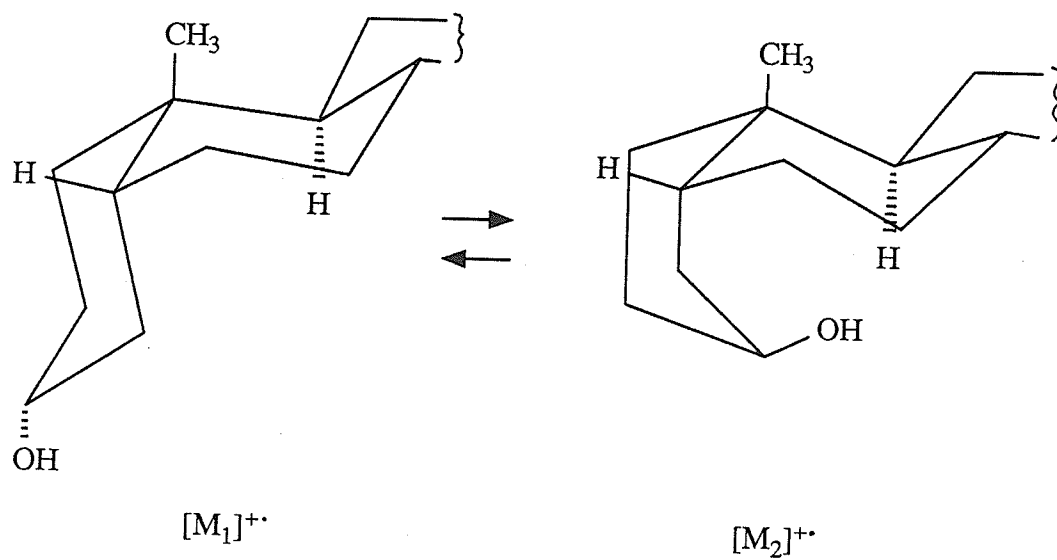
—▷ process confirmed by the observation of a metastable transition in at least one of the complexes.  
 —▶ unconfirmed but probable fragmentation.

**Scheme 3.** Suggested fragmentation pathways for the 3,17-diols.

greatly enhanced with respect to  $[M]^{+\cdot}$  in the spectra of  $5\beta$ -compared to  $5\alpha$ -steroids (compare (3,4)(c,d) with (3,4)(a,b)). Molecular models with the A-ring in the more stable chair conformation show a much shorter distance between C(3) and H(9) (the closest non-adjacent hydrogen) in the  $5\beta$ -epimer (29). There is a further enhancement in these ratios when the 3-OH is axial ( $\alpha$ ) as opposed to equatorial ( $\beta$ ). It is highly probable that in the case of the  $3\alpha$ -hydroxy- $5\beta$ -steroids (3c and 4c), the dehydration of the molecular ion is preceded by a chair-to-boat isomerization of ring A as shown in Scheme 4. This situation, which is not possible in  $5\alpha$ -steroids (trans A/B ring junction), reduces the C(3)-H(9) distance even more and increases the likelihood of interaction. In fact, models show that the C(9) tertiary hydrogen may be brought to within 0.4 Å of the 3-hydroxyl group in the boat conformation of ring A in  $5\beta$ -cholan- $3\alpha$ -ol (30). At such proximate distances, O-H bond formation can occur without the requirement of ring fission (thus lower activation energy). Deuterium labelling (31) has indeed established that hydrogen abstraction from C(9) occurs in the loss of  $H_2O$  from the molecular ion of  $5\beta$ -cholan- $3\alpha$ -ol (a different mechanism is assumed to operate in the respective  $3\beta$ -alcohols).

The  $[M - 75]^{+}/[M]^{+\cdot}$  and  $[M - 89]^{+}/[M]^{+\cdot}$  ratios exhibit the same trends as those just discussed. In addition to the metastable information given in Scheme 3, evidence garnered from the known fragmentations of the corresponding ketones would strongly suggest that  $[M - 75]^{+}$  is also formed by the loss of ( $H_2O+57$ ) from  $[M]^{+\cdot}$ . Since, as noted above, the  $[M - 57]^{+}$  fragment is insignificant in all diol





**Scheme 4.** Chair-to-boat isomerization of ring A in 3 $\alpha$ -hydroxy-5 $\beta$ -steroids.

spectra, dehydration of the molecular ion is presumed to occur more readily than loss of the other neutral fragment. Therefore, an alternative pathway to  $[M - 75]^+$  would be loss of  $H_2O$  from ring A of  $[M]^+$  (with its attendant stereochemical dependencies) followed by loss of part of ring D.

Interpretation of the  $[M - 18]^+ / [M]^+$ ,  $[M - 36]^+ / [M]^+$  and  $[M - 51]^+ / [M]^+$  ratios is complicated by the fact that the losses of water from rings A and D of  $[M]^+$  probably occur at competitive rates. In any event, a comparison of Tables 2 and 3 clearly reveals that there is little dependence of any of these ratios upon the orientation of the 17-hydroxyl group. All of these ratios are most strongly enhanced for the  $5\beta$  - vs  $5\alpha$  -steroids (compare (3,4)(c,d) with (3,4)(a,b)), with an additional smaller enhancement for  $3\alpha$  -hydroxy- vs  $3\beta$  -hydroxy-steroids (compare (3,4)(a,c) with (3,4)(b,d)).

#### D. SUMMARY

A definitive correlation between relative ion abundances and the stereochemistry at the A/B ring junction is established in the electron ionization mass spectra of the steroidal ketones and alcohols examined. The intensity ratios  $[M - 51]^+ / [M]^+$ ,  $[M - 75]^+ / [M]^+$  and  $[M - 89]^+ / [M]^+$  are greatly enhanced for  $5\beta$ - (cis A/B) compared to  $5\alpha$ - (trans A/B) steroids. As well, the  $[M - 18]^+ / [M]^+$ ,  $[M - 36]^+ / [M]^+$ ,  $[M - 76]^+ / [M]^+$  and  $[M - 91]^+ / [M]^+$  ratios for the 3,17-diols are much greater for  $5\beta$ - than for  $5\alpha$ -epimers. Elimination of  $H_2O$  is believed to occur at some stage in the formation of all fragment ions involved. Probably for this reason these ratios are further increased when a  $3\alpha$ -hydroxy group is present, particularly in a  $5\beta$ -steroid.

A general relationship between the dehydration of the molecular ion and the orientation of the -OH group at C(17) is not apparent from this study. Results suggest that C(17) elimination reactions may be influenced by the functional groups and conformation of ring A. Conformational effects are also observed in the ring D fragmentations of the 3-ketosteroids, where  $[M - 57]^+ / [M]^+$  and  $[M - 58]^+ / [M]^+$  ratios are significantly enhanced in the  $5\beta$ - versus  $5\alpha$ -epimers.

## CHAPTER II.

MASS SPECTRA OF  
FLUORINATED METAL  $\beta$ -DIKETONATES  
AND  
MONOTHIO- $\beta$ -DIKETONATES

## A. INTRODUCTION

Beginning with the pioneering work of Combes (32), Urbain (33) and Werner (34) near the turn of the century and continuing to the present day, the study of metal  $\beta$ -diketonates has been pursued by a countless number of investigators using many varied techniques. The bonding and structure of these complexes have been explored by spectral methods (infrared, electronic, n.m.r. and mass spectra), as well as through chromatographic (gas, column and thin-layer) and physical measurements (x-ray diffraction, vapour pressure, magnetic and dipole moments). A comparable body of evidence has been compiled for the metal complexes of monothio- $\beta$ -diketones since Chaston and Livingstone (35) first reported their synthesis in 1964. From a practical viewpoint, metal chelates of this type have seen applications as n.m.r. shift reagents, in solvent extraction studies, and in laser technology.

An exhaustive review of all of the chemical and physical studies reported to date on metal  $\beta$ -diketonates and monothio- $\beta$ -diketonates will not be attempted here. For this purpose, the reader is referred to several comprehensive reviews (36-39). Instead, when possible, discussion will focus upon studies which are of direct concern to the specific complexes under investigation, namely unsymmetric, fluorinated chelates of the form  $\text{Met}^{n+}[\text{RCXCHCOR}']_n$  (where Met = Al(III), Ga(III), Co(III), Ni(II), Pd(II), Cu(II), Zn(II); R = aryl or heterocycle; X = O or S; R' = fluorine-substituted alkyl; n = 2 or 3). Aspects to be considered include general chemistry and synthetic methods, x-ray

structural analysis, n.m.r. spectra and dipole moments. A more detailed treatment of previous mass spectral studies will also be given.

### 1. General Chemistry

As shown in Figure 18,  $\beta$ -diketones are capable of keto-enol tautomerism; in solution, the diketo form I is in equilibrium with the enol forms II and III. A great deal of effort has been expended in recent years on the study of keto-enol tautomerism in  $\beta$ -diketones. It has been found (see (36) and references cited therein) that the proportion of the enol isomer is increased when (a) an electron-withdrawing group is substituted for hydrogen on the  $\alpha$ -carbon, (b) the ligands are fluorinated or contain an aromatic ring, or (c) the  $\beta$ -diketone is in a non-polar solvent. As well, double-bond resonance and chelation through hydrogen-bonding further stabilize the enol form (see Figure 18). Conversely, substitution of one of the  $\alpha$ -hydrogens by a bulky group (e.g. alkyl) causes steric hindrance between R-group protons and this, combined with an alkyl group's inductive effect, often diminishes the extent of enolization. It should be noted that all of the ligands used in this study are unsubstituted at R'', fluorinated at R', and aryl-substituted at R.

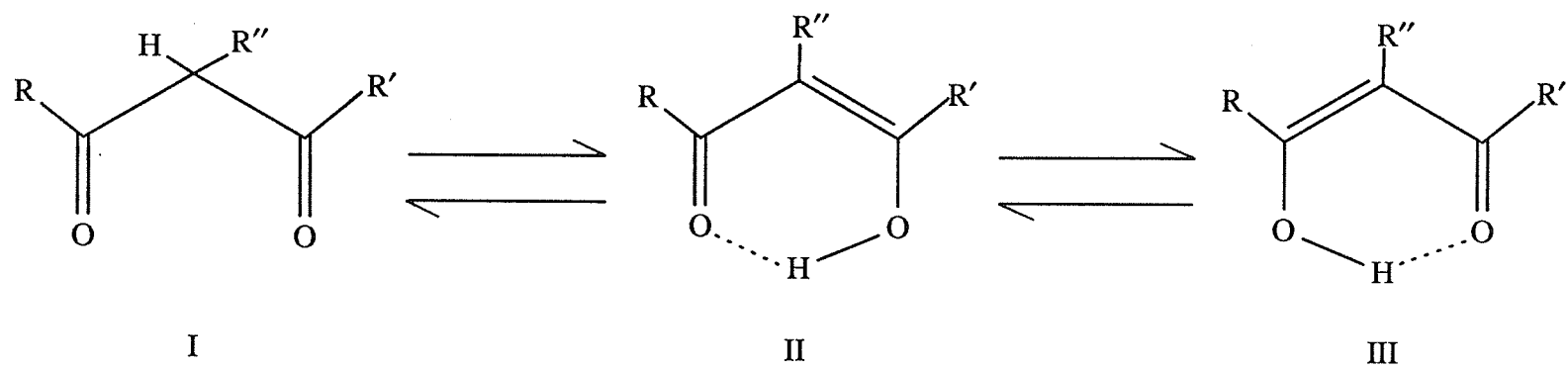
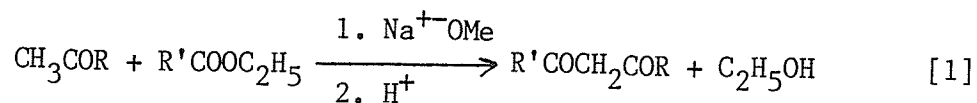


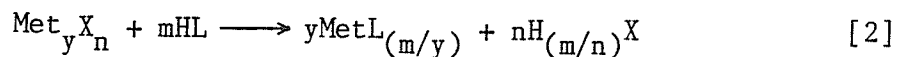
**Figure 18.** Tautomerism of  $\beta$ -diketones.

The most commonly-traveled synthetic route to  $\beta$ -diketones has been through a variation of the Claisen condensation, in which a ketone containing an  $\alpha$ -hydrogen undergoes a base-catalyzed reaction with an ester:



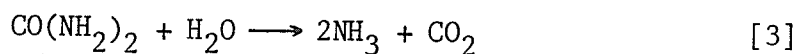
The methoxide ion abstracts a proton from the  $\alpha$ -carbon of the methyl ketone to form the carbanion, which in turn attacks the carbonyl carbon of the fluorine-substituted ethyl ester, displacing the ethoxide ion and giving the  $\beta$ -diketone. However, since the  $\alpha$ -hydrogens of a  $\beta$ -diketone are located alpha to two carbonyl groups, ionization yields a particularly stable carbanion. As a result, the  $\beta$ -diketone is a considerably stronger acid than ethanol and therefore reacts with the ethoxide ion to form ethanol and the  $\beta$ -diketo anion  $[\text{RCOCHCOR}']^-$ . Acidification at this stage yields the desired product.

Under the appropriate reaction conditions, the enolic proton of a  $\beta$ -diketone can be replaced by a metal to form a characteristic metal  $\beta$ -diketonate. The metal chelation reactions of  $\beta$ -diketones have, in the past, involved a number of different forms of starting materials: elemental metals, metal salts, metal oxides, metal carbonyls and others. The majority of the metal chelates used in my work were prepared from their metal salts, according to the general equation:

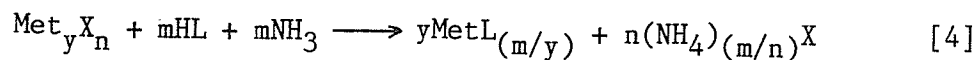




where  $\text{Met}_y\text{X}_n$  is the metal salt ( $X = \text{acetate, nitrate, chloride or sulfate}$ ), HL is the  $\beta$ -diketone ligand,  $y = 1$  or  $2$ ,  $n = 2$  or  $3$  and  $m = 2, 3$  or  $6$ . As discussed by Fernelius and Bryant (40), the main difficulty with this process is the accumulation of free acid, which brings the reaction to equilibrium short of completion. A pH control is therefore mandatory, with three approaches having been employed: (a) the use of metal acetates, (b) the use of a buffered reaction medium, and (c) the addition of a weak base such as ammonia. Metal acetates have proven to be very popular reactants by nature of their "natural" buffering action. The use of a buffer solution has the disadvantage of adding extraneous ions, which may in turn contaminate the final product. A drawback to the addition of ammonia is the possibility that high local concentrations of base might result in the precipitation of insoluble metal hydroxides. This problem can be avoided through the homogeneous generation of ammonia by urea hydrolysis:



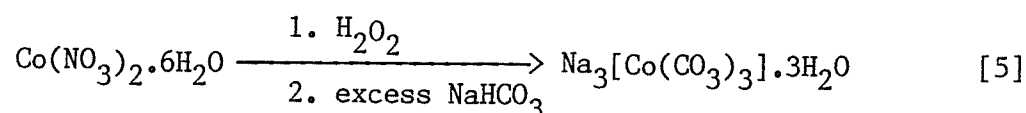
The general form of the synthesis then becomes:



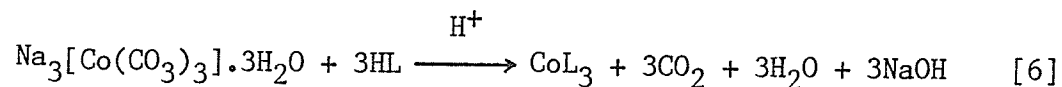
The reactions of  $\beta$ -diketones with metal salts in aqueous solution are often hampered by the low solubilities of many  $\beta$ -diketones in water. Such a problem can usually be overcome by using a partially non-aqueous solvent (an ethanol/water mixture for example) or by adding an alcoholic solution of the  $\beta$ -diketone to an aqueous solution of the metal salt.

Divalent transition metals typically exhibit coordination numbers greater than four for oxygen donors. Neutral  $\beta$ -diketonates of these metals often behave then as Lewis acids, forming addition compounds with bases such as water, ammonia or pyridine (41). In fact, the normal preparative methods for these complexes give hydrates. Nickel(II)  $\beta$ -diketonates, for example, are usually obtained as dihydrates, in which the coordination number of the metal atom is raised to six. In the absence of suitable bases, divalent metal  $\beta$ -diketonates are prone to self-association, giving polymeric species in which the oxygen atoms of one molecule are coordinated to the metal atom of another. Solid state structural analyses have confirmed the polymeric nature of many of these compounds.

The foregoing methodology has been found applicable to the synthesis of most of the first-row transition series metal chelates examined in this study. However, a variation was used for the preparation of the cobalt(III)  $\beta$ -diketonates. The most common route to Co(III) chelates involves the oxidation of the Co(II) ion in the presence of excess ligand, but this method can break down when applied to ligands which are sensitive to oxidation or where solvent may be an effective competitor for metal coordinating sites. As an alternative, a Co(III) intermediate, sodium tris-carbonatocobaltate(III) trihydrate, was prepared by the hydrogen peroxide-induced oxidation of Co(II) nitrate hexahydrate in the presence of excess sodium bicarbonate (42):



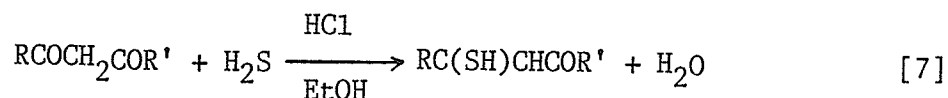
The  $\beta$ -diketone was then added, liberating  $\text{CO}_2$  and producing the desired compound (43):



Normally the volatility of carbon dioxide drives the reaction to completion, although occasionally acid is added.

Monothio  $\beta$ -diketones mimic their dioxo analogs by exhibiting three possible tautomeric forms as shown in Figure 19. The same criteria which favour the enol form of  $\beta$ -diketones (electron-withdrawing groups, aromatic substituents, non-polar solvents) also apply to the monothio derivatives. However, physical evidence (37,38,44 and references cited therein) suggests that in the solid state and in solution, monothio- $\beta$ -diketones exist predominantly in the intramolecularly hydrogen-bonded thienol form (VI).

The simplest preparation of monothio- $\beta$ -diketones involves the acid-catalyzed reaction of hydrogen sulfide with the corresponding  $\beta$ -diketone in ethanolic solution:



The above reaction was initially investigated by several researchers (45-47), albeit with little success; the major obstacles included low yields and a tendency for the reaction products to dimerize. Chaston

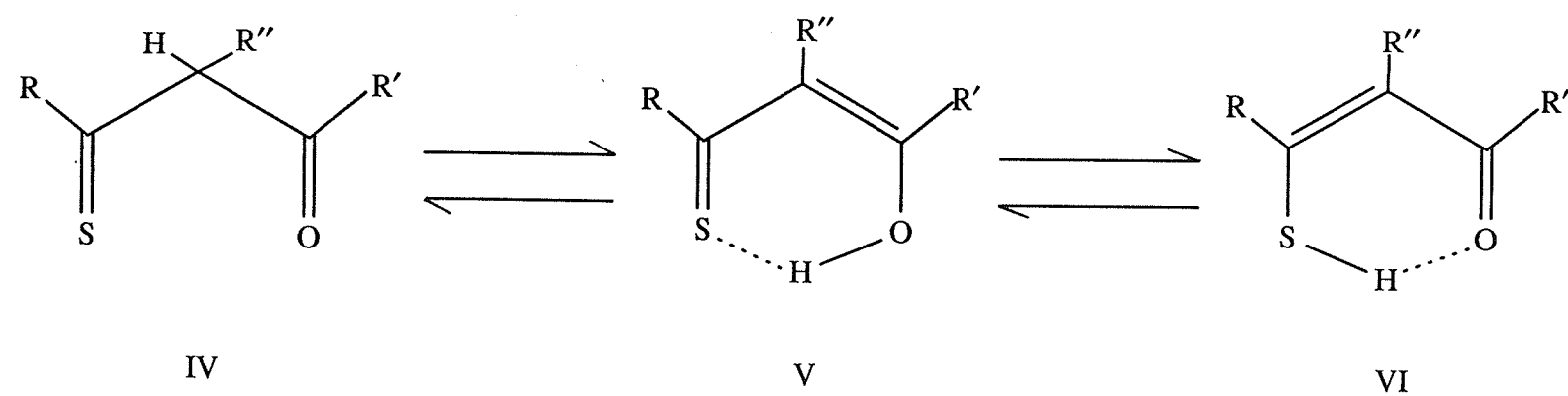
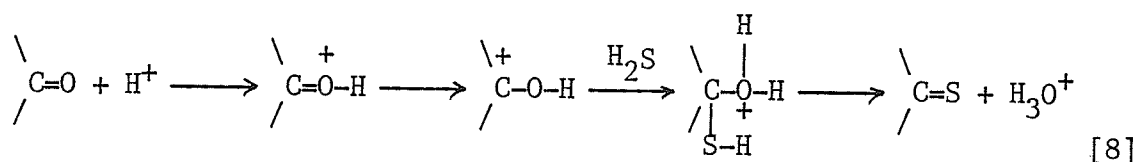


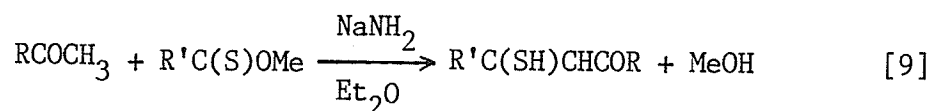
**Figure 19.** Tautomerism of Monothio- $\beta$ -diketones.

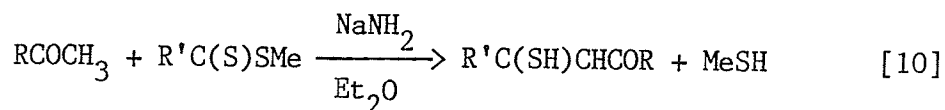
and co-workers (35,48) found that these problems could be alleviated by using a low concentration of the starting  $\beta$ -diketone and by keeping strict controls on reaction conditions. For example, they observed a correlation between the degree of enolization of the parent  $\beta$ -diketone and the concentration of HCl necessary for converting it into the thio derivative: the higher the percentage of enol tautomer initially present in the alcoholic solution, the higher the acid concentration required. Since hydrogen chloride enhances the polarity of the solvent, it was suggested that the reaction with hydrogen sulfide occurs primarily with the diketo isomer:



In all investigated cases of the reaction with asymmetrical  $\beta$ -diketones, evidence has shown that the nucleophilic attack by  $\text{H}_2\text{S}$  occurs at the carbonyl attached to the less electronegative R group, thereby producing the isomer  $\text{RC}(\text{SH})\text{CHCOR}'$  (electronegativity of  $\text{R} < \text{R}'$ ). The limitation to only one isomeric form is undoubtedly the primary drawback of this reaction procedure.

An alternative method of synthesizing monothio- $\beta$ -diketones was advanced by Uhlemann (49,50) and involves a Claisen-type condensation of ketones with thionic or dithionic esters:





This method has the advantage that where two structural isomers (RC(SH)CHCOR' and RCOCH(SH)CR') are possible, both can be prepared in good yield through a suitable choice of starting materials.

Unfortunately, the difficulty in obtaining thionic or dithionic esters having R' = perfluoroalkyl group, necessary for the preparation of the RCOCH(SH)CR' isomers, detracts from the general utility of this procedure.

Chelation of monothio- $\beta$ -diketones with most metals is known, usually by way of direct reaction of a metal halide or acetate with the ligand in a suitable solvent system (normally alcohol or aqueous alcohol). However, the reaction is often complicated by oxidation-reduction reactions of the metal ligand system, depending upon the nature of the metal (especially its oxidation state), the ligand and the reaction conditions. For instance, Chaston and Livingstone (51) demonstrated that in the presence of metal ions in high oxidation states (e.g. Fe(III), Mn(III)), the oxidation of monothio- $\beta$ -diketones to their corresponding disulfides readily occurs, while on the other hand, a metal in a low oxidation state may reduce some of the ligand and form a metal complex of a higher oxidation state (e.g. the oxidation of Fe(II) to Fe(III) and Co(II) to Co(III)). As well, the role of the terminal R-groups in determining the oxidation states of metal monothio- $\beta$ -diketonates was established (51) using a

Cu(I) - Cu(II) system; it was found that in general, strongly electron-withdrawing substituents decrease the negative charge density on the sulfur atom and stabilize the complex in its higher oxidation state.

In contrast to metal  $\beta$ -diketonates, monothio- $\beta$ -diketonates are generally anhydrous, soluble in most organic solvents, and monomeric in the solid state.

## 2. X-ray Structural Studies

Three fundamental physical parameters that can be garnered from the x-ray structural analysis of a given molecule include bond lengths, bond angles and molecular geometry. In metal  $\beta$ -diketonates and monothio- $\beta$ -diketonates, metal-oxygen (or metal-sulfur) bond distances, chelate ring planarity and molecular symmetry are all important structural characteristics. Unfortunately, very little single-crystal, three-dimensional x-ray data exist for the series of asymmetrical, fluorinated metal chelates of interest. As such, only work on compounds of comparative structure can be reported.

The most studied of all nickel(II)  $\beta$ -diketonates is bis(2,4-pentanedionato)nickel(II) ( $\text{Ni}(\text{acac})_2$ ;  $\text{R} = \text{R}' = \text{CH}_3$ ). Early work by Bullen (52) was initiated on the supposition that all diamagnetic Ni(II) complexes possess a planar structure, while paramagnetic species such as  $\text{Ni}(\text{acac})_2$  conform to a tetrahedral geometry. His results show three, nearly colinear nickel atoms in an asymmetric unit cell and,

while not ruling out square planar or tetrahedral coordination, suggest the possibility of an octahedral environment for the nickel atoms. An electron diffraction study by Shibata (53) on the same complex does not reach a definite conclusion regarding geometry, but suggests that the gas-phase results are consistent with a square planar arrangement of oxygen atoms about a nickel center. Bullen and co-workers (54,55) would later confirm the trimeric, octahedral coordination of the complex - specifically, a distorted octahedral geometry about each nickel atom resulting from the bridging of each pair of Ni atoms by three oxygen atoms as shown in Figure 20. Two types of Ni-O bonds appear to exist, depending on whether the oxygen is bonded to only one nickel atom (shorter) or shared between two nickel atoms. The space group is  $Oca2_1$  and the density calculated at twelve molecules per unit cell.

Nickel(II)  $\beta$ -diketonates are easily hydrated in air. Montgomery and Lingafelter (56) found that the nickel ion in diaquo-bis(2,4-pentanedionato)nickel(II) is surrounded by a tetragonally distorted octahedron, with the nickel atom slightly out of the plane of each flat acetylacetonate residue. Although corresponding metal atom displacements are evident in similar cobalt(II) (57) and zinc(II) (58) compounds, no explanations have been proposed. The crystals are monoclinic with space group  $P2_1/c$  and two molecules per unit cell.

Bullen et al. (54) suggest that trimerization can be expected in complexes similar to  $Ni(acac)_2$  provided that the chelating ligands do not present a steric hinderance to such an association. This idea is



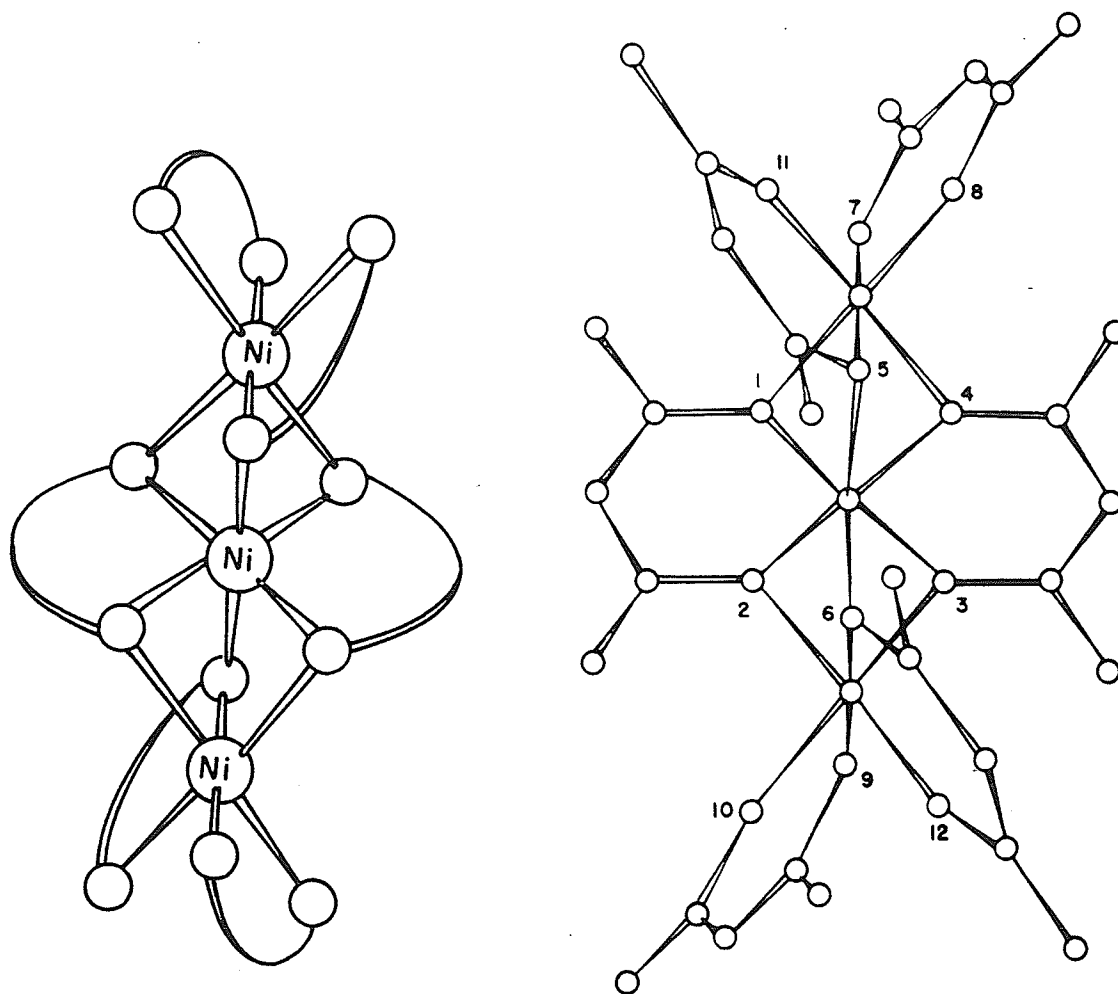


Figure 20. Trimeric structure of Ni(II) acetylacetonate (55).

confirmed by Cotton and Wise (59) in the x-ray structural analysis of bis(2,2,6,6-tetramethyl-3,5-heptanedionato)nickel(II). With the added bulk of the tert-butyl groups, exclusively monomeric, square planar structures are found as shown in Figure 21. The unit cell is monoclinic, space group  $P2_1/a$  and contains two formula units. Of particular interest in this study are the Ni-O bond distances, which are significantly shorter than those observed for octahedral  $Ni(acac)_2$  or  $Ni(acac)_2 \cdot 2H_2O$ . The absence of electrons from the antibonding d orbital of the low-spin square planar Ni(II) complex is proposed as the main reason for the shortened metal-oxygen bonds.

A single-crystal structure of the monothio- $\beta$ -diketonate bis(4-mercapto-pent-3-en-2-onato)Ni(II), as determined by Siiman et al. (60), shows a nearly planar, monomeric molecule in which the nickel atom is surrounded by a square-planar arrangement of oxygen and sulfur atoms (see Figure 22). The molecule adopts a cis configuration of sulfur atoms about nickel, that, according to the authors, is the result of favourable non-bonded interactions between sulfur atoms. The interatomic distances in the chelate ring, while consistent with substantial delocalization of the  $\pi$ -bond system, reveal more double bond character in the C-O bond than in the C-S bond and a slightly shorter C-C bond adjacent to C-S than the C-C bond adjacent to C-O. These observations support the view of a predominantly thienol chelate ring structure. The crystals are orthorhombic, space group  $P_{bca}$ , and contain eight molecules per unit cell.

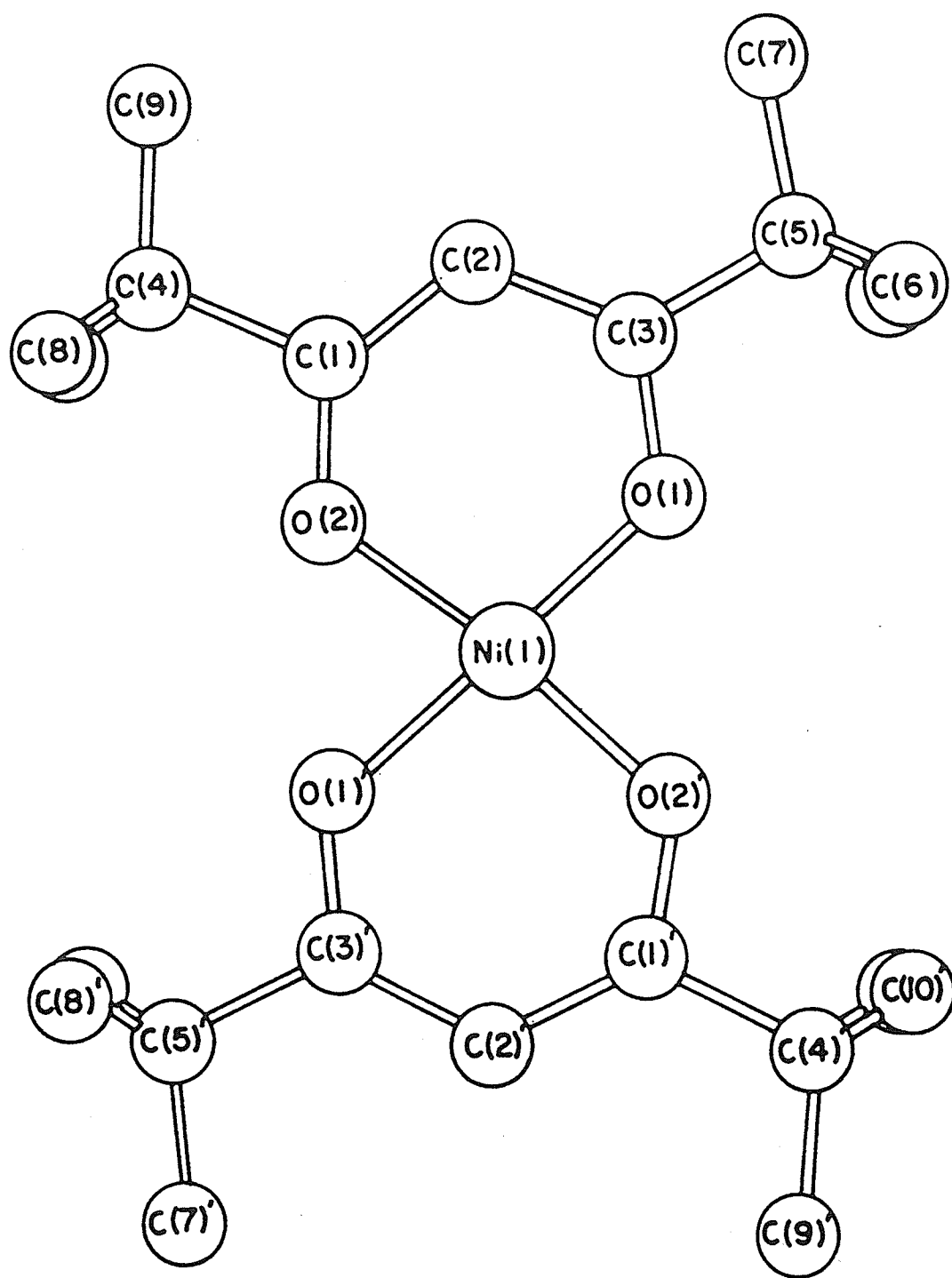
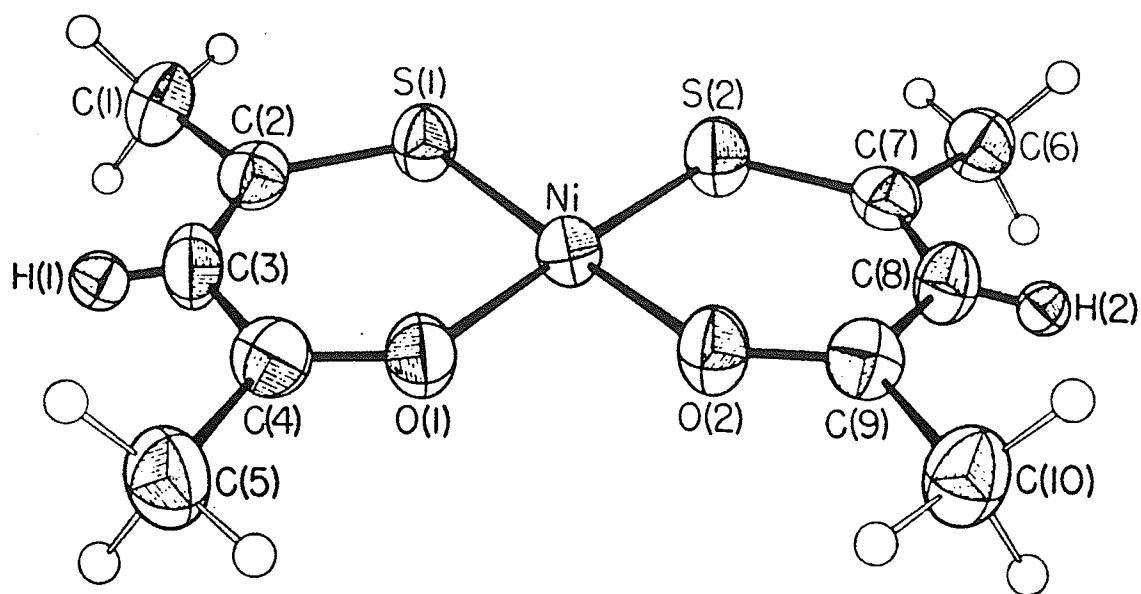


Figure 21. Molecular structure of bis(2,2,6,6-tetramethyl-3,5-heptanedionato)Ni(II) (59).



**Figure 22.** Molecular structure of bis(4-mercapto-pent-3-en-2-onato)Ni(II) (60).

Conclusions reached by Craig and co-workers (61) concerning the solid state structure of bis(1,1,1-trifluoro-4-mercapto-pent-3-en-2-onato)nickel(II) ( $R = \text{CH}_3$ ,  $R' = \text{CF}_3$ ) show the configuration about the nickel to be cis square-planar (see Figure 23). The authors rationalize the cis configuration on the basis of a greater ease of Ni-S  $\pi$ -bonding when the groups are inclined at  $90^\circ$  rather than  $180^\circ$ . The space group is  $P2_1/c$  with four molecules per unit cell.

With the exception of adduct derivatives, comparatively few x-ray crystal structures of Pd(II)  $\beta$ -diketonates have been published. Hon and co-workers (62) report that the palladium and four oxygen atoms found in bis(1-phenyl-1,3-butanedionato)palladium(II) are coplanar and form a parallelogram centered on the palladium (see Figure 24). Pd-O bond lengths are 1.965 and 1.976 Å and the phenyl substituents are trans to one another and at  $23^\circ$  to the plane of the chelate ring (insufficient to destroy conjugation to the chelate ring). The observed C-O bond distances indicate that the carbon-oxygen bond adjacent to the methyl group has more double bond character than the one next to the phenyl group, suggesting a conjugated "enol" single-double bond arrangement in the chelate ring. The crystals are monoclinic, space group  $P2_1/c$  with two molecules per unit cell. Recently, a Japanese research group published an x-ray analysis of the cis isomer of bis(1-phenyl-1,3-butanedionato)palladium(II). The work of Okeya and associates (63) shows that the palladium atom is coordinated in a square-planar fashion by the four oxygen atoms. As well, bond angle measurements indicate that the phenyl and chelate ring

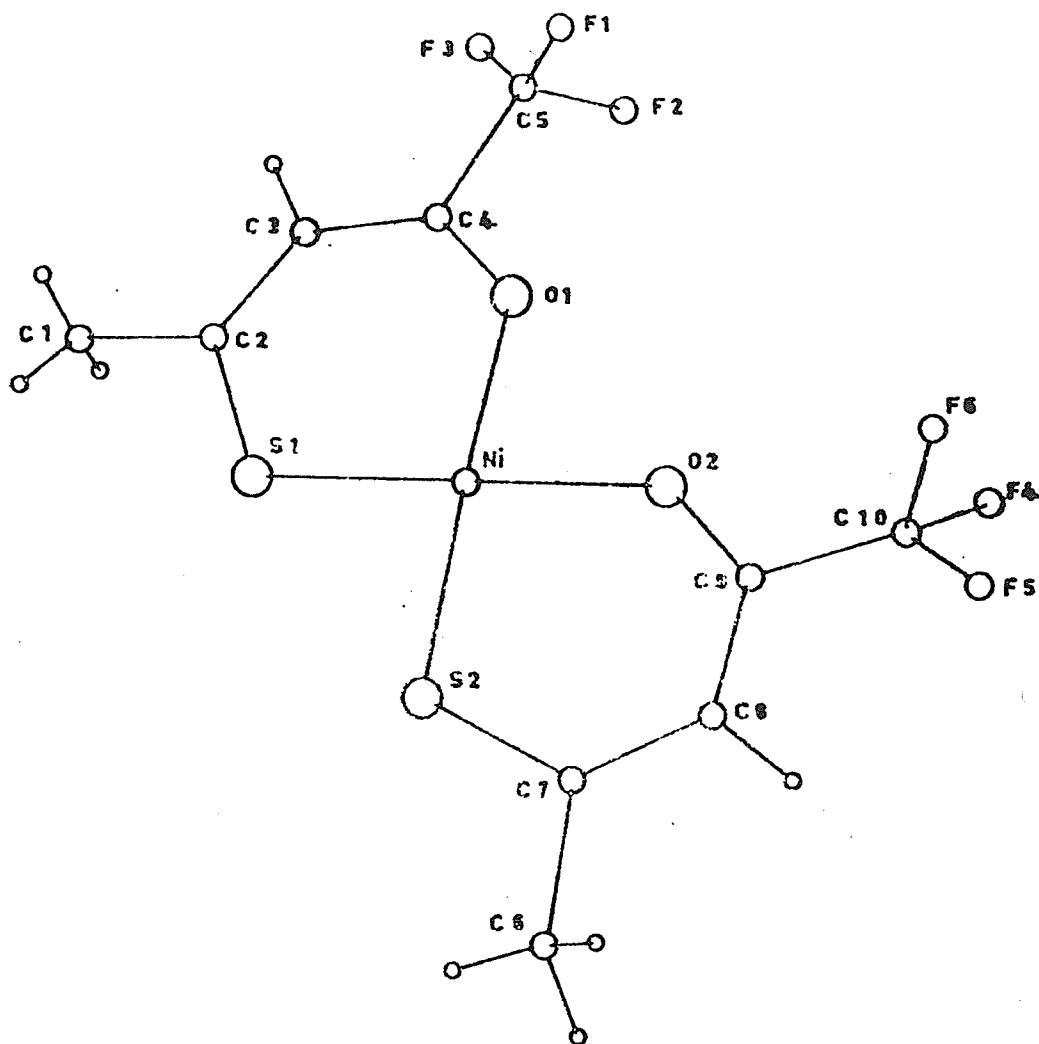


**Figure 23.** Molecular structure of bis(1,1,1-trifluoro-4-mercapto-pent-3-en-2-onato)Ni(II) (61).

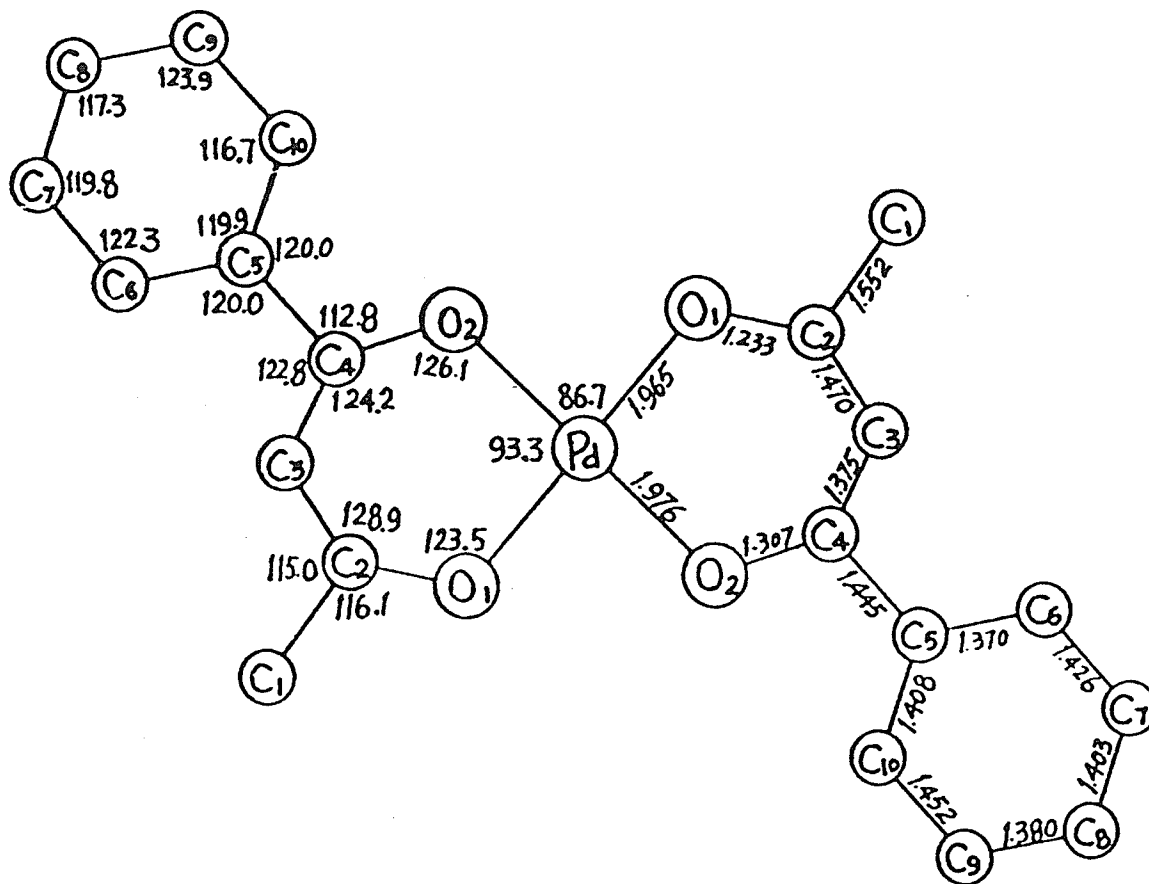


Figure 24. Molecular structure of bis(1-phenyl-1,3-butanedionato)Pd(II) (62).

moieties are approximately coplanar. However, the authors do not find any structural evidence to support the claim of Hon et al. (62) concerning inter-ring conjugation.

One of the only available crystal structures of a Pd(II) monothio- $\beta$ -diketonate is that of bis(1,3-diphenyl-3-mercapto-prop-2-en-1-onato)palladium(II) by Shugan et al. (64). A cis stereochemistry of sulfur atoms about a square-planar Pd center is reported. The crystals belong to the space group  $P2_1/c$  and there are four molecules per unit cell.

Hon and co-workers (65) examined the molecular structure of the trans form of bis(1-phenyl-1,3-butanedionato)copper(II) by x-ray methods and found that the copper and four oxygens form a coplanar parallelogram centered on copper, a geometry very similar to that of the Pd(II) analog discussed above. The pattern of bond lengths around the chelate ring resembles that found for Pd(II), as do the crystal parameters: monoclinic, space group  $P2_1/c$ , two molecules per unit cell. However, a difference is detected in the metal-oxygen bond lengths, where the Cu-O bond is shortened on the side to which the phenyl group is attached. This behavior is similar to that observed by these authors for bis(1-phenyl-1,3-butanedionato)vanadyl(IV) (66) and is attributed to an electron-donating resonance interaction between the phenyl and chelate rings. Such an effect demands a degree of conjugation between these two moieties, which is possible despite the fact that the phenyl ring carbons are twisted  $14^\circ$  out of the plane of the chelate ring (the overlap integral between two  $p\pi$  orbitals twisted



by an angle  $\tau$  falls off as  $\cos \tau$ ;  $\cos 14^\circ = 0.97$ , therefore resonance interaction should be 97% of the value for complete coplanarity). Kidd, Sager and Watson (67) make brief mention of the crystal structure of bis(1,1,1-trifluoro-4-phenyl-2,4-butanedionato)copper(II) and report a  $P2_1/c$  space group with two molecules per unit cell. From symmetry considerations, they argue that the ligands are required to adopt a square-planar configuration about the central copper atom.

The trimeric structure discussed earlier for bis(2,4-pentanedionato)Ni(II) appears to be applicable to both bis(2,4-pentanedionato)zinc(II) (55) and bis(1,1,1-trifluoro-2,4-pentanedionato)zinc(II) (67). Montgomery and Lingafelter's (58) investigation of monoquo-bis(2,4-pentanedionato)zinc(II) indicates that the structure is comprised of discrete molecules and that oxygen atoms are coordinated to the zinc in a geometry intermediate between tetragonal pyramidal and trigonal bipyramidal. This is somewhat in contrast to an earlier report by Lippert and Truter (68) which states that the complex has a distorted trigonal bipyramidal geometry. Lippert and Truter later recanted their claim (58). The unit cell contains two molecules and is space group  $P2_1$ .

A single-crystal, three-dimensional x-ray study of bis(2,2,6,6-tetramethyl-3,5-heptanedionato)Zn(II) by Cotton and Wood (69) indicates a distorted tetrahedral geometry about the metal center (see Figure 25). The crystal is tetragonal, space group  $I4_1/a$  with four molecules per unit cell. The C-O and C-C bond distances in the chelate rings correspond to the delocalized  $\pi$ -bonding (or resonance) structures

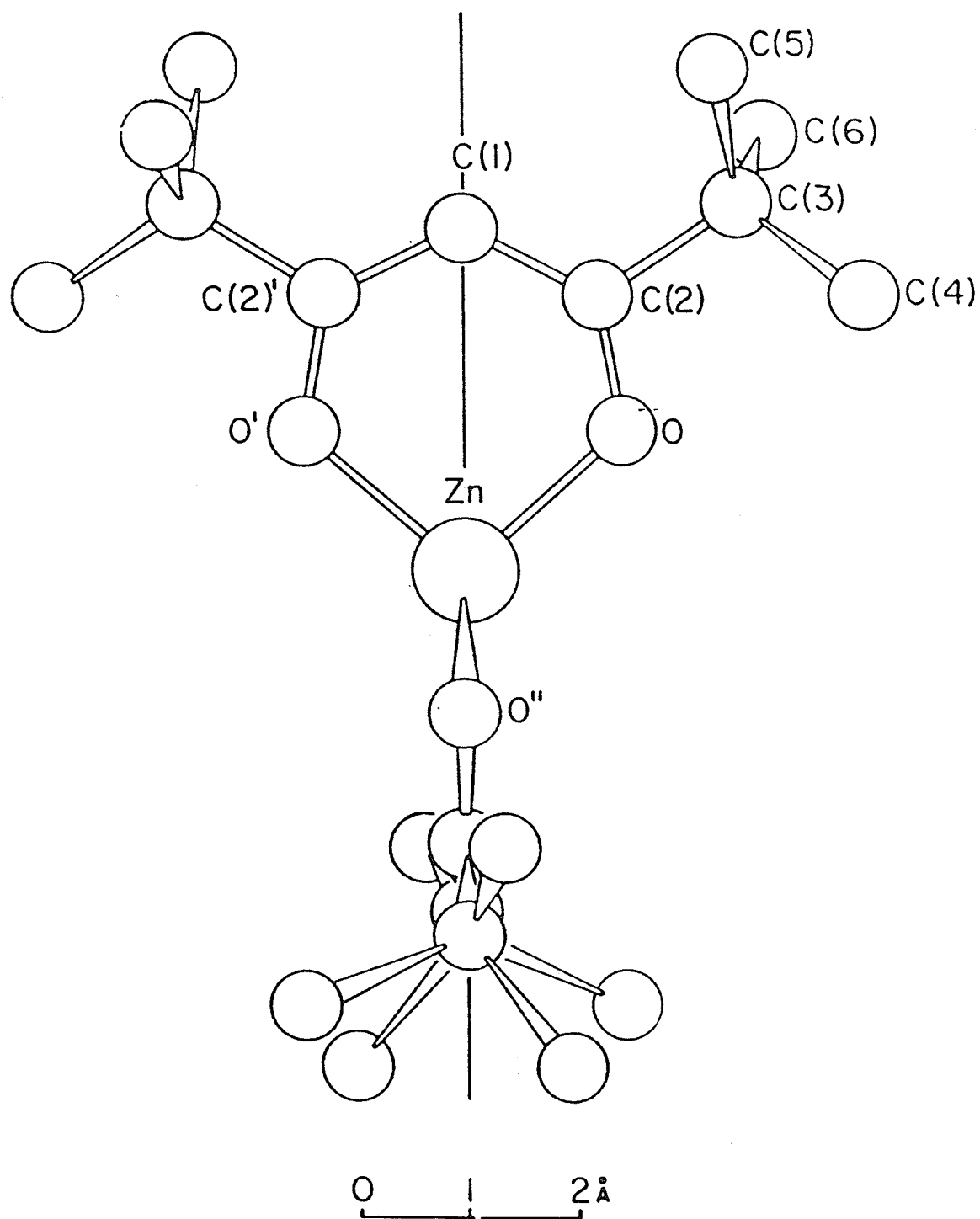


**Figure 25.** Molecular structure of bis(2,2,6,6-tetramethyl-3,5-heptanedionato)Zn(II) (69).

postulated for 2,4-pentanedionato rings. Symmetry dictates that the pairs of C-O and C-C bonds in each ring must be exactly equal in length, a fact confirmed by experimental results.

Ollis and co-workers (70) describe the single-crystal structure of tris(1,1,1-trifluoro-4-mercapto-4-phenyl-but-3-en-2-onato)cobalt(III). As shown in Figure 26, the molecule is centered on a three-fold axis of symmetry and has a facial octahedral configuration with all three sulfur atoms mutually cis. The crystal is hexagonal, space group  $R\bar{3}$  with six molecules per unit cell.

### 3. Nuclear Magnetic Resonance Studies

In 1958, Holm and Cotton (71) published the proton nuclear magnetic resonance spectra of ten metal acetylacetonates, thereby providing the first nmr examination of metal  $\beta$ -diketonates. By observing the resonance of the  $\alpha$ -hydrogen, the authors attempted to establish a correlation between the electronic distribution in the chelate rings and the particular metal atom present. They found, however, that the magnitude of the chemical shifts appeared to be independent of the nature of the metal. Although the chemical shifts approximated those of olefinic protons, Holm and Cotton were reluctant to endorse the concept of aromaticity in the ring moiety. Subsequent studies (72,73) by others also proved inconclusive in establishing an aromatic character for metal acetylacetonates.

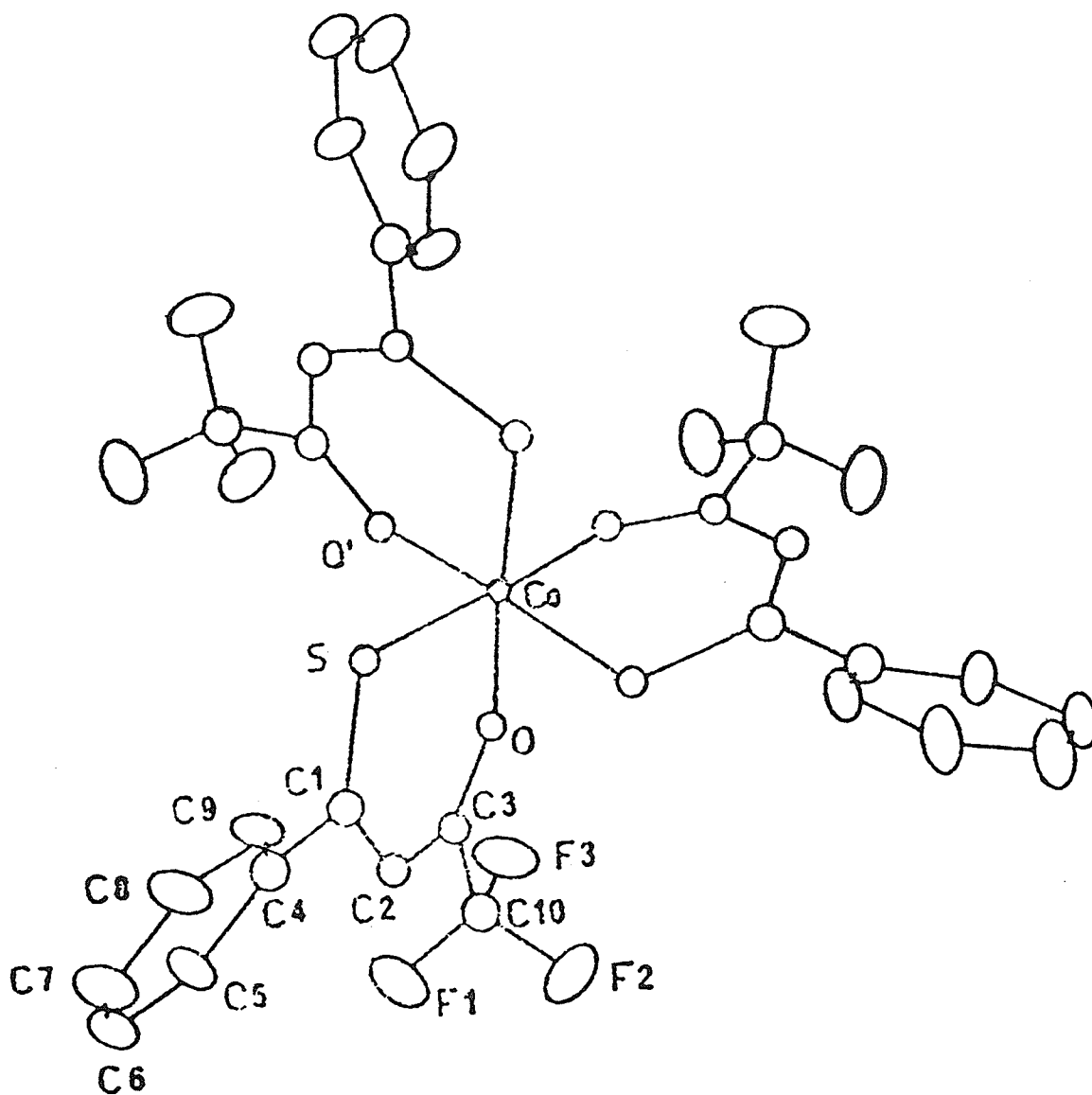


**Figure 26.** Molecular structure of tris(1,1,1-trifluoro-4-mercapto-4-phenyl-but-3-en-2-onato)Co(III) (70).

More recently, nmr spectroscopy has been put to productive use for the investigation of geometrical isomerism in metal tris  $\beta$ -diketonates. If the chelate rings of the complex are unsymmetrical, there exists the possibility of cis/trans isomerization. Figure 27 depicts two diastereomeric forms of an octahedrally-coordinated tris  $\beta$ -diketonate. The cis isomer has a three-fold axis of symmetry, whereas there is no such symmetry axis in the trans form. Fay and Piper (43,74,75) were among the first to use nmr to study cis and trans isomerism in unsymmetrical tris  $\beta$ -diketonates. They examined a series of chelates of the form  $\text{Met}(\text{RCOCHCOR}')_3$  (R = methyl, phenyl; R' = methyl, trifluoromethyl; Met = Cr(III), Co(III), Rh(III), Mn(III), Fe(III), Al(III), Ga(III) and In(III)) by  $^1\text{H}$  and  $^{19}\text{F}$  nmr techniques. The  $^{19}\text{F}$  nmr results for the inert Cr(III), Co(III) and Rh(III) chelates show two distinct forms in solution: a soluble, polar form giving a single line resonance (an identical signal for each ring substituent) and a less soluble, less polar component giving three resonance lines, one for each  $\text{CF}_3$  substituent group. The two forms are assigned as cis and trans respectively on the basis of equivalent and nonequivalent ring environments. The spectra of the Al(III), Ga(III), Mn(III), Fe(III) and In(III) compounds reveal that these labile complexes exist as equilibrium mixtures of cis and trans isomers while in solution. The rates of isomerization can be estimated (75) by determining the temperature at which the four resonance lines in the  $^{19}\text{F}$  nmr spectra of the trifluoro derivatives merge into a single line. This coalescence is attributed to rapid interconversion between cis and trans isomers; the environment of the three trifluoromethyl groups lies between those

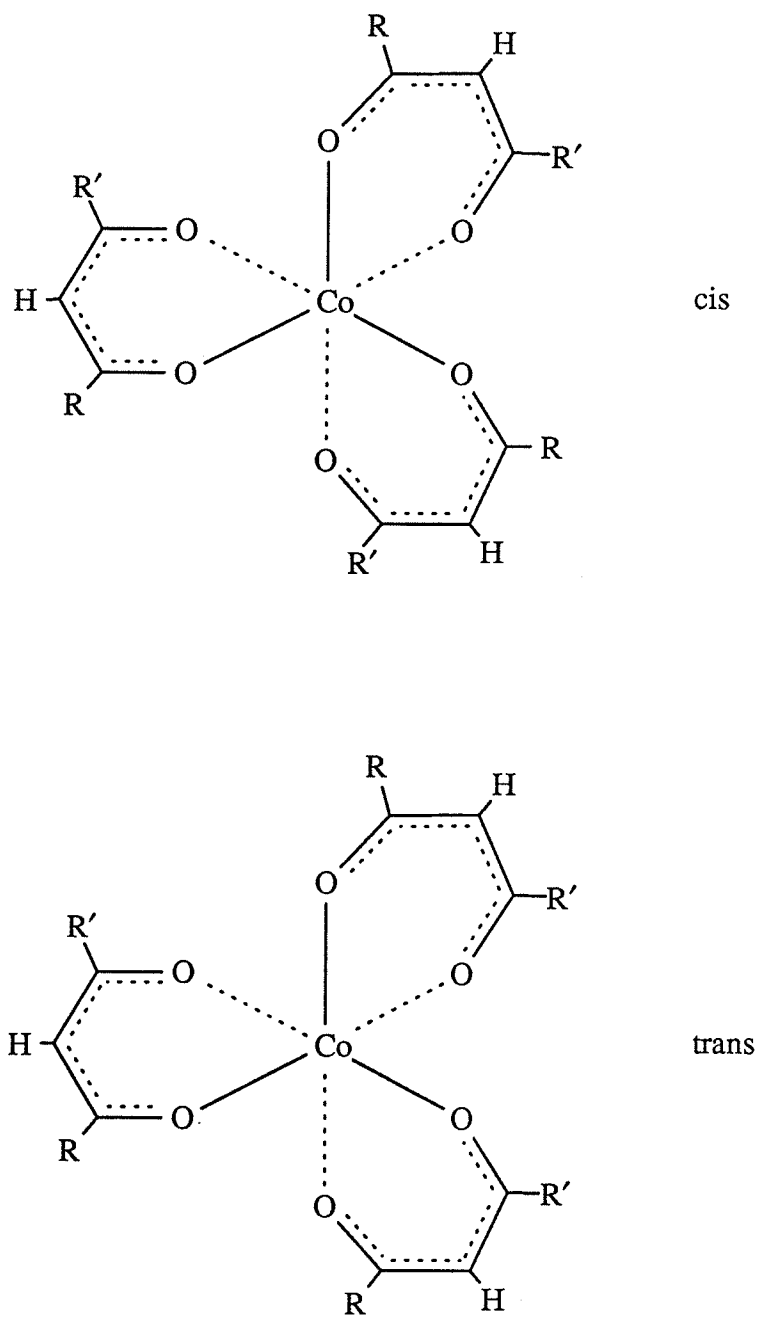


**Figure 27.** Configurations of cis and trans isomers in Co(III)  
 $\beta$ -diketonates.

of the four possible nonequivalent sites of the cis and trans isomers. Based on  $^{19}\text{F}$  nmr evidence, Fay and Piper reject the likelihood of a dissociative, intermolecular mechanism for these stereochemical rearrangements in favour of an intramolecular, single metal-oxygen bond rupture process. However, the possibility that one or more intramolecular twisting mechanisms (76-78) may be at work cannot be discounted.

Haworth, Das and co-workers (79,80) continued the nmr-based examination of stereochemically non-rigid metal tris- $\beta$ -diketonates by studying a series of novel aluminum(III), gallium(III) and indium(III) chelates ( $\text{R} = \text{phenyl}, 2\text{-naphthyl}, 4\text{-fluorophenyl}, 4\text{-methylphenyl}$  and  $2\text{-thienyl}$ ;  $\text{R}' = \text{difluoromethyl}$  and  $\text{trifluoromethyl}$ ). Four  $^{19}\text{F}$  resonances - corresponding to an equilibrium mixture of the cis (one signal) and trans (three signals) isomers - are observed for each complex. The fluorine signals coalesce into one resonance at a temperature unique to each complex; this information can then be used to establish rates of, and energy barriers to, rearrangement. A single metal-oxygen bond rupture mechanism proceeding through a square pyramidal intermediate is suggested as being responsible for the rapid intramolecular exchange phenomenon.

Eight bis ( $\beta$ -diketonato) palladium(II) chelates containing fluorinated, unsymmetrical ligands ( $\text{R} = \text{CH}_3, \text{C}_6\text{H}_5, \text{C}_4\text{H}_3\text{S}$ ;  $\text{R}' = \text{CHF}_2, \text{CF}_3, \text{C}_2\text{F}_5$  and  $\text{C}_3\text{F}_7$ ) have been examined by Haworth et al. (81) using  $^{13}\text{C}$  and  $^{19}\text{F}$  nmr spectroscopy. The observation of dual carbon and fluorine resonances in several of these square-planar complexes suggests the

existence of both cis and trans isomers. A preference for the trans isomer is indicated in the averaged relative peak intensities of each pair of  $^{19}\text{F}$  signals (cis:trans ratio of 1:1.3 to 1.5).

Metal monothio- $\beta$ -diketonates can display geometrical isomerism as well: cis or trans square-planar in bis chelates and facial or meridional configurations in octahedral complexes (see Figure 28).

In a series of articles, Haworth and Das (82-85) discuss the  $^{13}\text{C}$  and  $^{19}\text{F}$  nmr characteristics of a number of nickel(II), palladium(II), zinc(II) and cobalt(III) monothio- $\beta$ -diketonates ( $\text{R} = \text{C}_6\text{H}_5$ ,  $\text{C}_4\text{H}_3\text{S}$ ,  $\text{C}_{10}\text{H}_7$  and substituted -phenyl;  $\text{R}' = \text{CHF}_2$ ,  $\text{CF}_3$ ,  $\text{C}_2\text{F}_5$  and  $\text{C}_3\text{F}_7$ ), with particular emphasis on structure and isomerism. The data show that the  $^{13}\text{C}$  nmr chemical shifts of the diketonate carbon ring resonances vary between complexes having different metal centers. Similarly, the  $^{19}\text{F}$  results indicate that the fluorines nearest the metal give chemical shifts that are metal dependent. The authors are reluctant to speculate as to whether these effects are a result of molecular geometry or the nature of the metal complexed. Exceptions to this behavior are the fluorine signals in the chelates having  $\text{R}' = \text{C}_3\text{F}_7$ ; it is suggested that the increased inductive effect of  $\text{C}_3\text{F}_7$  (relative to H, F or  $\text{CF}_3$ ) cancels any shielding change of the  $\text{CF}_2$  resonance that might arise from metal coordination and/or configuration. All of the cobalt(III) complexes exhibit a cis (fac) geometry as evidenced by only single resonances for each type of carbon atom in the  $^{13}\text{C}$  nmr spectra (a meridional configuration, which lacks the  $\text{C}_3$  symmetry axis of the facial isomer, would show a unique resonance for each respective



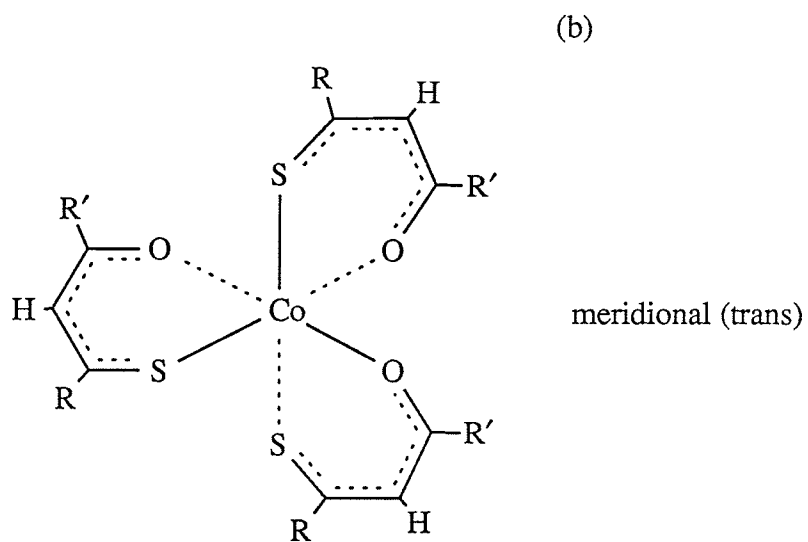
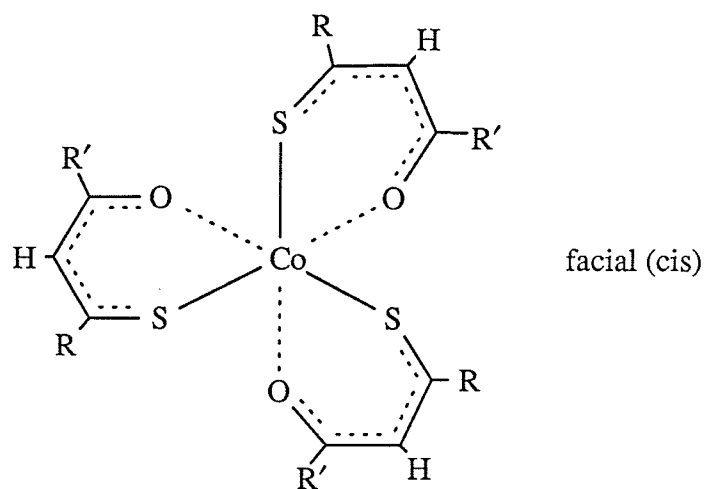
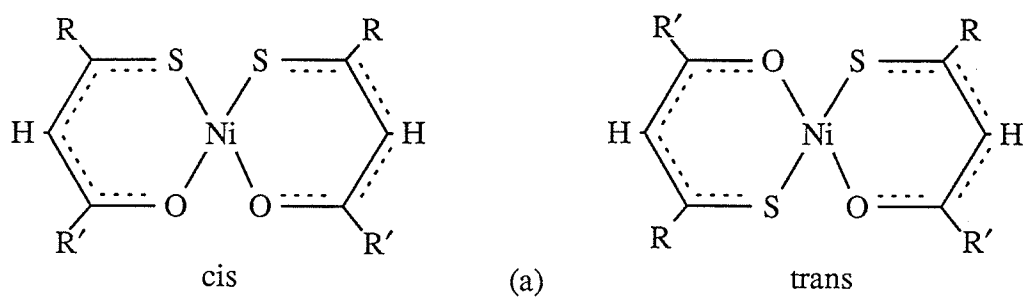


**Figure 28.** Geometrical isomerism in (a) square-planar Ni(II) and (b) octahedral Co(III) monothio- $\beta$ -diketonates.

carbon). The preference for the formation of the cis-structure may be attributed to the fact that all three sulfur atoms are at right angles to each other and to the central metal atom, thus maximizing metal-sulfur  $\pi$ -bonding opportunities. Weak, non-bonded S-S interactions may also play a role (60,86).

Haworth and Das broadened their  $^{13}\text{C}$  and  $^{19}\text{F}$  nmr study of monothio- $\beta$ -diketonates to include alkyl-substituted compounds (87-89), gallium(III) and indium(III) chelates (90) and some second- and third-row transition metal complexes (91). The results for the alkyl-substituted chelates are much the same as those reported above. On the basis of variable-temperature  $^{19}\text{F}$  nmr work, the gallium and indium complexes appear non-rigid, existing in solution as equilibrium mixtures of cis and trans isomers. The  $^{13}\text{C}$  and  $^{19}\text{F}$  nmr results for the rhodium(III), palladium(II) and platinum(II) complexes (91) reveal chemical shift data that are geometry (or metal) dependent. A facial octahedral geometry for the rhodium chelates is confirmed.

#### 4. Dipole Moments

Dipole moment measurements can yield valuable information concerning the structure of complexes in solution. For example, the existence of cis-trans isomerism in unsymmetrical metal  $\beta$ -diketonates and monothio- $\beta$ -diketonates has been established by dipole moment determinations. Square-planar complexes with negligible dipole moments can be classified as likely having a trans configuration, while those

possessing significant moments may be cis isomers. Similarly, a high dipole moment for an octahedrally-coordinated metal chelate suggests a facial (cis) geometry, whereas lower dipole values indicate the presence of a meridional (trans) isomer.

Relatively few dipole moment studies concerning metal  $\beta$ -diketonates have been published, perhaps because their limited solubility in organic solvents renders them unsuitable for solution phase work. Nevertheless, Holm and Cotton (92) report the dipole moments of bis(1,1,1-trifluoro-2,4-pentanedionato)Be(II), Co(II) and Cu(II) as calculated from static polarization measurements. Their results indicate that the beryllium compound is tetrahedral, while the latter two each exist as mixtures of cis- and trans-square-planar complexes (estimated cis:trans ratio of 3:2).

Das and Livingstone (93) have determined the dipole moments for the copper(II) complexes of several trifluoro- $\beta$ -diketones ( $R = C_6H_5$ ,  $C_4H_3S$ ,  $p\text{-MeC}_6H_4$ ,  $p\text{-ClC}_6H_4$ ,  $m\text{-ClC}_6H_4$ ,  $p\text{-BrC}_6H_4$  and  $m\text{-BrC}_6H_4$ ). The authors suggest that the appreciable sizes of the observed dipole moments are indicative of a cis square-planar configuration. Their rationale is based on the assumption that a highly conjugated metal chelate ring aided by the presence of aromatic substituents on the C-4 carbon atom might allow  $\pi$ -bonding to occur between the metal and oxygen atoms, thereby giving rise to a measure of stereoselectivity in the formation of these complexes. Das and Livingstone do not appear to consider the possibility that a mixture of cis and trans isomers may be present.

Recently, Haworth et al. (81) used dipole moment measurements to examine the geometrical configuration of a series of palladium(II) chelates containing fluorinated, unsymmetrical  $\beta$ -diketone ligands. The dipole moment data suggest that these compounds co-exist in solution as a mixture of cis and trans isomers.

The first measurements of the dipole moments of metal monothio- $\beta$ -diketonates were made by Eddy and co-workers (94), who examined the nickel(II), palladium(II) and platinum(II) chelates of 1,3-diphenyl-3-mercapto-prop-2-en-1-one. Molecular models of these square-planar complexes show that a small dipole moment might be expected for the trans isomers due to a non-planar arrangement of the phenyl rings vis-à-vis the four donor atoms. However, the large dipole values imply that the cis form predominates in solution. This concept was reinforced when attempts to establish the co-existence of both isomers proved unsuccessful.

The dipole moments of a wide range of metal monothio- $\beta$ -diketonates have been reported by Das, Livingstone and co-workers (95-103). The complexes studied include nickel(II), palladium(II), platinum(II), copper(II), zinc(II), iron(III), cobalt(III) and rhodium(III); R =  $C_4H_9S$ ,  $C_{10}H_7$ ,  $C_6H_5$  and numerous alkyl- and halogen-substituted phenyl groups; R' =  $CHF_2$ ,  $CF_3$ ,  $C_2F_5$  and  $C_3F_7$ . A cis square-planar configuration is indicated by the large dipole moments of the nickel, palladium, platinum and copper complexes. However, the appreciably lower values obtained for the copper compounds as compared to the Ni, Pd and Pt chelates implies significant distortion from square-planar

towards a tetrahedral geometry; data for the corresponding zinc complexes, which are known to be tetrahedral, show even further lowering. The dipole moment measurements also suggest facial (cis) octahedral structures for the iron, cobalt and rhodium compounds. The preferential formation of cis structures in the transition metal chelates of sulfur-containing ligands is attributed to  $d\pi-d\pi$  metal-sulfur bonding and weak, non-bonded S-S attractive forces as discussed earlier. In general, the magnitude of the dipole moments increases in the order: tetrahedral < distorted square-planar < square-planar < octahedral. In a separate publication, Livingstone (104) discusses the results and conclusions put forth in these papers, paying particular attention to the various R groups and their influence upon the observed dipole moments.

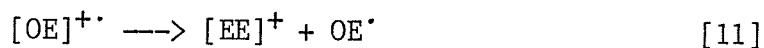
The dipole moments of three fluorinated monothio- $\beta$ -diketone chelates of gallium(III) and indium(III) are reported by Haworth and Das (90). Their dipole moments are lower than those of complexes known to have a facial octahedral structure (e.g. Co(III) and Rh(III) monothio- $\beta$ -diketonates). This fact supports the concept of a fluxional, facial-meridional equilibrium for these complexes in solution.

## 5. Mass Spectrometry Studies

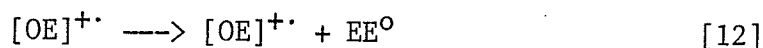
From the time of Macdonald and Shannon's authoritative 1966 paper "Mass Spectrometry and Structures of Metal Acetylacetonate Vapours" (105) to the present day, over seventy-five articles concerning the mass spectral behavior of metal  $\beta$ -diketonates and monothio- $\beta$ -diketonates have appeared in the literature. These studies encompass over four hundred different complexes of the alkali earth, lanthanide and transition metal series and have involved nearly all of the ionization techniques available in modern mass spectrometry. Two reference compilations of these works are given in Appendices 1 and 2. Several excellent reviews of the subject are also available (36,39,106,107).

This section will be divided into three parts: first, a brief discussion of the concept of metal valency change in the mass spectra of metal chelates, followed by a summary of previous works concerned with the mass spectrometry of metal  $\beta$ -diketonates, and finally an examination of similar work conducted on metal monothio- $\beta$ -diketonates. Discussion will focus on chelates of a given ligand type and upon metals which are of direct interest to this study. Although the vast majority of work in this field involves positive-ions produced by electron ionization (EI), techniques such as negative-ion chemical ionization (NCI), secondary ion mass spectrometry (SIMS) and laser desorption (LD) will also be considered.

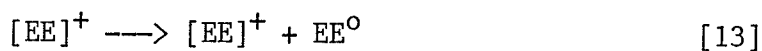
When discussing the mass spectra of coordination complexes such as metal  $\beta$ -diketonates, the concept of metal valency change is of fundamental importance (108,109). The idea of changing the valence state of the metal is essentially an offshoot of the 'even-electron rule', an oft-quoted generalization important for the understanding and prediction of the mass spectral behavior of organic compounds (8,110). It basically states that odd-electron  $[\text{OE}]^{+\cdot}$  cations (such as molecular ions or fragment ions formed by rearrangements) eliminate either odd-electron neutrals  $\text{OE}^\cdot$ :



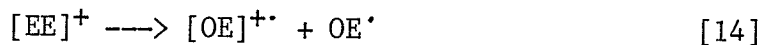
or even-electron neutrals  $\text{EE}^\circ$ :



but that decompositions of even-electron ions  $[\text{EE}]^+$  (such as fragments formed by a single bond cleavage) are strongly influenced by a preference for the formation of an  $[\text{EE}]^+$  ion and an  $\text{EE}^\circ$  neutral:



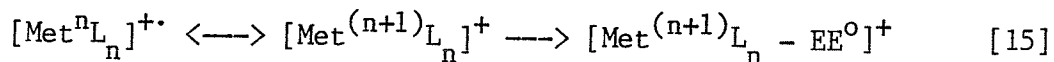
Production of an  $[\text{OE}]^{+\cdot}$  ion from an  $[\text{EE}]^+$  ion must be accompanied by the formation of an odd-electron neutral species, involving the energetically unfavorable separation of an electron pair:



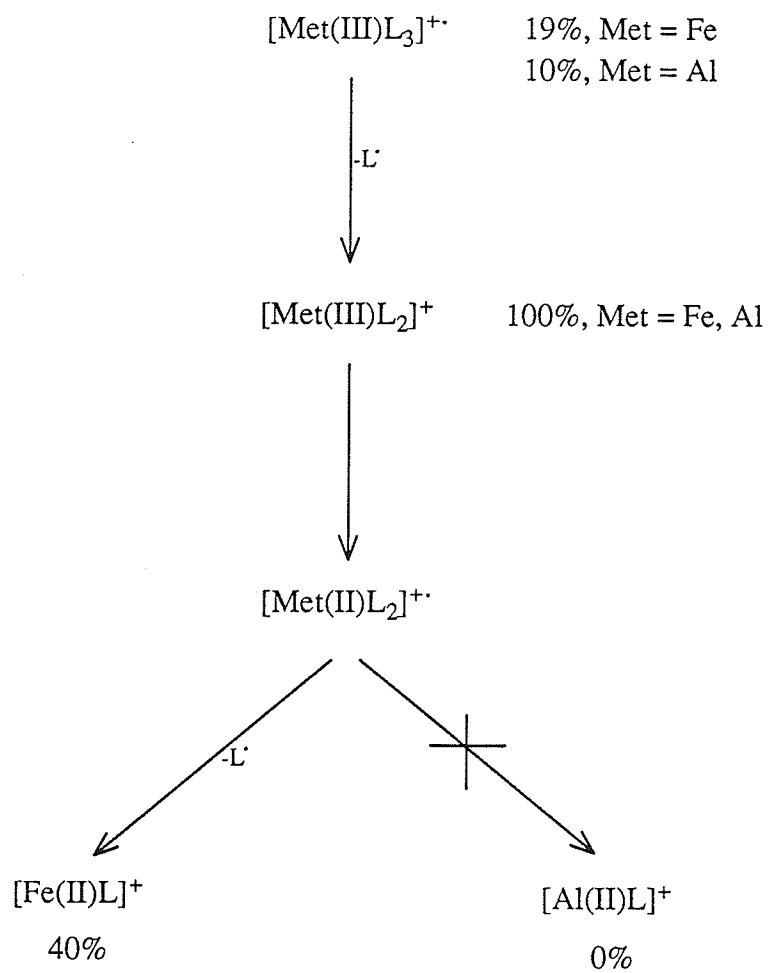
The odd- or even-electron character of a metal-containing ion is determined by the capacity of the complexed metal atom to accept one or

more electrons from the ligands (valence decrease in metal) or to donate one or more electrons to the ligands (valence increase in metal). The mass spectra of metal  $\beta$ -diketonates can often best be explained if valence changes in the bonded metal are assumed to occur during the ion dissociation reactions. In fact, many proposed fragmentation mechanisms appear to be dependent on the oxidation states normally adopted by the metal. For example, both tris (2,4-pentanedionato)iron(III) and tris (2,4-pentanedionato)aluminum(III) give molecular ions and abundant fragment ions due to the loss of a ligand radical (Scheme 5). However, the loss of two ligand radicals is observed only in the ferric compound, presumably because Fe(III), but not Al(III), can readily assume a lower oxidation state. The representations  $[\text{Met(III)L}_2]^+$  and  $[\text{Met(II)L}_2]^+$  in Scheme 1 may be considered canonical contributions to a resonance hybrid possessing a certain degree of radical character.

The three postulates put forth by Westmore (106) concerning the relationship between metal oxidation states and molecular ion stabilities can be used to rationalize much of what has been observed in the mass spectra of metal  $\beta$ -diketonates and monothio- $\beta$ -diketonates. First, the molecular ion will be stabilized if metal-to-ligand  $\pi$ -electron donation is favored, i.e. if a facile increase in metal oxidation state can occur. The molecular ion will be relatively abundant and the loss of even-electron neutral species from the molecular ion will be enhanced:

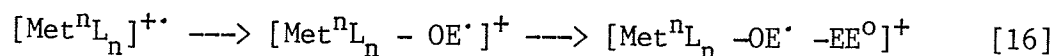




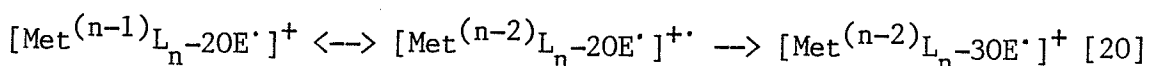
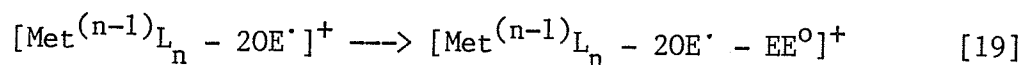
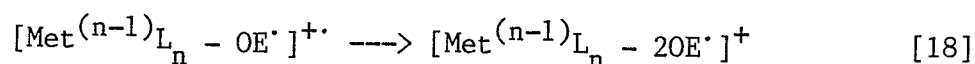
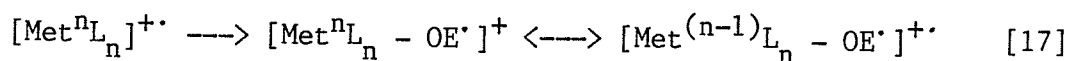


**Scheme 5.** Principal fragmentation pathways of the Al(III) and Fe(III) complexes of 2,4-pentanedione (106).

Secondly, should the metal not be amenable to either an increase or decrease in valency, the molecular ion is not appreciably stabilized and hence may be of low abundance. Fragmentation typically proceeds through the loss of a neutral radical, followed by loss of even-electron neutrals:

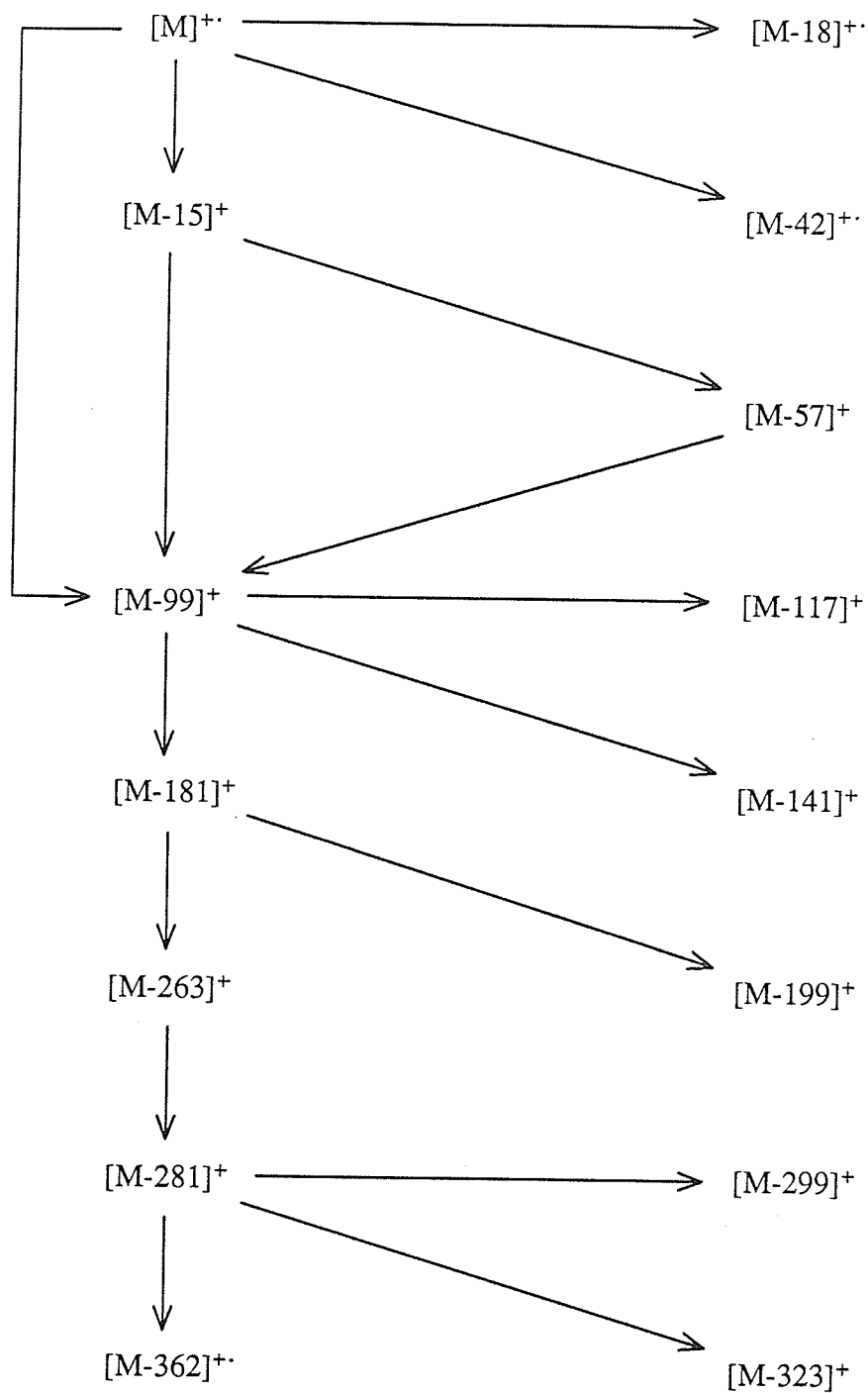


Finally, if the metal is subject to a facile decrease in oxidation state, then the molecular ion may be destabilized. Fragmentation usually occurs via two successive losses of neutral radicals. Succeeding losses will occur through the elimination of odd- or even-electron neutrals, depending upon the ease of a further reduction in metal oxidation state:

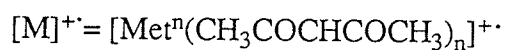
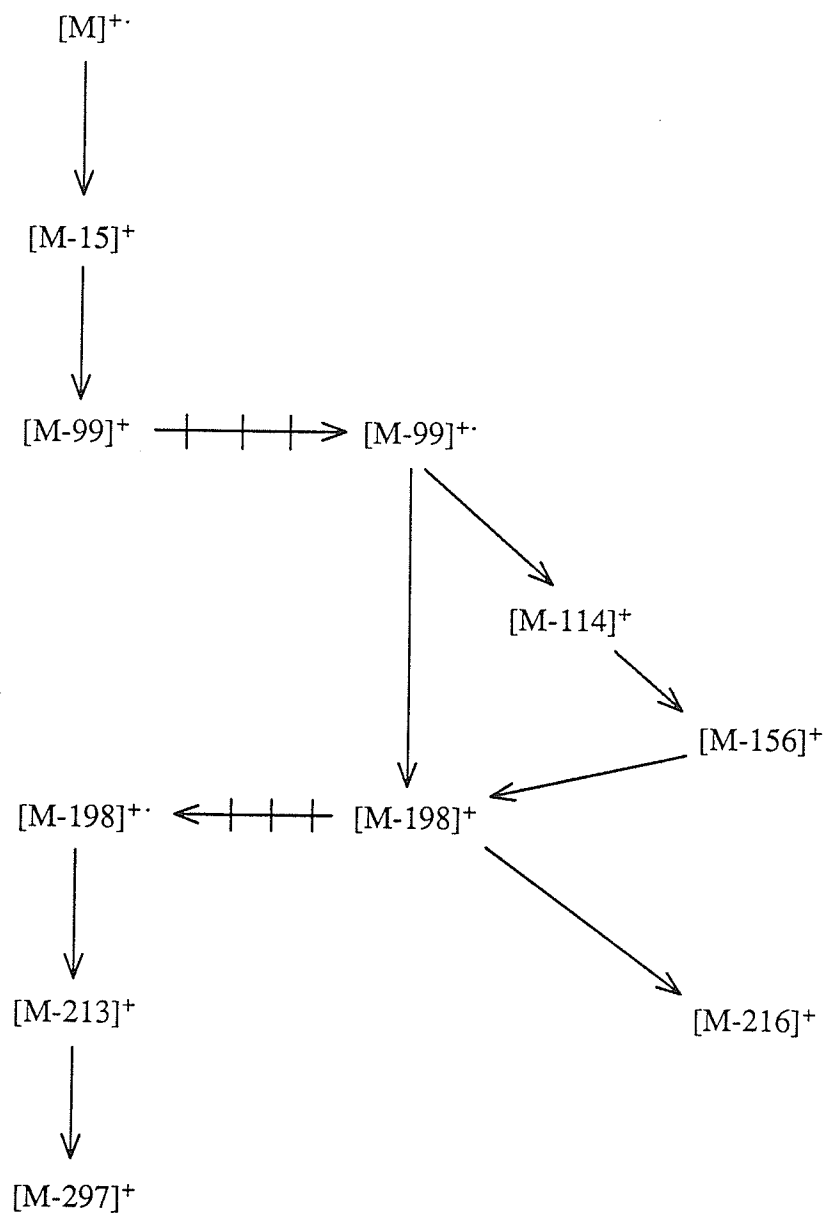


The consecutive losses of odd-electron neutrals may, although not necessarily, involve chemically-equivalent species, of which one or more may be a ligand moiety (L').

As mentioned earlier, Macdonald and Shannon (105) were the first to systematically record the positive-ion, EI mass spectra of metal  $\beta$ -diketonates, specifically twenty metal chelates of 2,4-pentanedione (acetylacetone; Hacac). Their results support the idea of metal valency change and the tendency of ions to dissociate along particular pathways depending upon their odd- or even-electron character and ability to change oxidation state. For example, the primary fragmentation process for the molecular ion  $[\text{Met}^n(\text{acac})_n]^+$  is the loss of an OE' neutral: either a methyl radical ( $[\text{M} - 15]^+$ ) when  $n$  is 1 or 2, or a ligand radical ( $[\text{M} - 99]^+$ ) when  $n$  is 3 or 4. The preference for loss of a ligand radical in tri- and tetravalent complexes is attributed to a lower activation energy for this process as compared to the mono- and divalent species. Elimination of  $\text{CH}_3\cdot$  from the molecular ion is often followed by successive losses of  $\text{CH}_2\text{CO}$  or a single loss of  $\text{CH}_3\text{COCHCO}$ , both  $\text{EE}^0$  neutrals, to give  $[\text{M} - 99]^+$ . Notably, the peak at  $[\text{M-L}]^+$  forms the base peak in many of the spectra; regardless of the pathway followed for its formation, this ion does not require a formal change in the oxidation state of the metal. The ion decompositions requiring no change in metal valency are summarized in Scheme 6. After the initial loss of an OE' neutral, all subsequent neutral fragments are  $\text{EE}^0$  species. Fragmentation pathways requiring a decrease in metal valency are presented in Scheme 7. Repeated losses of OE' neutrals are evident in the mass spectra of tris (2,4-pentanedionato)Cr(III), Mn(III), Fe(III) and Co(III), and bis (2,4-pentanedionato)Cu(II) and Ni(II), which is in keeping with the established stability of lower oxidation states for these metals.



**Scheme 6.** Fragmentation pathways for metal chelates of 2,4-pentanedione involving no change of metal oxidation state (105).

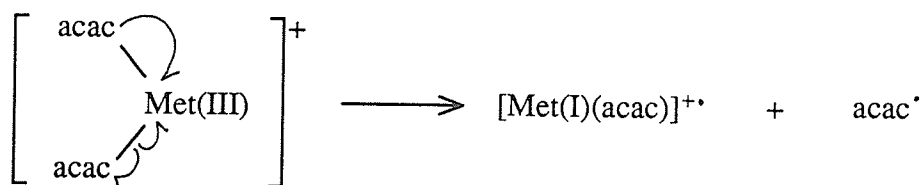


$\xrightarrow{\text{||||}}$  reaction step in which a decrease in metal oxidation state is proposed.

**Scheme 7.** Fragmentation pathways for metal chelates of 2,4-pentanedione involving a reduction of metal oxidation state (105).

Shortly after Macdonald and Shannon's work was published, several reports of similar mass spectral investigations appeared in the literature. Sasaki et al. (111) measured the EI mass spectra of fifteen metal acetylacetonates and correlated the observed fragmentations with the electronegativity of the central metal atom. In a series of articles, Westmore and co-workers (112-114) tabulated the mass spectra and appearance potentials of both divalent and trivalent transition metal chelates of 2,4-pentanedione. Generally, the results obtained were analogous to those reported by Macdonald and Shannon. However, a peak at  $[M - 98]^+$  was evident in the spectra of the divalent nickel and copper species (114). The ion was assigned the structure  $[\text{MetH}(\text{acac})]^+$  and assumed to be the result of hydrogen transfer from a methyl group to the metal atom. A recent paper by Bhattacharjee and co-workers (115) supports this conclusion.

The EI mass spectra of the tris (2,4-pentanedione) chelates of gallium(III) and indium(III) have been discussed by Charalambous et al. (116). Both complexes give a molecular ion  $[\text{Met}(\text{acac})_3]^+$  of low abundance, which proceeds to fragment by consecutive losses of ligand radicals to give the ions  $[\text{Met}(\text{acac})_2]^+$ ,  $[\text{Met}(\text{acac})]^+$  and  $[\text{Met}]^+$ . The authors propose that the elimination of acac from  $[\text{Met}(\text{acac})_2]^+$  is accompanied by the transfer of two electrons to the metal atom (one from the 'leaving' ligand, the other from the remaining ligand), reducing its formal oxidation state to +1:



A stable +1 oxidation state is known for both gallium and indium compounds. The subsequent decomposition of  $[\text{Met(I)(acac)}]^+$  to the bare metal ion provides added support for the suggested mechanism. The  $\text{EE}^+$  ion  $[\text{Met(acac)}_2]^+$  also undergoes dissociation by losses of  $\text{EE}^\circ$  neutrals. Of particular interest is the elimination of the species  $\text{CH}_3\text{COCHCO}$  from  $[\text{Ga(acac)}_2]^+$ ; this process implies methyl migration to the metal, a hitherto undocumented reaction in the mass spectra of metal acetylacetonates.

Cooks and co-workers (117,118) have studied the secondary ion mass spectra (SIMS) of several transition metal acetylacetonates, with a view to probing the significance of SIMS as a tool for molecular characterization and as a means of determining the structure of surfaces. The tris (2,4-pentanedionato) Fe(III), Mn(III) and Cr(III) complexes all yield simple spectra, typified by the absence of an intact molecular ion and the dominance of the fragment ion  $[\text{Met(acac)}_2]^+$ . However, under the appropriate ionization conditions, many structurally-informative adduct ions are produced, eg.  $[\text{Na} + \text{Met(acac)}_3]^+$ ,  $[\text{Ag} + \text{Met(acac)}_3]^+$ , and  $[\text{Met} + \text{Met(acac)}_3]^+$ . Respectively, these secondary ions are a result of cationization by  $\text{Na}^+$  from a NaCl matrix and  $\text{Ag}^+$  from the silver support, and self-cationization from the complex itself. In contrast to the tris

( $\beta$ -diketonato) complexes, divalent Ni(II) and Cu(II) metal chelates of 2,4-pentanedione exhibit a tendency towards metal cluster formation under SIMS conditions. Laser desorption (LD) data given for the cobalt(III) and iron(III) chelates compare well with SIMS, including the generation of cationized species and cluster-ion formation at the sample surface. Parallels between LDMS and SIMS of metal acetylacetonates have been drawn by others (119).

The EI mass spectra of metal complexes of 1,3-diphenyl-1,3-propanedione (120) reveal that the molecular ions' primary mode of decomposition involves the loss of an  $OE^\bullet$  neutral (either a ligand or phenyl radical). The loss of  $C_6H_5^\bullet$  is usually followed by the elimination of the remainder of the ligand, the  $EE^O$  species  $C_6H_5COCHCO$ . As with metal acetylacetonates, the loss of a second  $OE^\bullet$  neutral occurs only in complexes where the metal can readily undergo a valency decrease (eg. Cr(III), Fe(III) and Cu(II)). The remaining fragmentations revolve around hydrogen atom eliminations and transfers:

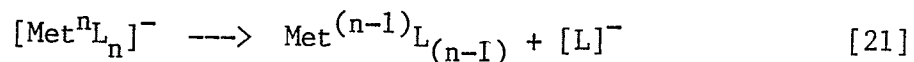
- (a) loss of a hydrogen atom from the molecular ion to give  $[M - 1]^+$ ,
- (b) hydrogen transfer to a phenyl group followed by elimination of the  $EE^O$  neutral  $C_6H_6$  from ions such as  $[Met(II)L]^+$ ,
- (c) the formation of  $[MetLH]^+$  by transfer of an ortho-hydrogen from a phenyl group to the metal (Met = Ni(II), Co(II)) followed by loss of an  $EE^O$  fragment, and
- (d) transfer of a bridging hydrogen into the neutral product (Met = Cu(II)), leading to the formation of the  $[CuL - H]^+$  ion.

The electron ionization mass spectra of a series of bis (1-methyl-3-alkyl-1,3-dionato)Cu(II) complexes (121) show a repetitious

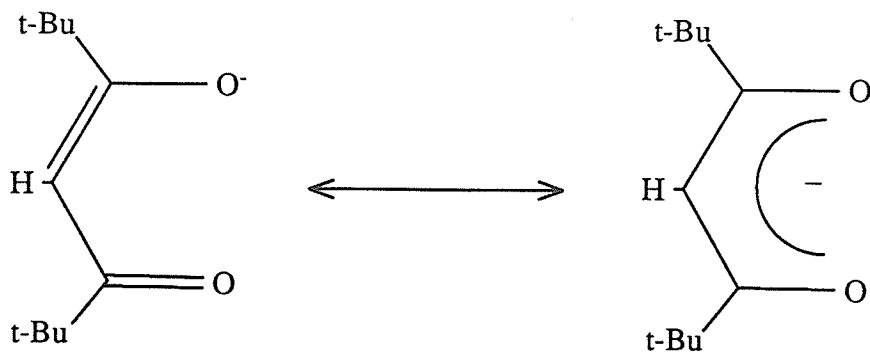


fragmentation pattern involving the stepwise elimination of the alkyl groups around the periphery of the chelate ring structure. Results suggest that as alkyl radical stability increases, the population of copper ions containing that alkyl group decreases.

Negative-ion, electron capture mass spectra have been reported by Gregor and co-workers (122) for the Sc(III), Cr(III), Mn(III), Fe(III), Co(III), Al(III), Ga(III), In(III), Co(II), Ni(II), Cu(II) and Zn(II) chelates of 2,2,6,6-tetramethyl-3,5-heptanedione. The spectra are characterized by their simplicity, with the molecular anion being the principal peak in most instances. The stability of  $[M]^-$  is influenced by the availability of energetically-accessible and unoccupied metal d-orbitals. For example, ion currents carried by the molecular anion for the first transition series metals decrease from 99% for Sc(III) ( $d^0$ ) to 60% for Co(III) ( $d^6$ ). For the  $d^{10}$  Zn(II) complex,  $[M]^-$  carries <20% of the total ion current, which is consistent with the non-availability of an appropriate metal-based LUMO to accommodate the reacting electron. In contrast, each of the Co(II), Ni(II) and Cu(II) chelates form molecular ions that carry ca. 90% of their respective ion currents. The only major fragmentation process observed is:



where the neutral product contains the metal in a lowered oxidation state. The ligand fragment ion is presumably stabilized through delocalization of the negative charge:



Fluorine-substituted metal  $\beta$ -diketonates are more volatile than their non-fluorinated counterparts, thus making them ideal candidates for mass spectral studies. The metal chelates derived from 1,1,1-trifluoro-2,4-pentanedione (trifluoroacetylacetone) and 1,1,1,5,5,5-hexafluoro-2,4-pentanedione (hexafluoroacetylacetone) have, in particular, received thorough examination. Two groups of researchers, one led by Westmore (123-125) and the other by Koob (126-128), have independently studied the EI mass spectra of the Al(III), Fe(III), Cr(III), Co(III), Fe(II), Cu(II) and Zn(II) chelates of these ligands. The following is a summary of their observations.

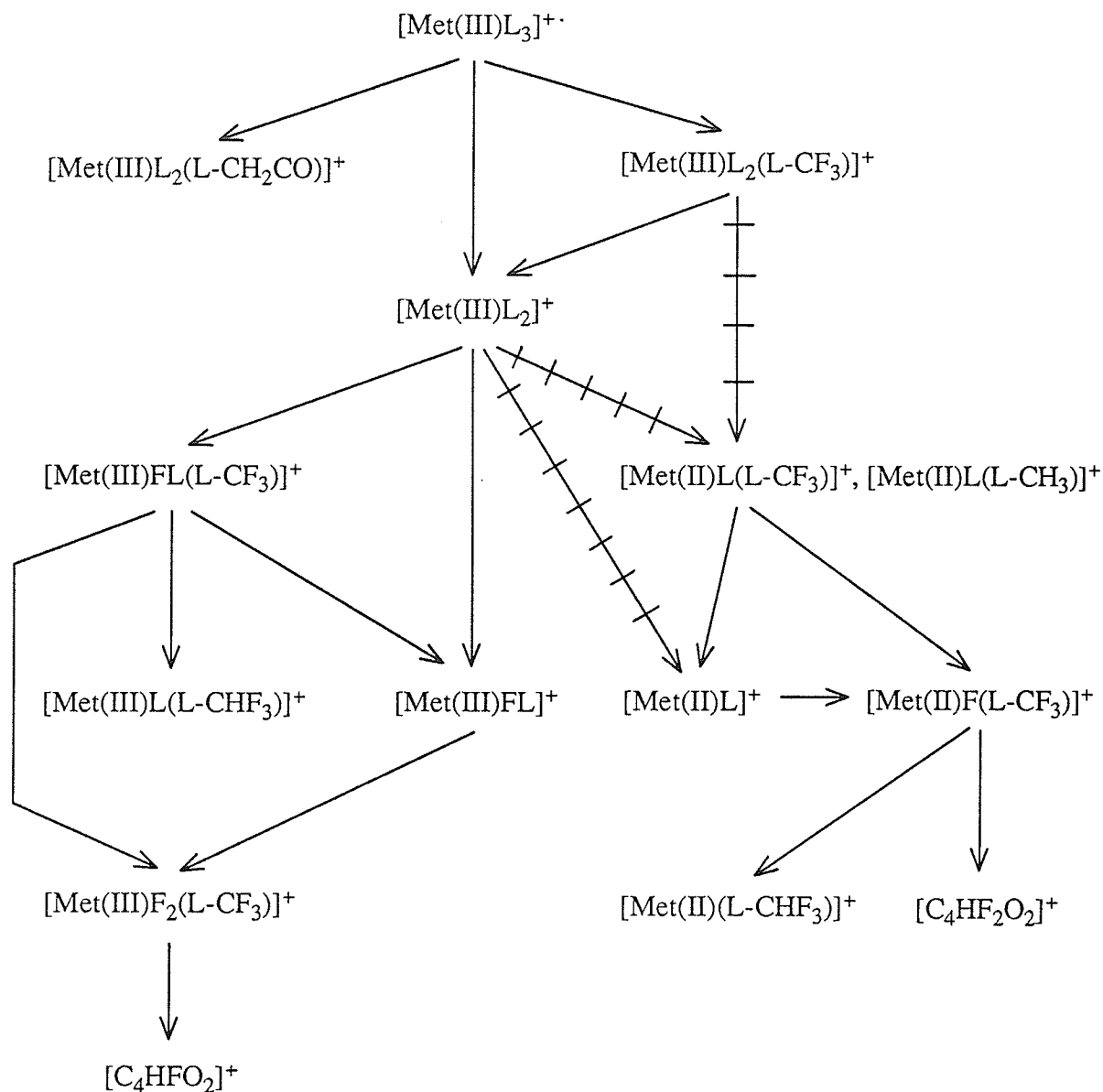
Substitution of  $\text{CF}_3$  for  $\text{CH}_3$  in metal acetylacetonates leads to extensive fragmentation of the molecular ion. This is perhaps the most striking feature of the spectra and is believed to be a result of the comparatively weak nature of the  $\text{C}-\text{CF}_3$  bonds. As such, ions produced by the elimination of  $\text{CF}_3^\cdot$  are very abundant.

The tendency towards the formation of  $\text{EE}^+$  ions, accompanied by metal valence change where necessary, is a powerful driving force in the decompositions of metal tri- and hexafluoroacetylacetonates.

Fragmentation of the  $OE^+$  molecular ion generally proceeds via the loss of  $OE$  neutrals ( $F$ ,  $CF_3$ ,  $CH_3$  and  $L$ ) to produce relatively stable  $EE^+$  fragment ions. Further elimination of  $OE$  neutrals is favored in complexes of Cr(III), Fe(III), Co(III) and Cu(II), where metal valency change (reduction) can occur. Otherwise,  $EE^+$  ions tend to lose  $EE^0$  neutral species ( $CF_2$ ,  $CH_2CO$  and  $(L-F)$ ) with no change in metal oxidation state.

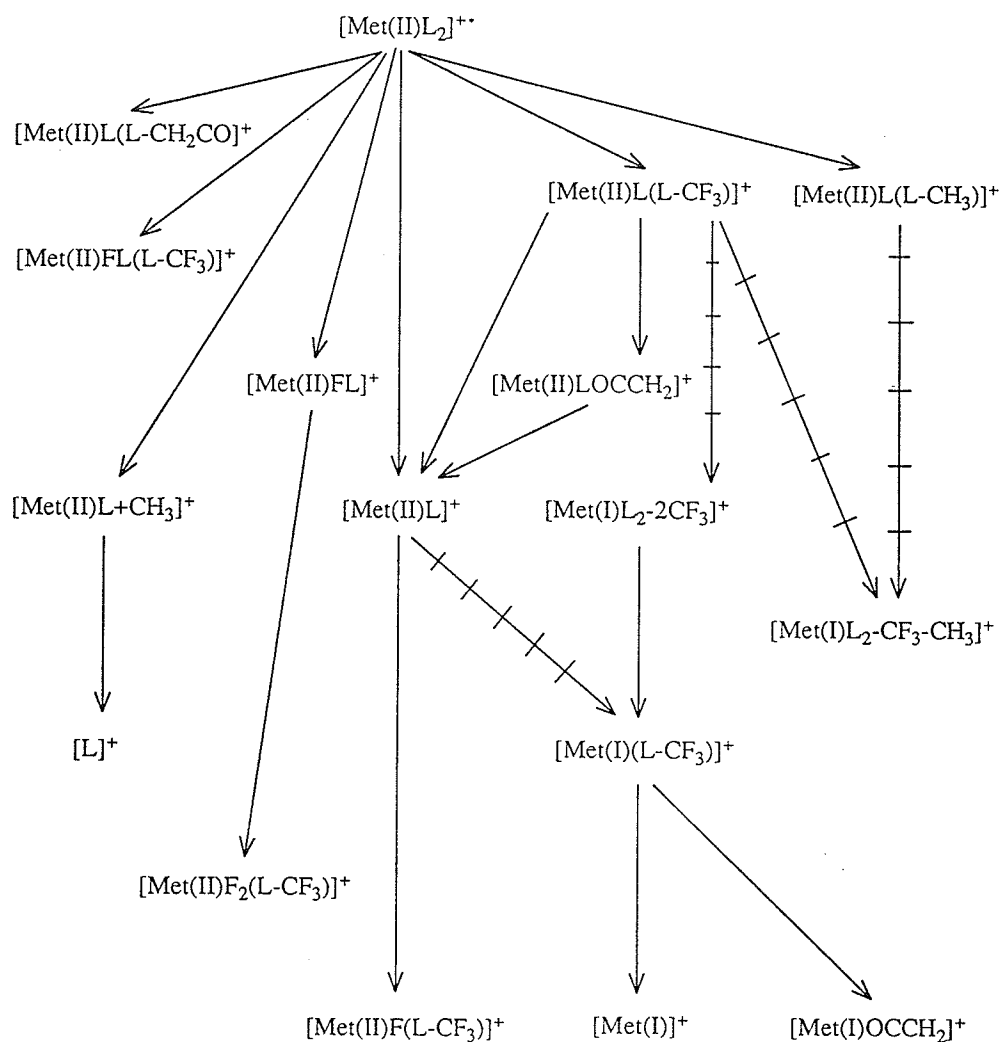
The elimination of  $CF_2$  requires an accompanying fluorine atom rearrangement. The two most likely acceptor sites for the fluorine include the metal atom and the electron-deficient carbon generated as the  $C-CF_3$  bond is broken. Evidence for the formation of a metal-fluorine bond is furnished by the loss of neutral metal fluorides in the mass spectra of several tris  $\beta$ -diketonates; metastable transitions are documented for the elimination of  $AlF_3$ ,  $CrF_3$ ,  $FeF_3$ ,  $FeF_2$  and  $CoF_2$  from appropriate metal-containing fragments. The loss of the difluorides  $FeF_2$  and  $CoF_2$  from  $Met(III)L_3$  precursors also suggests that a change in metal valency occurs in these complexes.

The proposed ion dissociation pathways for the 1,1,1-trifluoro-2,4-pentanedione and 1,1,1,5,5,5-hexafluoro-2,4-pentanedione transition metal chelates discussed above are shown in Schemes 8 (tris complexes) and 9 (bis complexes). The most important influence of the coordinated metal in these processes would appear to be its reducibility. On the other hand, the ligand composition is crucial in determining the nature of the fragments, since essentially all fragmentation proceeds via the loss of all or a portion of a ligand.



$\text{---} \times \times \times \rightarrow$  reaction step in which a decrease in metal oxidation state is proposed.

**Scheme 8.** Fragmentation routes for tris metal complexes of 1,1,1-trifluoro-2,4-pentanedione and 1,1,1,5,5,5-hexafluoro-2,4-pentanedione (106).



++ → reaction step in which a decrease in metal oxidation state is proposed.

**Scheme 9.** Fragmentation routes for bis metal complexes of 1,1,1-trifluoro-2,4-pentanedione and 1,1,1,5,5,5-hexafluoro-2,4-pentanedione (106).

Charalambous and co-workers (116) have investigated the mass spectra of gallium(III) and indium(III) complexes derived from 1,1,1-trifluoro-2,4-pentanedione. The molecular ions of these compounds fragment by ligand radical elimination to give  $[\text{MetL}_2]^+$  ions, which in turn decompose in a sequence of reactions involving losses of  $\text{CF}_2$ ,  $\text{HF}$  and  $\text{CH}_2\text{CO}$ . The presence of  $[\text{LMetF}]^+$  and  $[\text{LMetF-CF}_2]^+$  indicates fluorine migration to the metal, although confirmatory evidence (such as formation of neutral metal fluorides) is absent. The stability of the +1 oxidation state of gallium is exemplified in the ions  $[\text{Met(I)L}]^+$  and  $[\text{Met(I)}]^+$ ; these species were previously seen in the mass spectra of Ga(III) and In(III) acetylacetonates (116).

The introduction of fluorine into  $\beta$ -diketonates is also of significance insofar as electron attachment and negative ion formation is concerned. In an extended series of reports, I.K. Gregor and co-workers have attempted to rationalize the various ion decomposition pathways of a number of bis- and tris-metal  $\beta$ -diketonates. The negative-ion mass spectra of metal chelates of 1,1,1-trifluoro-2,4-pentanedione (129) and 1,1,1,5,5,5-hexafluoro-2,4-pentanedione (130-132) are distinguished by their extreme simplicity vis-à-vis the corresponding positive-ion spectra. In general, the molecular anion predominates, with the ligand ion being the only major fragmentation product. This is consistent with a reaction pathway involving decomposition of the molecular ion to yield the ligand anion and a metal-containing neutral in a reduced oxidation state (see Equation [17]). Although fragmentation is minimal, proof of fluorine

rearrangement is found in the ions  $[L_2\text{MetF}]^-$ ,  $[\text{LMetF}_2]^-$  and  $[\text{LMetF}]^-$ . These species are significantly more abundant for the metals magnesium, manganese, cobalt and zinc than for nickel or copper; a similar trend in the gas phase reactivity of these metals has been discerned from positive-ion spectra.

Gregor has also examined electron capture processes in several odd-electron  $d^9$  copper(II) (133) and even-electron  $d^8$  nickel(II) (134)  $\beta$ -diketonates of the form  $\text{Met}(\text{RCOCHCOR}')_2$ , where R is an alkyl or aryl group and R' is a perfluoroalkyl group. Once again, the negative-ion mass spectra of these complexes are simple;  $[\text{MetL}_2]^-$  and  $[\text{L}]^-$  ions predominate. However, the presence of aryl substituents in the ligands results in some novel rearrangements, leading to the formation of  $[\text{LMetR}]^-$  and  $[\text{RMetR}]^-$ . Fluorine atom transfers of the type observed in the tri- and hexafluoro derivatives are also evident.

Dillow and Gregor (135) have identified several reactions involving radical additions and ligand displacements in the chloride ion NCI mass spectra of the zinc(II) complexes  $\text{Zn}(\text{RCOCHCOR}')_2$  (R, R' = CH<sub>3</sub>; R, R' = tert-butyl; R = CH<sub>3</sub>, R' = CF<sub>3</sub>; R, R' = CF<sub>3</sub>). Major ions include  $[\text{ZnL}_2\text{Cl}]^-$ ,  $[\text{ZnL}_2]^-$ ,  $[\text{ZnLCl}_2]^-$ ,  $[\text{ZnLCl}]^-$  and  $[\text{ZnCl}_3]^-$ . According to the authors, the tendency of the complexes to undergo resonance electron capture is dependent upon the degree of fluorination in the ligands; the increasing ion currents carried by  $[\text{ZnL}_2]^-$  as the number of fluorine atoms increases provides evidence of an enhanced cross-section for resonance electron capture in the fluorinated chelates.

One of the few applications of positive chemical ionization to the study of metal  $\beta$ -diketonates is found in a report by Gregor et al. (136) concerning the interaction of divalent manganese, cobalt, nickel, copper and zinc hexafluoroacetylacetonates with pyridine under CI conditions. Significant ions include  $[\text{MetLpy}_2]^+$ ,  $[\text{MetLpy}_3]^+$  and  $[\text{MetL}_2\text{py}_2]^+$  (py = pyridine). Metastable peaks corresponding to the loss of pyridine from the above ions indicate the reversibility of pyridine addition to these metal chelates.

Olefin chemical ionization mass spectra of Cu(II) acetylacetonates, trifluoroacetylacetonates and hexafluoroacetylacetonates have been published by Morris and Koob (137). Reactions include fragmentation of the complex, reduction of copper(II) to copper(I), and subsequent complexation of the Cu(I) species with the reagent olefin. This sequence is most pronounced when the ligand is hexafluoroacetylacetone, suggesting that the mechanism leading to ionization and dissociation of  $\text{CuL}_2$  (presumably proton transfer from the olefin to the unsaturated diketonate ligand) is considerably more exothermic for bis(1,1,1,5,5,5-hexafluoro-2,4-pentanedionato)Cu(II) than for either the acetylacetonate or trifluoroacetylacetonate complexes.

Morris and Johnston (138) have described the multiphoton ionization and fragmentation of selected transition metal  $\beta$ -diketonates. The spectra obtained for the complexes  $\text{Met}^n(\text{RCOCHCOR}')_n$  (Met = Cr(III), Co(III), Fe(III), Co(II), Ni(II); R, R' =  $\text{CH}_3$ ; R =  $\text{CH}_3$ , R' =  $\text{CF}_3$ ; R, R' =  $\text{CF}_3$ ) display extensive fragmentation; the bare metal ion is the base peak in all cases. In contrast to the large metal-organic ions formed



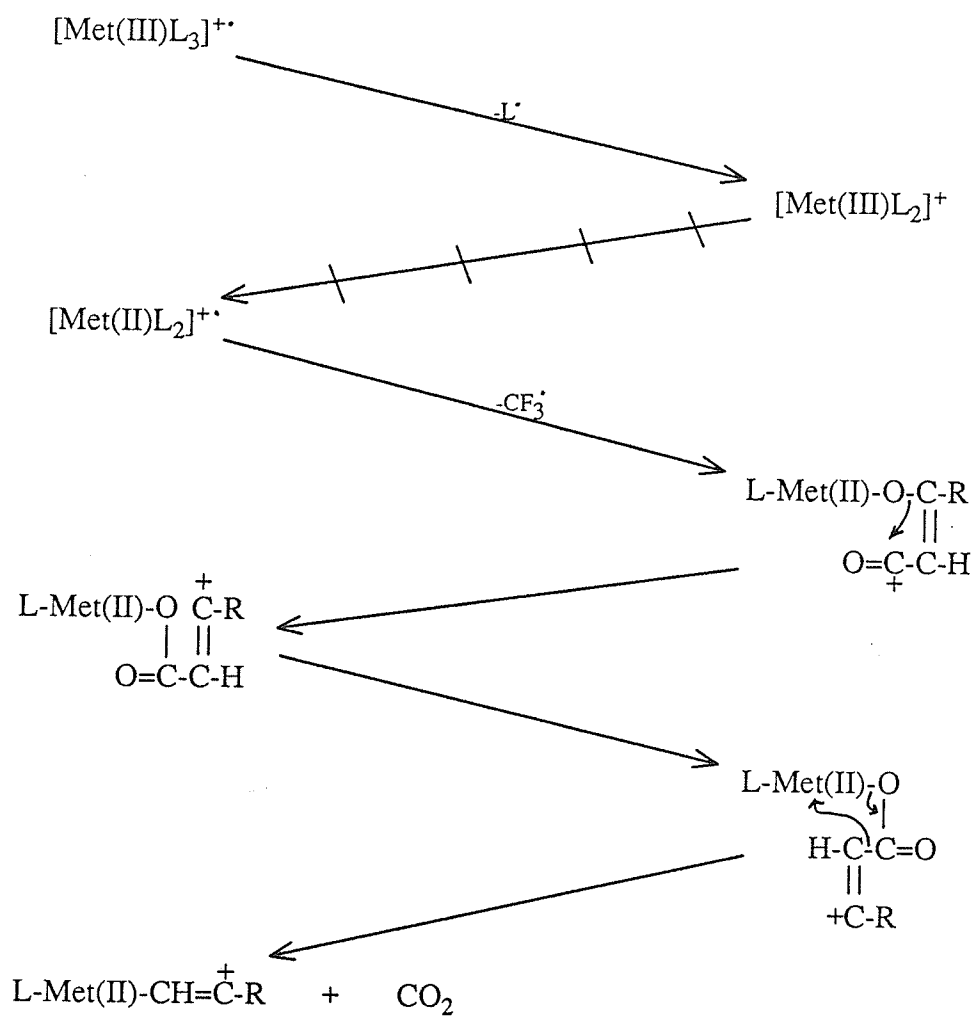
in EI, multiphoton ionization (MPI) produces small clusters between metal atoms and electronegative species (eg.  $[\text{MetO}]^+$ ,  $[\text{MetF}]^+$ ,  $[\text{MetF}_2]^+$ ). The exclusive production of these ions suggests that the dominant mechanism for MPI of metal chelates is dissociation to the bare metal atom (or a small rearrangement cluster) followed by ionization.

Fukuda and Campana's laser photodissociation study (139) of the mass-selected molecular ions of several transition metal chelates of 2,4-pentanedione and 1,1,1-trifluoro-2,4-pentanedione has revealed a fragmentation pattern dependent upon both the nature of the metal center and the composition of the ligand. In general, chelates of the trivalent metals Cr(III), Mn(III), Fe(III) and Co(III) fragment via the loss of a single intact ligand, while the divalent species Mn(II), Co(II), Fe(II), Ni(II), Cu(II) and Zn(II) eliminate the terminal R' substituent from the ligand (R,R' = CH<sub>3</sub> for acetylacetonate; R' = CF<sub>3</sub> for trifluoroacetylacetonate). The non-transition metal  $\beta$ -diketonates studied (those of Al(III) and Ga(III)) do not readily photodissociate. These results suggest that a metal d-orbital interaction may be involved in the photodissociation process, perhaps as a charge-transfer, metal-to-ligand ( $d \rightarrow \pi$ ) transition.

Evidence suggesting the loss of carbon dioxide in the mass spectra of some partially-fluorinated metal(III)  $\beta$ -diketonates has been presented by Clobes, Morris and Koob (140). Elimination of CO<sub>2</sub> is observed for fragment ions derived from chelates of the type  $\text{Met}(\text{RCOCHCOCF}_3)_3$ , where Met = Fe(III), Co(III) and R = phenyl,

substituted phenyl and 2-thienyl. The unusual skeletal rearrangement necessary to yield  $\text{CO}_2$  (the oxygen atoms in a  $\beta$ -diketone are separated by three carbon atoms) apparently requires the presence of both the metal and an aromatic substituent on the chelate ring; carbon dioxide elimination is not observed in the uncomplexed ligand or when R is an aliphatic group. The variety of aromatic substituents capable of supporting this reaction suggests that instead of being structurally associated with the elimination, these groups act in a stabilizing manner by way of electrostatic or resonance effects. A proposed mechanism is shown in Scheme 10. Although the precise role of the metal is not known, the particular metal involved appears crucial; studies of comparable Cr(III) and Al(III) complexes show no tendencies towards the loss of carbon dioxide.

Globes, Morris and Koob (128) have discussed the mass spectra of the Al(III), Cr(III), Fe(III) and Co(III) complexes of 1,1,1,5,5,5-hexafluoro-2,4-pentanedione, 1,1,1-trifluoro-2,4-pentanedione, 1,1,1-trifluoro-4-phenyl-2,4-butanedione and the Fe(III) chelate of 1,1,1-trifluoro-4-(2'-thienyl)-2,4-butanedione. In accordance with the earlier observations of Macdonald and Shannon (105), the fragmentation pathways are dependent upon the ability of the complexed metal to change valence state, thereby determining whether an even-electron or radical fragment is apt to be eliminated. Decompositions common to all of the chelates include the losses of a ligand radical,  $\text{CF}_3^\cdot$  and  $\text{CF}_2$  (accompanied by fluorine migration to the metal). The elimination of the  $\text{EE}^0$  species HF is seen in most of the complexes, but only in ions that already have a fluorine attached to the metal, eg.  $[\text{LMetF}(\text{L-CF}_3)]^+$

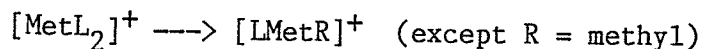


$\text{---}\times\times\text{---}\rightarrow$  reaction step in which a decrease in metal oxidation state is proposed.

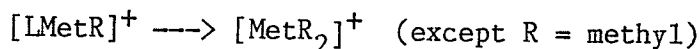
**Scheme 10.** Fragmentation pathway involving loss of  $\text{CO}_2$  from some fluorinated Fe(III) and Co(III)  $\beta$ -diketonates (140).

loses HF to form  $[\text{LMet}(\text{L}-\text{CHF}_3)]^+$ , implying that the metal-bonded fluorine forms part of the leaving group. The introduction of asymmetry into the ligands clearly demonstrates their influence in determining the nature of the fragmentation. The phenyl- and thienyl-substituted  $\beta$ -diketonates give the ion  $[\text{LMetR}]^+$ , formed as a result of a direct aryl group migration ( $\text{R} = \text{phenyl}$  or  $\text{thienyl}$ ) from the ligand to the metal. The relative stability of the aryl-metal bond versus the alkyl-metal bond is reflected by the absence of  $[\text{LMetR}]^+$  when  $\text{R} = \text{CH}_3$  or  $\text{CF}_3$ .

The EI and CI mass spectra of several gallium(III) and indium(III) chelates of  $\text{RCOCH}_2\text{COCF}_3$  ( $\text{R} = \text{methyl}$ ,  $\text{phenyl}$ ,  $4\text{-fluorophenyl}$ ,  $4\text{-methylphenyl}$ ,  $4\text{-methoxyphenyl}$ ,  $2\text{-thienyl}$  and  $2\text{-naphthyl}$ ) have been reported by Das (141). In the electron ionization spectra, the base peak is the  $\text{EE}^+$  fragment ion  $[\text{MetL}_2]^+$ . Additional reactions include the loss of  $\text{CF}_2$  from  $[\text{MetL}_2]^+$ , the elimination of the metal-bonded fluorine from  $[\text{MetL}_2\text{-CF}_2]^+$  in the form of HF or  $\text{RCOF}$ , and migration of R to the metal in the reactions:



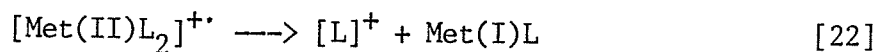
and

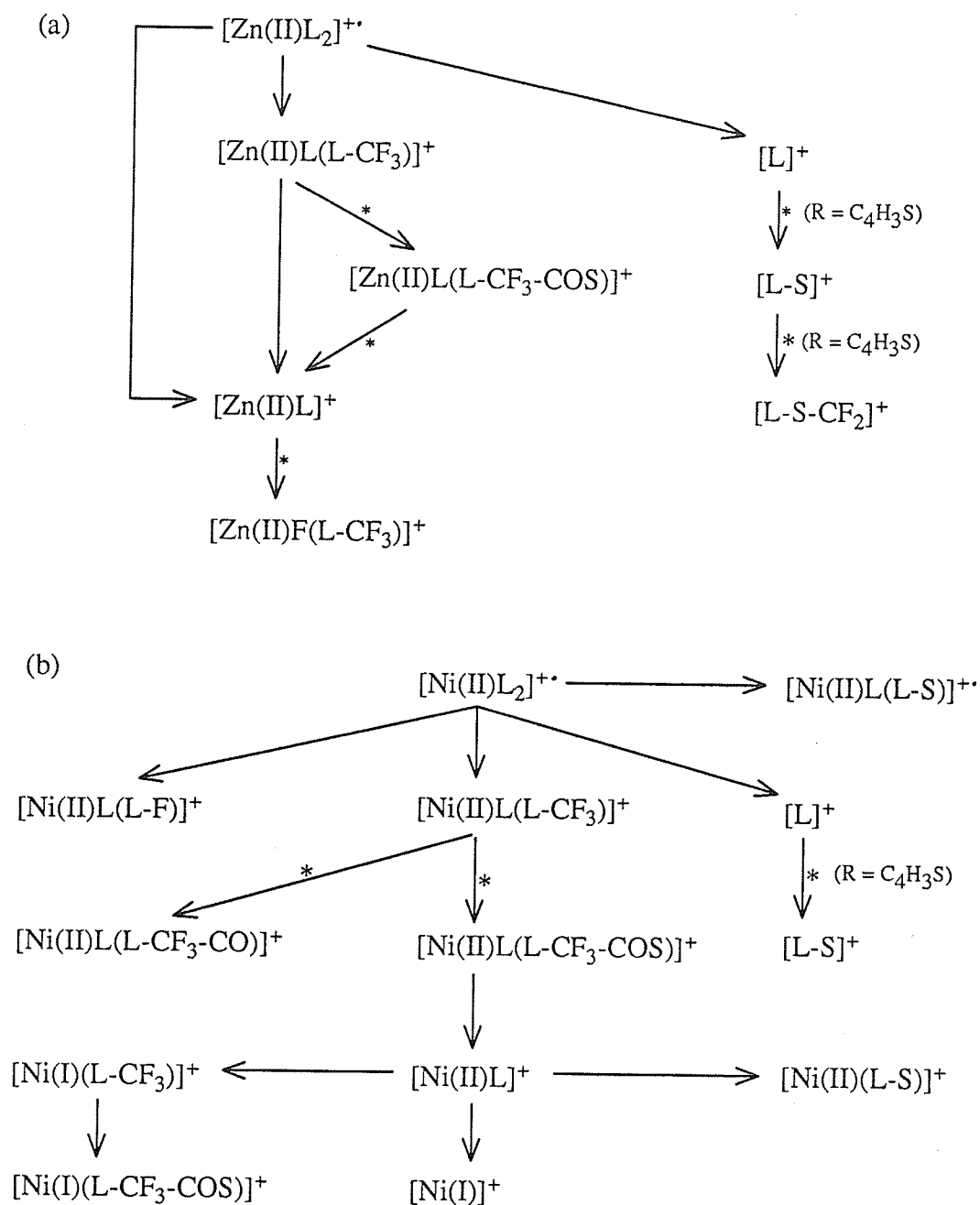


The major ions in the  $\text{H}_2$ -CI spectra are the protonated molecular ion  $[\text{MetL}_3\text{H}]^+$ ,  $[\text{MetL}_3\text{H}-\text{HCF}_3]^+$ ,  $[\text{MetL}_3\text{H}-\text{RH}]^+$ ,  $[\text{MetL}_3\text{H}-\text{HF}]^+$  and  $[\text{MetL}_2]^+$ .

Das (142) has published the mass spectra of selected palladium(II) chelates of fluorinated  $\beta$ -diketones:  $\text{Pd}(\text{RCOCHCOR}')_2$  where  $\text{R}' = \text{CF}_3$ ,  $\text{R} = \text{methyl, 2-furyl, phenyl, 2-thienyl}$ ;  $\text{R}' = \text{C}_2\text{F}_5, \text{C}_3\text{F}_7$ ,  $\text{R} = \text{phenyl, 2-thienyl}$ . Prominent ions include the molecular ion, those formed through R migrations to the metal, and those involving the loss of CO. Notably absent from the spectra are ions associated with the transfer of fluorine to palladium.

Most of the mass spectral studies concerning metal monothio- $\beta$ -diketonates have been reported by S.E. Livingstone and M. Das. Their investigations have covered a wide range of transition metal chelates of fluorinated monothio- $\beta$ -diketones possessing both alkyl and aryl substituents. For example, the major fragmentation routes arising from electron ionization of the zinc(II) and nickel(II) chelates  $\text{Met}(\text{RCSCHCOCF}_3)_2$  ( $\text{R} = \text{phenyl, 4-methylphenyl, 2-thienyl and methyl}$ ) (143) are summarized in Scheme 11. The zinc complexes give strong peaks for  $[\text{ZnL-CF}_2]^+$ ,  $[\text{HL}]^+$ ,  $[\text{L}]^+$ ,  $[\text{RCSCH}]^+$  and  $[\text{RCS}]^+$ , while the most intense signals in the nickel chelate spectra include  $[\text{NiL}_2]^+$ ,  $[\text{NiL}_2\text{-F}]^+$ ,  $[\text{NiL}_2\text{-CF}_3]^+$ ,  $[\text{NiL}_2\text{-COCF}_3]^+$ ,  $[\text{NiL}]^+$ ,  $[\text{Ni}]^+$  and  $[\text{L}]^+$ . In many instances, metastable peaks help to confirm reaction pathways. A strong signal corresponding to  $[\text{L-S}]^+$  is evident in the zinc and nickel chelates of 1,1,1-trifluoro-4-mercapto-4-(2'-thienyl)-but-3-en-2-one. The intense  $[\text{L}]^+$  peak present in all of the spectra results from a process involving a decrease in the oxidation state of the metal:



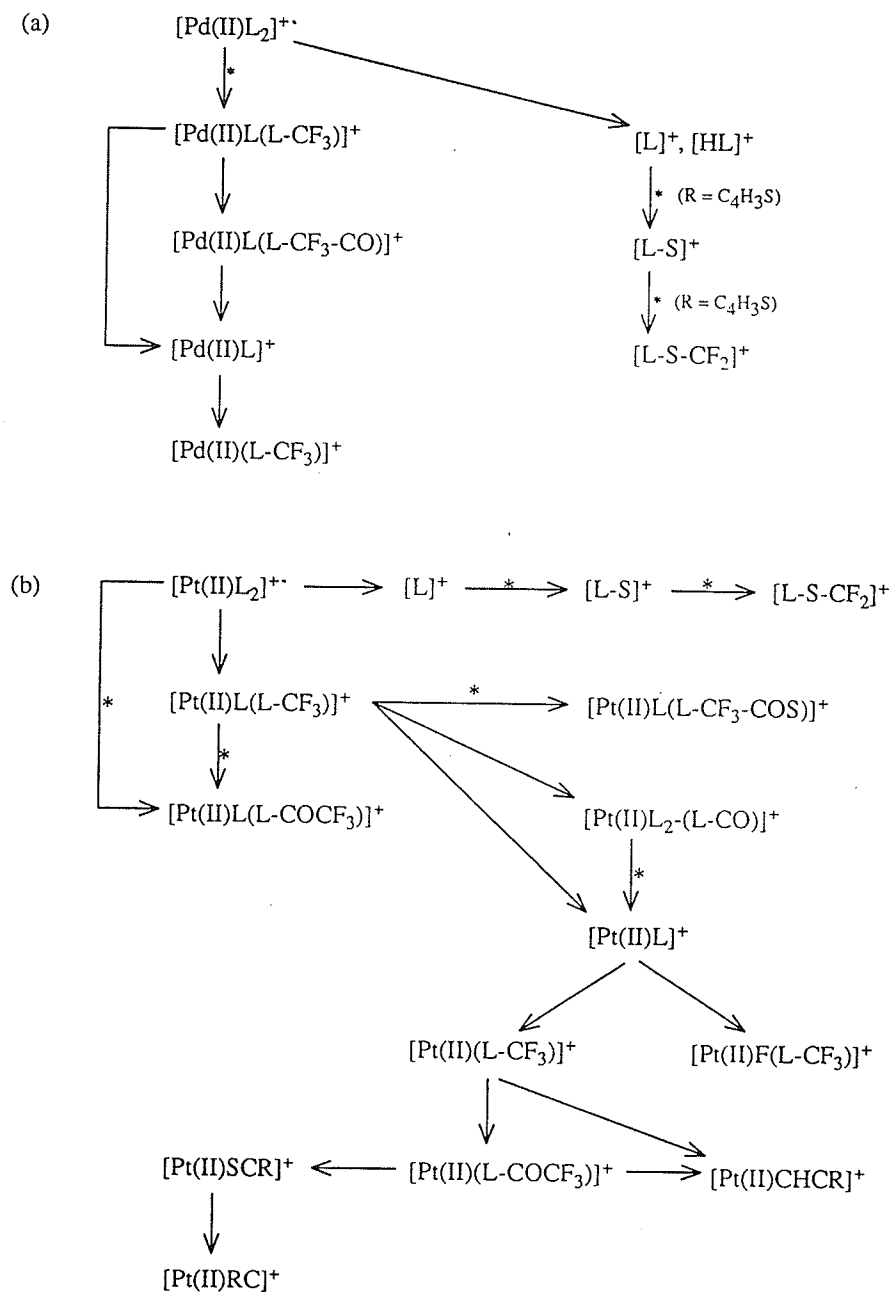


\* reaction confirmed by the observation of a metastable transition.

**Scheme 11.** Fragmentation pathways for (a) Zn(II) and (b) Ni(II) chelates  $\text{Met}(\text{RCSCHCOCF}_3)_2$  ( $\text{R} = \text{C}_6\text{H}_5$ ,  $p\text{-CH}_3\text{C}_6\text{H}_4$ ,  $\text{C}_4\text{H}_3\text{S}$  and  $\text{CH}_3$ ) (143).

Das and Livingstone (144) have reported the mass spectra of the palladium(II) and platinum(II) chelates  $\text{Met}(\text{RCSCCHCOCF}_3)_2$ , where R = phenyl, 4-methylphenyl, 4-bromophenyl, 4-nitrophenyl, 2-thienyl and methyl (Pd only). The major fragmentation routes for the Pd and Pt complexes are summarized in Scheme 12. The palladium chelates give intense signals for  $[\text{PdL}_2]^+$ ,  $[\text{PdL}_2\text{-CF}_3]^+$ ,  $[\text{PdL}]^+$ ,  $[\text{LH}]^+$ ,  $[\text{L}]^+$ ,  $[\text{RCSCH}]^+$  and  $[\text{RCS}]^+$ , while the dominant ions in the platinum mass spectra are  $[\text{PtL}_2]^+$ ,  $[\text{PtL}_2\text{-COCF}_3]^+$ ,  $[\text{PtL}_2\text{-CF}_3\text{-COS}]^+$ ,  $[\text{PtL}]^+$ ,  $[\text{PtL-CF}_2]^+$ ,  $[\text{PtL-CF}_3]^+$ ,  $[\text{PtL-COCF}_3]^+$ ,  $[\text{LH}]^+$ ,  $[\text{L}]^+$ ,  $[\text{L-S}]^+$ ,  $[\text{L-S-CF}_2]^+$ ,  $[\text{RCSCH}]^+$  and  $[\text{RCS}]^+$ . In general, the platinum chelates yield more intense and more numerous metal-containing fragments than their palladium counterparts. The ion  $[\text{L-S}]^+$  appears in the spectra of three of the platinum complexes (R = phenyl, 4-methylphenyl and 2-thienyl) but in only one of the palladium chelates (R = 2-thienyl). A degree of resonance stabilization in the platinum-derived  $[\text{L-S}]^+$  ions is proposed. As well, formation of metal-fluorine bonds is evident only in the platinum chelates.

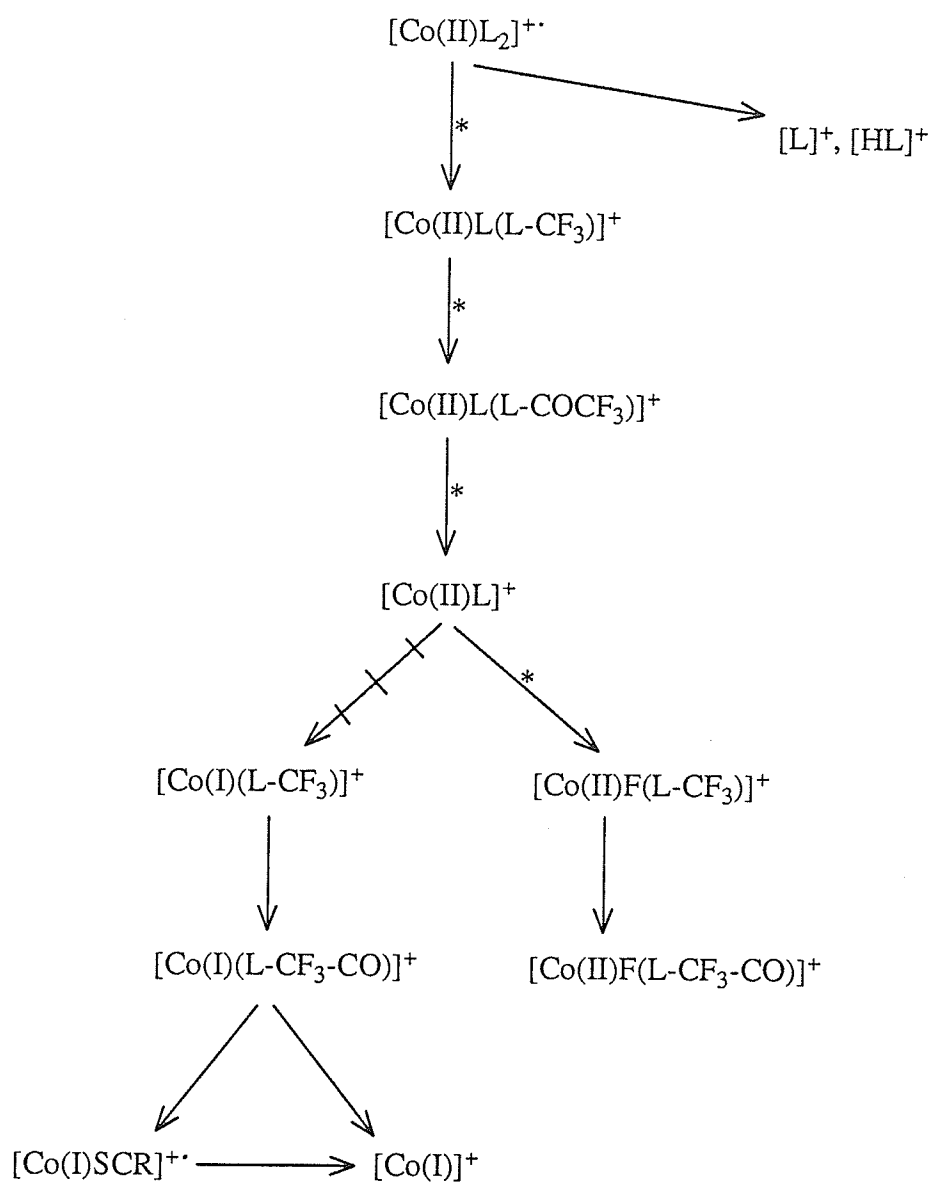
A report by Das and Livingstone (145) concerning the EI mass spectra of the tris cobalt(III) chelates  $\text{Co}(\text{RCSCCHCOCF}_3)_3$  (R = phenyl, 4-methylphenyl, 4-bromophenyl, 4-fluorophenyl, 2-thienyl and methyl) has appeared in the literature. The major fragmentation pathways are presented in Scheme 13. The lack of a molecular ion is probably the most noteworthy aspect of these spectra. The parent molecule is believed to undergo thermal degradation in the mass spectrometer to yield the divalent  $\text{CoL}_2$  species and a ligand radical. Although cobalt(III) molecular ions are visible in chelates of fluorinated  $\beta$ -



\* reaction confirmed by the observation of a metastable transition.

**Scheme 12.** Fragmentation pathways for (a) Pd(II) and (b) Pt(II) chelates  $\text{Met}(\text{RCSCHCOCF}_3)_2$  ( $\text{R} = \text{C}_6\text{H}_5$ ,  $p\text{-CH}_3\text{C}_6\text{H}_4$ ,  $p\text{-BrC}_6\text{H}_4$ ,  $p\text{-NO}_2\text{C}_6\text{H}_4$ ,  $\text{C}_4\text{H}_3\text{S}$  and  $\text{CH}_3$ ) (144).





\* reaction confirmed by the observation of a metastable transition.

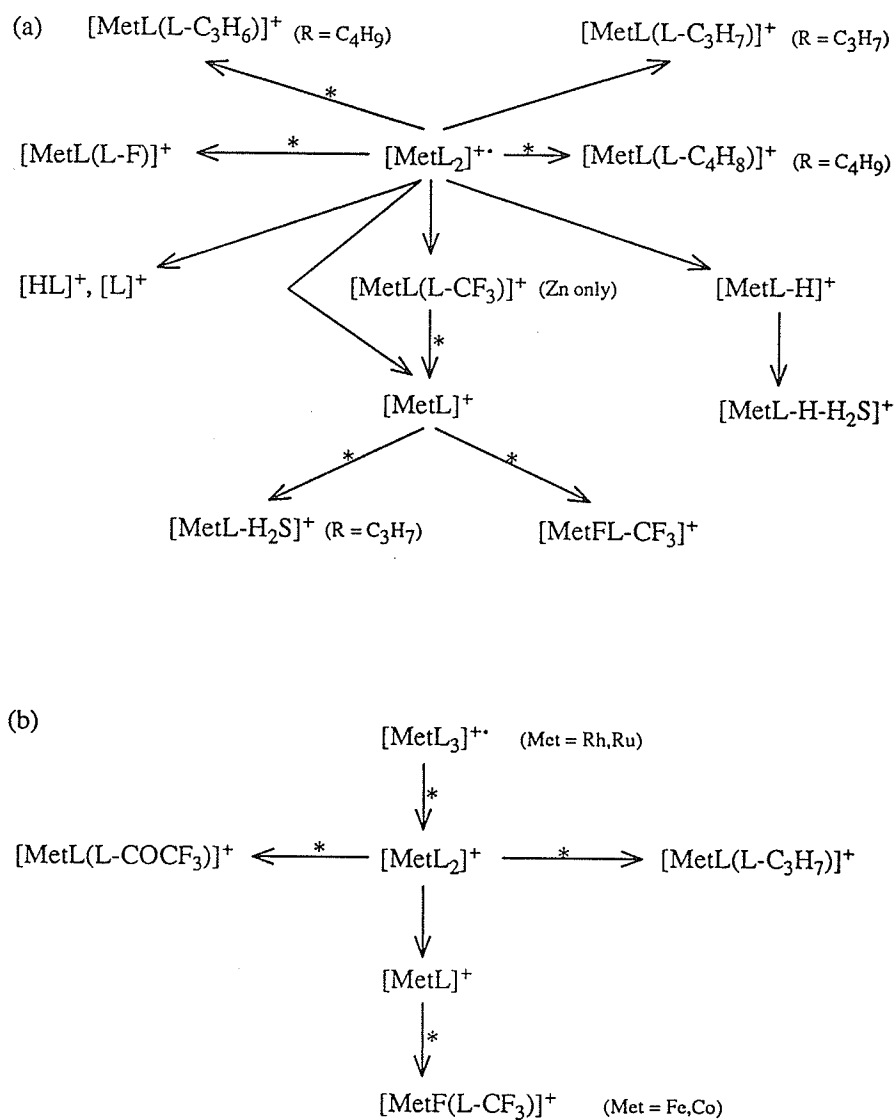
$\times \times \rightarrow$  process in which a decrease in metal oxidation state is proposed.

**Scheme 13.** Fragmentation pathways for the cobalt(III) chelates  
 $\text{Co(RCSCHCOCF}_3)_3$  (R =  $\text{C}_6\text{H}_5$ ,  $p\text{-CH}_3\text{C}_6\text{H}_4$ ,  $p\text{-BrC}_6\text{H}_4$ ,  $p\text{-FC}_6\text{H}_4$ ,  
 $\text{C}_4\text{H}_3\text{S}$  and  $\text{CH}_3$ ) (145).

diketones (128), the substitution of a sulfur for an oxygen in the chelate ring apparently lowers the thermal stability of the resulting monothio complex. Major ions in the cobalt spectra include  $[\text{CoL}_2]^+$ ,  $[\text{CoL}]^+$ ,  $[\text{CoL-CF}_2]^+$ ,  $[\text{CoL-CF}_2\text{-CO}]^+$ ,  $[\text{CoL-CF}_3]^+$ ,  $[\text{L}]^+$  and  $[\text{CF}_3]^+$ . A further reduction in the oxidation state of cobalt (from +2 to +1) is necessary in order to rationalize the loss of the OE' neutral  $\text{CF}_3$  from the  $\text{EE}^+$  ion  $[\text{Co(II)L}]^+$ .

Livingstone and Saha (146) have obtained mass spectral data on the nickel(II), palladium(II), platinum(II), zinc(II) and rhodium(III) chelates  $\text{Met}^{\text{II}}(\text{RCSCHCOCF}_3)_n$  (R = isopropyl, isobutyl) and on the analogous iron(III), ruthenium(III) and cobalt(III) complexes where R = isopropyl. The major fragmentation routes for the divalent and trivalent species are summarized in Scheme 14. Not all fragmentations shown are common to every complex. The novel features of the spectra are the occurrence of the ions  $[\text{MetL}_2\text{-(R-H)}]^+$ ,  $[\text{MetL}_2\text{-R}]^+$ ,  $[\text{MetL-H}]^+$  and the loss of  $\text{H}_2\text{S}$  from  $[\text{MetL}]^+$  and  $[\text{MetL-H}]^+$ . Attempts to obtain the mass spectra of the copper(II) chelates of these alkyl-substituted monothio- $\beta$ -diketones proved unsuccessful, possibly because of thermal decomposition in the ion source.

The monothio- $\beta$ -diketone 1,1,1-trifluoro-4-mercapto-4-(2'-naphthyl)-but-3-en-2-one (R =  $\text{C}_{10}\text{H}_7$ , R' =  $\text{CF}_3$ ) and its iron(III), ruthenium(III), cobalt(III), rhodium(III), nickel(II), palladium(II), platinum(II) and zinc(II) chelates have been examined by Livingstone and Moore (147). Many of the observed fragmentations are consistent with those of other monothio- $\beta$ -diketonates of these metals. However,



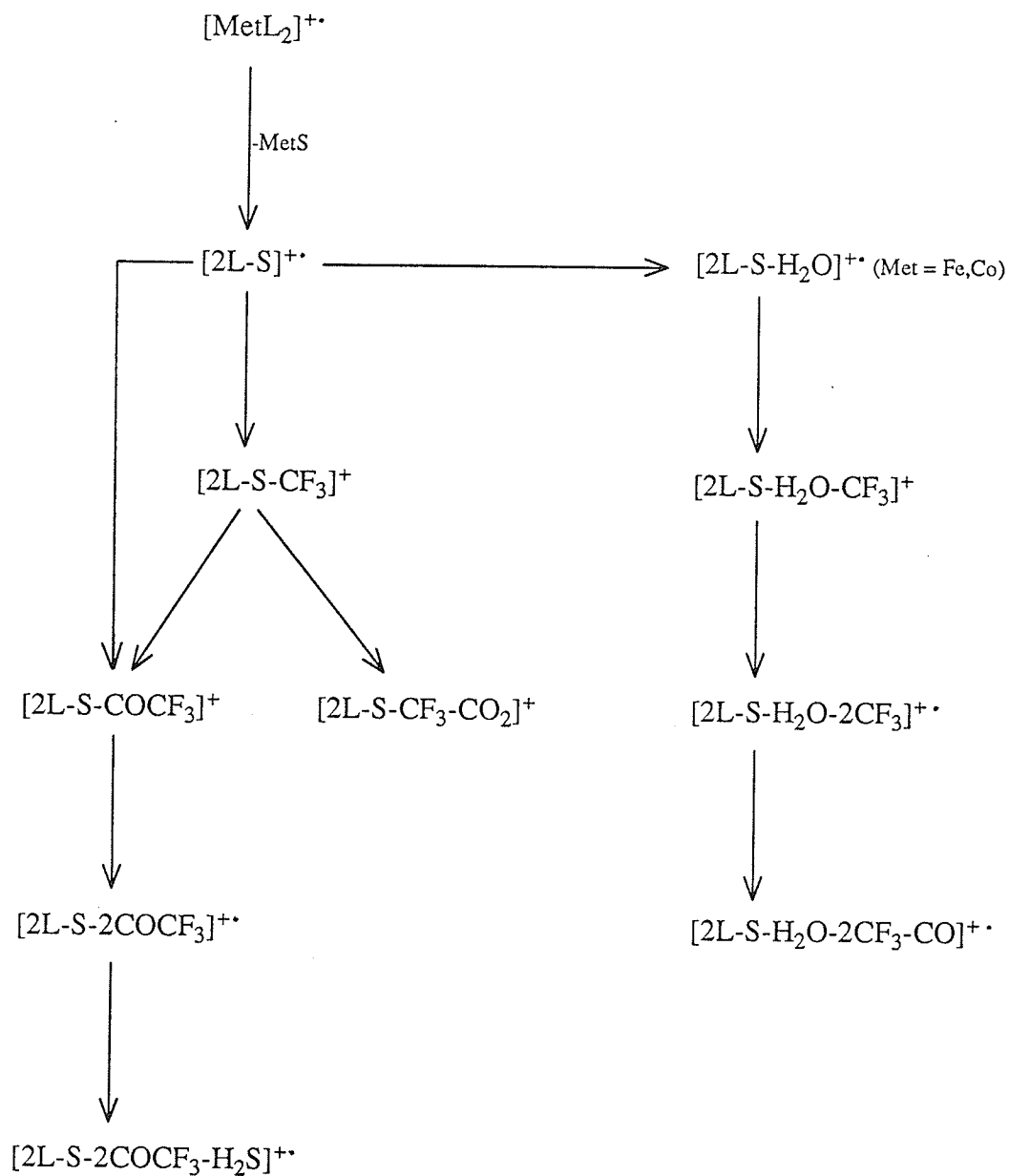
\* reaction confirmed by the observation of a metastable transition.

**Scheme 14.** Fragmentation pathways for (a) Ni(II), Zn(II), Pd(II), Pt(II) and Rh(III) chelates  $\text{Met}^n(\text{RCSCHCOF}_3)_n$  (R = iso-C<sub>3</sub>H<sub>7</sub>, iso-C<sub>4</sub>H<sub>9</sub>) and (b) Fe(III), Ru(III) and Co(III) chelates  $\text{Met}(\text{RCSCHCOF}_3)_3$  (R = iso-C<sub>3</sub>H<sub>7</sub>) (146).

with the exception of the zinc complex, all of the metal chelates exhibit a number of unique, high-mass, metal-free peaks derived from the loss of MetS from  $[\text{Met(II)L}_2]^+$ . The major fragmentation routes emanating from the  $[\text{MetL}_2\text{-MetS}]^+$  ion are shown in Scheme 15.

The electron ionization mass spectra of several nickel(II), zinc(II) and cobalt(III) complexes of the monothio- $\beta$ -diketone  $\text{RC(SH)=CHCOCHF}_2$  (R = phenyl, 2-thienyl, 4-methylphenyl) have been discussed by Das (99). Losses of 32 and 111 mass units from the molecular ions of the nickel complexes result in the species  $[\text{NiL}_2\text{-S}]^+$  and  $[\text{NiL}_2\text{-CHF}_2\text{-COS}]^+$ , respectively. These decompositions have also been observed in the mass spectra of the nickel(II) derivatives of  $\text{RC(SH)=CHCOCF}_3$  (R = phenyl, 2-thienyl, 4-methylphenyl) (143). The zinc chelate  $\text{Zn}(\text{C}_4\text{H}_3\text{SCSCHCOCHF}_2)_2$  shows the loss of HF from the molecular ion (the proton eliminated is believed to originate from the  $\text{CHF}_2$  group) but an absence of  $\text{CF}_2$  loss from  $\text{ZnL}$ . Loss of  $\text{CF}_2$  would involve the unfavorable migration of a proton to the metal; conversely, migration of fluorine to the metal would require the release of CHF, a relatively unstable species vis-à-vis  $\text{CF}_2$ . The Co(III) spectra lack both a molecular ion ( $[\text{CoL}_3]^+$ ) and evidence of fluorine transfer to the metal.

An investigation into the influence of ligand substituents and donor atom sets on the gas phase electron attachment reactions of a series of nickel(II) chelates has been carried out by Gregor and co-workers (148,149). The complexes studied are of the form  $\text{Ni}(\text{R}'\text{CXCHCYR})_2$ , where (X,Y) represent the three possible donor atom combinations, namely



**Scheme 15.** Fragmentation pathways involving loss of MetS (Met = Ni, Pd, Pt, Fe, Co, Ru, Rh) from chelates of 1,1,1-trifluoro-4-mercapto-4-(2'-naphthyl)-but-3-en-2-one (147).

(O,O), (O,S) and (S,S), and  $R' = \text{CH}_3, \text{CF}_3$  or  $\text{C}_2\text{H}_5\text{O}$ ,  $R = \text{CH}_3$ ;  $R' = \text{C}_6\text{H}_5, \text{CH}_3$  or  $\text{CF}_3$ ,  $R = \text{C}_6\text{H}_5$ ;  $R', R = \text{tert-C}_4\text{H}_9$ . The negative ion mass spectra are very simple; they are characterized by the domination of molecular and ligand ion peaks. While the ligand substituents exert considerable influence over the various ion decompositions, the relative  $[\text{NiL}_2]^-$  intensities are largely dependent upon the ligand donor atom sets, with stabilities decreasing in the order  $(\text{O},\text{O}) > (\text{O},\text{S}) > (\text{S},\text{S})$ . The relative ease of reductive elimination of  $\text{Ni}(\text{I})\text{L}$  (see Equation [21]) appears to increase as the number of co-ordinating sulfur atoms increases, a possible consequence of the greater degree of covalency of the Ni-S bond as compared to the Ni-O bond. As well, the dithioenolate anion ( $[\text{L}]^-$ ) is appreciably stabilized through charge delocalization.

#### 6. Hard and Soft Acids and Bases: Applications to Rearrangements in the Mass Spectra of Halogenated Metal $\beta$ -diketonate Complexes

Molecular ions formed under 70eV electron bombardment have sufficient activation energy to undergo not only simple cleavage, but also rearrangements involving both cleavage and bond formation. In the case of organometallic compounds, the most interesting rearrangements are those involving the central metal atom, either accompanied by the transfer of an atom (or group of atoms) to the metal in a fragment ion, or in the expulsion of a neutral metal-containing species from an ion (150). Metal  $\beta$ -diketonates are certainly not immune to these processes; the migration of fluorine to the central metal and the elimination of neutral metal fluorides is a well-documented phenomenon

in appropriately-substituted metal chelates. However, the underlying basis for the rearrangements and the reasons behind the bonding preferences shown by various metals towards the migrating species is not as well understood. One concept which shows some promise in this regard is the Principle of Hard/Soft Acids and Bases (HSAB). This section will describe the HSAB principle in some detail, including its characteristics and theoretical rationale. Applications to the mass spectra of halogenated metal complexes will also be discussed.

One of the most important classes of chemical reaction is the generalized acid-base reaction:



where, according to the Lewis definition, a base (B) is an atom, molecule or ion possessing at least one pair of valence electrons which are not already being shared in a covalent bond, and an acid (A) is a unit in which at least one atom has a vacant orbital capable of accommodating a pair of electrons. The nature of A:B may be that of a coordination compound or complex ion (in which A is a metal atom or ion), an ordinary inorganic or organic molecule, or a charge transfer complex, among others. In all instances, it can be assumed that A is acting in part as an electron acceptor and B as an electron donor.

The special case where A is a metal ion has been studied extensively, and many of the associated equilibrium constants for Equation [23] are known. Ahrland, Chatt and Davies (151) were among the first to correlate the relative affinities of donor atoms (ligands,

Lewis bases) for metal acceptor molecules and ions. They concluded that there was no uniform pattern of relative co-ordinating affinities of all ligand atoms for all acceptors, but rather a dependence existed upon the particular acceptor or donor concerned. However, two general rules did emerge: (i) a significant difference in co-ordinating attraction exists between the first and the second element from each of Groups VA, VIA and VIIA of ligand atoms i.e. between N and P, O and S, F and Cl; (ii) acceptor ions and molecules are of two well-defined types: class (a), which form their most stable complexes with the first ligand atom of each Group, and class (b), which form their most stable complexes with the second or subsequent ligand atoms of each Group. The division between the two classes is by no means definite; each oxidation state of the metal can be regarded as a unique acceptor (eg. Cu(I) has considerably more class (b) character than Cu(II), while Fe(III) exhibits more class (a) behavior than Fe(II)). Even when the oxidation state is specified, the boundary remains slightly diffuse, depending in its detail on the specific group of ligand atoms under consideration.

The rules of Ahrland, Chatt and Davies were used by Pearson (152) to classify other kinds of generalized Lewis acids. He observed that the features common to class (a) acceptors are small size, high positive oxidation state and few easily-distorted or removable valence electrons, while class (b) acids are characterized by low charge, large size and several valence electrons capable of being easily-distorted or removed. Since the features which promote class (a) behavior are those which lead to high electronegativity and low polarizability, and those



which favour type (b) behavior lead to low electronegativity and high polarizability, Pearson found it convenient to call class (a) acids "hard acids" and class (b) acids "soft acids". In subsequent reports (153-155), he defined a "hard base" as one which possesses a donor atom low in polarizability, high in electronegativity and difficult to oxidize, and a "soft base" as one in which the donor atom is of high polarizability, low electronegativity and easily oxidized.

Comprehensive listings of hard and soft acids and bases are given in Tables 4 and 5. These classifications of hardness and softness led Pearson to propose a simple rule governing the stability of acid-base complexes: hard acids prefer to bind to hard bases and soft acids prefer to bind to soft bases. This principle, while not a formal law, has nevertheless been invaluable in qualitatively predicting and correlating the results of a vast number of acid-base equilibria.

The most important properties that determine softness in Lewis acids include size, oxidation state, electronic structure and other attached groups. For instance, in elements of variable valence, there is usually a smooth increase in hardness as the oxidation state increases. It appears safe to assume that the increase in charge leads to a sharp decrease in polarizability and hence a strengthening of the (a) character. The importance of d-electrons for metal ions has been stressed by Ahrland (156), who noted that all good class (b) acceptors have a large number (six or more) of d-electrons in their outer shell. The existence of many d-electrons, however, does not necessarily constitute a soft acceptor; electrons in orbitals outside the d-shell

**Table 4.** Classification of hard and soft acids.Hard Acids

$H^+$ ,  $Li^+$ ,  $Na^+$ ,  $K^+$ , ( $Rb^+$ ,  $Cs^+$ )

$Be^{2+}$ ,  $Be(CH_3)_2$ ,  $Mg^{2+}$ ,  $Ca^{2+}$ ,  $Sr^{2+}$  ( $Ba^{2+}$ )

$Sc^{3+}$ ,  $La^{3+}$ ,  $Ce^{4+}$ ,  $Gd^{3+}$ ,  $Lu^{3+}$ ,  $Th^{4+}$ ,  $U^{4+}$ ,  $UO_2^{2+}$ ,  $Pu^{4+}$

$Ti^{4+}$ ,  $Zr^{4+}$ ,  $Hf^{4+}$ ,  $VO^{2+}$ ,  $Cr^{3+}$ ,  $Cr^{6+}$ ,  $MoO^{3+}$ ,  $WO^{4+}$ ,  $Mn^{2+}$ ,  $Mn^{7+}$ ,  $Fe^{3+}$ ,  $Co^{3+}$

$BF_3$ ,  $BCl_3$ ,  $B(OR)_3$ ,  $Al^{3+}$ ,  $Al(CH_3)_3$ ,  $AlCl_3$ ,  $AlH_3$ ,  $Ga^{3+}$ ,  $In^{3+}$

$CO_2$ ,  $RCO^+$ ,  $NC^+$ ,  $Si^{4+}$ ,  $Sn^{4+}$ ,  $CH_3Sn^{3+}$ ,  $(CH_3)_2Sn^{2+}$

$N^{3+}$ ,  $RPO_2^+$ ,  $ROPO_2^+$ ,  $As^{3+}$

$SO_3$ ,  $RSO_2^+$ ,  $ROSO_2^+$

$Cl^{3+}$ ,  $Cl^{7+}$ ,  $I^{5+}$ ,  $I^{7+}$

HX (hydrogen-bonding molecules)

Borderline Acids

$Fe^{2+}$ ,  $Co^{2+}$ ,  $Ni^{2+}$ ,  $Cu^{2+}$ ,  $Zn^{2+}$

$Rh^{3+}$ ,  $Ir^{3+}$ ,  $Ru^{3+}$ ,  $Os^{2+}$

$B(CH_3)_3$ ,  $GaH_3$

$R_3C^+$ ,  $C_6H_5^+$ ,  $Sn^{2+}$ ,  $Pb^{2+}$

$NO^+$ ,  $Sb^{3+}$ ,  $Bi^{3+}$

$SO_2$

**Table 4.** (continued).Soft Acids

$\text{Co}(\text{CN})_5^{3-}$ ,  $\text{Pd}^{2+}$ ,  $\text{Pt}^{2+}$ ,  $\text{Pt}^{4+}$

$\text{Cu}^+$ ,  $\text{Ag}^+$ ,  $\text{Au}^+$ ,  $\text{Cd}^{2+}$ ,  $\text{Hg}^+$ ,  $\text{Hg}^{2+}$ ,  $\text{CH}_3\text{Hg}^+$

$\text{BH}_3$ ,  $\text{Ga}(\text{CH}_3)_3$ ,  $\text{GaCl}_3$ ,  $\text{GaBr}_3$ ,  $\text{GaI}_3$ ,  $\text{Tl}^+$ ,  $\text{Tl}(\text{CH}_3)_3$

$\text{CH}_2$ , carbenes

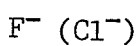
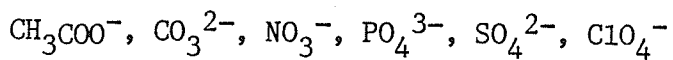
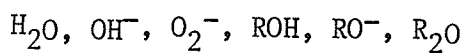
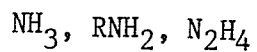
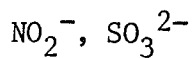
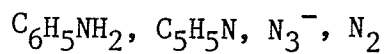
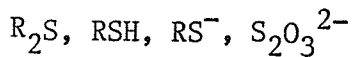
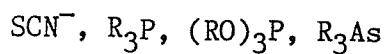
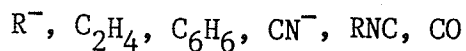
$\pi$ -acceptors: trinitrobenzene, chloroanil, quinones, tetracyanoethylene

$\text{HO}^+$ ,  $\text{RO}^+$ ,  $\text{RS}^+$ ,  $\text{RSe}^+$ ,  $\text{Te}^{4+}$ ,  $\text{RTe}^+$

$\text{Br}_2$ ,  $\text{Br}^+$ ,  $\text{I}_2$ ,  $\text{I}^+$ ,  $\text{ICN}$ , etc.

$\text{O}$ ,  $\text{Cl}$ ,  $\text{Br}$ ,  $\text{I}$ ,  $\text{N}$ ,  $\text{RO}$ ,  $\text{RO}_2$

$\text{M}^0$  (metal atoms) and bulk metals

**Table 5.** Classification of hard and soft bases.Hard BasesBorderline BasesSoft Bases

can produce considerable weakening of the (b) properties, presumably due to a shielding effect on the outer d-electrons.

The hardness of a given acceptor is also a function of the other groups bonded to it. The introduction of soft, polarizable substituents can soften an otherwise hard acid, while the addition of electron-withdrawing groups often reduces the softness of a site. Further, the presence of "hard" groups on an acceptor facilitates the addition of other hard substituents to it, while "soft" donors on the acceptor make it easy to add other soft bases. Jorgensen (157) was the first to comment on this important effect, coining the term "symbiosis" to describe it. Symbiotic behavior in metal complexes can be rationalized if one considers that it is the actual charge on the central atom, rather than the formal charge, which determines softness.

An explanation of why the HSAB principle works requires a consideration of all of the factors which determine the strength of chemical bonds. No one component seems universally responsible, and several theories have been proposed by investigators looking at different aspects of acid-base behavior.

The oldest and simplest explanation for hard-hard and soft-soft interactions is the ionic-covalent theory. Hard acids are assumed to bind to hard bases primarily by ionic or electrostatic forces; small size and high positive (acceptor) and negative (donor) charges favour such bonding. On the other hand, soft acids bind soft bases mainly by covalent bonds. Clearly, Pearson's criteria of low charge, high

polarizability and low electronegativity for soft-soft complex formation meld easily into the classical interpretation of covalent bonding.

Chatt's theory of  $\pi$ -bonding (158,159) has been proposed as a possible explanation for HSAB behavior. In this context, the important features of soft acids are their low oxidation states and abundance of loosely-held, outer d-orbital electrons. These electrons can form  $\pi$ -bonds by donation to ligands for which suitable empty orbitals exist on the basic atom. Many soft ligands presumably use vacant d-orbitals to accommodate the extra electrons; the increase in (b) acceptor affinity between the first donor atoms of each Group (i.e. the hard bases N, O and F, none of which have d-orbitals of the same principal quantum number as the bonding electrons), and the following ones (soft bases P, As, S and I, where such orbitals exist and are vacant) is generally greater than that predicted on the basis of increases in polarizability alone. Unsaturated ligands such as carbon monoxide and isonitriles would also be able to accept metal electrons by means of empty, but not too unstable  $\pi^*$  molecular orbitals. Conversely, hard basic atoms such as oxygen and fluorine can form  $\pi$ -bonds in the opposite sense, by donating electrons from the ligand to the empty, energetically-accessible orbitals of the class (a) acid. With soft acids, there would be a repulsive interaction between the filled orbitals on the metal and those associated with the hard base.

Pitzer (160) points out that London dispersion energies increase with increasing size and polarizability and thus might stabilize a bond

between two soft atoms. It seems reasonable to assume that some small degree of stabilization due to London forces will always exist in a complex formed between a polarizable acid and a polarizable base.

Mulliken (161) offers an alternative explanation for the extra stability of bonds formed between soft acids and soft bases. He proposes that d-p orbital hybridization occurs so that both the  $\pi$ -bonding molecular orbitals and the  $\pi^*$  antibonding orbitals contain some admixed d character. This has the two-fold effect of strengthening the bonding orbital by increasing overlap and weakening the antibonding orbital by decreasing overlap. Mulliken's theory and Chatt's  $\pi$ -bonding theory are essentially alike except for the added stabilization due to the antibonding molecular orbital. According to Mulliken, this effect can be more important than the more usual  $\pi$ - $\pi$  bonding because the antibonding orbital is more antibonding than the bonding orbital is bonding, if overlap is included. This condition greatly lessens the electronic repulsions found in soft-soft systems, where there is considerable mutual penetration of charge clouds.

Quantum mechanical perturbation theory has also been applied to the problem. Klopman's method (162) emphasizes the importance of charge and frontier-controlled effects. The frontier orbitals are the highest occupied orbitals of the base (donor) and the lowest unoccupied orbitals of the acid (acceptor). When the difference in energy of these orbitals is large, very little electron transfer occurs and a charge-controlled, ionic interaction results. When the frontier orbitals are of similar energy, significant electron transfer from the

donor to the acceptor can take place, resulting in a frontier-controlled, covalent bond. By considering the energies of the frontier orbitals and the changes in solvation energy that accompany electron transfer, Klopman has succeeded in calculating a set of characteristic energy values for many cations and anions. These numbers show a good correlation with the known hard or soft behavior of the ions and can be used to predict the stability of a given acid-base complex. While the apparent success of Klopman's approach speaks well for the ionic-covalent theory, there is no reason to discount the possibility that  $\pi$ -bonding and electron correlation (London dispersion and Mulliken's hybridization effects) play an important role in some instances.

Miller and co-workers (163) were the first to apply Hard/Soft Acid/Base theory to rearrangements in the mass spectra of organometallic compounds. Their study of a series of Group IVA and VA perfluoro-phenyl complexes of the type  $(C_6F_5)_n Met^{n+}$  (Met = Si(IV), Sn(IV), Ge(IV), Pb(IV), P(III), As(III) and Sb(III)) revealed spectral evidence for Met-F bond formation, especially in the Sn(IV), Si(IV) and Sb(III) compounds. They also examined a set of mercury(II) complexes  $(C_6X_5)_2Hg$  (X = F, Cl and Br) and reported observing several Hg-Br bonded ions, but no Hg-F or Hg-Cl containing species. Assigning the halide as the base and the central atom as the acid, these results conform quite closely with the tenets of the HSAB theory. Mercury, being a particularly soft acid, will favour bromide addition in preference to fluoride or chloride. The Groups IVA and VA metals for which fluorine transfer is favoured can all be considered hard acids,



so the migration of a hard base such as  $F^-$  is not unexpected. It should be noted that in separate studies (164-166) concerning the transfer of fluorine from a fluoroaromatic ring to a central carbon, nitrogen or oxygen atom, Miller found no evidence of fluorine migration. He suggests that one of the requirements for fluorine transfer is the presence of a vacant orbital on the central atom (such orbitals are absent for the C, N and O derivatives). This line of reasoning is in keeping with Chatt's theory of  $\pi$ -bonding in hard-hard acid-base complexes.

The extension of the HSAB principle to the mass spectra of fluorinated metal  $\beta$ -diketonates has been carried out by Morris and Koob (167). Rearrangement of fluorine to the metal to form either Met-F containing ions or neutrals is reported in the Co(II), Fe(III), Fe(II), Cr(III), Al(III), Zn(II), Ni(II) and Mn(II) complexes of 1,1,1,5,5,5-hexafluoro-2,4-pentanedione ( $R = R' = CF_3$ ). All of the metals mentioned above can be considered hard or borderline hard acids. Fluorine migration to these centers is therefore in keeping with HSAB theory (the two electron-withdrawing  $CF_3$  groups on the ligand would be expected to "harden" the borderline metals, making them more receptive to a fluorine transfer). Fluorine rearrangement is notably absent, however, in the spectrum of the copper(I) complex; Cu(I) is recognized as a soft acid and so would not be expected to bind with fluorine. Comparing the hexafluoroacetylacetonate results with those obtained when R is methyl, ethyl, isopropyl, tert-butyl, phenyl and 2'-thienyl reveals a striking dependence of the rearrangement ions' intensities on the nature of the substituent. Replacing a  $CF_3$  group with a more

electron-rich species softens the acidity of the metal, so fluorine rearrangement becomes less prevalent. This phenomenon is also seen in the reactions in which the species HF is eliminated. When one of the  $\text{CF}_3$  groups is replaced by methyl or phenyl, the relative abundances for the ions resulting from HF loss increase dramatically; softening the metal environment weakens its ability to compete with H for the fluorine.

Morris and Koob (168) have provided an interesting test of the HSAB theory as applied to non-fluorine halogenated  $\beta$ -diketonates. The Cu(II), Co(II), Mn(II), Al(III), Cr(III) and Fe(III) complexes of 1,1,1-trichloro-2,4-pentanedione give mass spectra in which the rearrangement of chlorine from the ligand to the metal emerges as a dominant reaction. The facile Cl transfer competes effectively with the internal reduction step associated with fragments arising from an OE neutral loss from an  $\text{EE}^+$  ion, a process shown to be important for many metal complexes of other  $\beta$ -diketones. In terms of HSAB theory, chloride is considered a softer base than fluoride, and as such is expected to soften the otherwise hard central metal. The combination of a softer base and a softened acid environment results in a good match between the chloride and the complexed metal.

## B. EXPERIMENTAL

### 1. Mass Spectra

Low resolution, positive-ion EI mass spectra of the metal chelates were initially recorded on an Hitachi RMU-6D single-focusing magnetic sector instrument (Hitachi, Ltd.; Tokyo, Japan) using the following operating parameters: accelerating voltage, 1800 V; resolution, 700 (nominal); electron beam energy, 70 eV (except where noted); total emission, 50  $\mu$ A; ion source temperature, 100-150  $^{\circ}$ C; scan time, 300 seconds ( $m/z$  12 - 600). All samples were introduced into the ion source via a direct-inlet probe and heated to produce an even rate of volatilization and to ensure reproducible mass spectra. All spectra were recorded on a Honeywell model 1508 Visicorder using uv-sensitive chart paper. A minimum of one background scan was taken prior to each spectral acquisition.

Later, spectra were acquired on a VG7070E-HF double-focusing mass spectrometer (VG Analytical Ltd.; Manchester, England) equipped with a DEC Micro PDP-11/73 data system (Digital Equipment Corporation; Maynard, Mass.). The following operating parameters were used: accelerating voltage, 6 kV; resolution, 1400; electron beam energy, 70 eV (except where noted); trap current, 200  $\mu$ A; ion source temperature, 200  $^{\circ}$ C; scan rate, 1.0 sec/decade. Sample introduction was accomplished in a manner similar to that described above. Perfluorokerosene (PFK) was admitted into the ion source through a

heated septum inlet and used as a calibrant for all mass spectra. Reported results were the average of at least three representative scans.

Linked-scanning experiments were also performed on the VG7070E-HF double-focusing mass spectrometer. Constant B/E and constant neutral loss scans of selected metal chelates were obtained as per the prescribed operating procedures. Collision-induced dissociation (CID) was implemented to increase the abundance of metastable ions; helium gas was introduced into a collision cell located in the first field-free region (FFR) of the spectrometer. The pressure in the collision cell was adjusted so that approximately 50% attenuation of the molecular ion beam was achieved.

The following linked-scanning experiments were performed (see Table 6 for an explanation of number codes):

<u>Complex</u>	<u>Function Type</u>	<u>Function Mass</u>
<b>A1-3a</b>	Daughter	457
	"	407
	"	261
	Neutral loss	50
<b>Ga-3a</b>	Daughter	535
	"	321
	Neutral loss	50

<b>Co-8a</b>	Daughter	501
	"	432
	"	280
	"	230
	Neutral loss	44
<b>Ni-2a</b>	Daughter	464
	"	413
	"	261
	Neutral loss	96
<b>Pd-8a</b>	Daughter	548
	"	410
	"	327
<b>Cu-13a</b>	Daughter	593
	"	474
	"	355
	"	328
	"	209
<b>Zn-8a</b>	Daughter	506
	"	437
	"	285
<b>Co-14b</b>	Daughter	633
	"	514
	"	486
	"	346
	Neutral loss	32

<b>Ni-5b</b>	Daughter	556
	"	459
	"	307
	"	210
	Neutral loss	32
<b>Pd-7b</b>	Daughter	628
	"	367
	Neutral loss	97
<b>Zn-7b</b>	Daughter	586
	"	517
	"	325
	"	275

## 2. Ligand Synthesis

All ligands were synthesized by Dr. Manoranjan Das or purchased commercially. Literature references are given in parentheses at the end of each synthetic procedure.

### (a) Fluorinated $\beta$ -Diketones

{1}  $\text{RCOCH}_2\text{COCHF}_2$  (R = phenyl, 2-thienyl).

Equimolar quantities (0.1 mole) of ethyl difluoroacetate ( $\text{CHF}_2\text{COOC}_2\text{H}_5$ ) and the appropriate methyl ketone ( $\text{CH}_3\text{COR}$ ) were added to a suspension of sodium methoxide, which was prepared by the

reaction of Na (3 g) and methanol (15 mL) in dry ether (100 mL). After standing at room temperature overnight, the mixture was treated with a solution of  $\text{KHSO}_4$  until slightly acidic (pH paper). A saturated aqueous copper acetate solution (200 mL) was then added, with stirring. The ether was removed over a steambath and the green copper complex of the  $\beta$ -diketone filtered and washed with ethanol. The copper complex was resuspended in ether (400 mL) and  $\text{H}_2\text{S}$  was passed through the solution for one hour. The resulting copper sulfide precipitate was filtered off with the aid of Whatman cellulose powder. The filtrate was dried over anhydrous  $\text{Na}_2\text{SO}_4$ , the ether evaporated off, and the crude product recrystallized from a small volume of ethanol (99).

{2}  $\text{RCOCH}_2\text{COCF}_3$  (R = phenyl, 2-thienyl, 2-furyl, 2-naphthyl).

These ligands are available from commercial sources; Aldrich Chemical Co. (R = phenyl, 2-thienyl) and Eastman Kodak Co. (R = 2-furyl and 2-naphthyl).

{3}  $\text{RCOCH}_2\text{COCF}_3$  (R = 4-fluorophenyl, 4-chlorophenyl, 4-methylphenyl, 4-methoxyphenyl).

These ligands were prepared by a Claisen condensation method analogous to that reported in part {1} above, using ethyl trifluoroacetate and the appropriate para-substituted acetophenone (169).

{4}  $\text{RCOCH}_2\text{COCF}_3$  (R = 5-chloro-2-thienyl, 5-methyl-2-thienyl).

These ligands were prepared by a Claisen condensation of methyl ketone ( $\text{RCOCH}_3$ ) and ethyl trifluoroacetate ( $\text{CF}_3\text{COOC}_2\text{H}_5$ ), using a procedure similar to that described in part {1}.

- {5}  $\text{RCOCH}_2\text{COC}_2\text{F}_5$  (R = phenyl, 2-thienyl, 2-naphthyl).

These ligands were prepared by a Claisen condensation of methyl ketone ( $\text{RCOCH}_3$ ) and ethyl pentafluoropropanoate ( $\text{CF}_3\text{CF}_2\text{COOC}_2\text{H}_5$ ) as in part {1}.

- {6}  $\text{RCOCH}_2\text{COC}_3\text{F}_7$  (R = phenyl, 2-thienyl, 2-naphthyl).

These ligands were prepared by a Claisen condensation of methyl ketone ( $\text{RCOCH}_3$ ) and ethyl heptafluorobutanoate ( $\text{CF}_3\text{CF}_2\text{CF}_2\text{COOC}_2\text{H}_5$ ) as in part {1}.

(b) Fluorinated Monothio- $\beta$ -diketones

- {1}  $\text{RCSHCHCOCF}_3$  (R = phenyl, 4-fluorophenyl, 4-methylphenyl, 4-methoxyphenyl).

Dry  $\text{H}_2\text{S}$  was passed at a rapid rate for 30 minutes through a solution of the  $\beta$ -diketone (4 g) in dry ethanol (250 mL), cooled to  $-70^\circ\text{C}$  in an ethanol/dry ice bath. Dry HCl was then passed for 15 min at a rapid rate. The reaction flask was fitted with a  $\text{CaCl}_2$  drying tube to prevent the access of moisture. The mixture was allowed to stand at room temperature for about 20 h. The resulting deep red solution was poured into ice-cold water (400 mL) with constant stirring, whereupon a deep red solid separated. The mixture was allowed to stand in an ice bath for 30 min with occasional stirring. The products were red liquids at room temperature, which could be extracted from the aqueous mixture with light petroleum. After drying over anhydrous  $\text{Na}_2\text{SO}_4$ , the extract was concentrated to a volume of 200 mL and a solution of lead



acetate trihydrate (4 g) in 90% alcohol (100 mL) added. Water (200 mL) was then added, and the lead complex was separated by filtration, washed with hot water, and dried over phosphorus pentoxide. The dried lead complex from three batches was suspended in light petroleum (300 mL) and dry  $H_2S$  passed for 90 min. The resulting lead sulfide was removed by filtration and the filtrate dried over anhydrous sodium sulfate. The solvent was evaporated off to yield the pure monothio- $\beta$ -diketone as a red oil (169,170).

{2}  $RCSHCHCOCF_3$  (R = 2-thienyl, 5-methyl-2-thienyl).

The ligands were prepared by the HCl-catalyzed action of dry  $H_2S$  gas on an alcoholic solution of the  $\beta$ -diketones in a manner similar to that described in part {1}, with the exception that after standing in an ice bath for 30 min, the aqueous ligand mixture was filtered, washed with water, dried over silica gel, and recrystallized from light petroleum to give red crystals (98).

{3}  $RCSHCHCOCF_3$  (R = 2-naphthyl).

Dry  $H_2S$  was passed at a rapid rate for 30 minutes through a solution of the  $\beta$ -diketone (5 g) in dry alcohol (200 mL) at  $-70^\circ C$  (ethanol/dry ice bath). Dry HCl was then passed through for 15 min. The reaction mixture was allowed to stand at room temperature for 2 hours, whereupon  $H_2S$  and HCl were again passed as before at  $-70^\circ C$ . After standing at room temperature overnight, the mixture was poured, with vigorous stirring, into ice water (400 mL) and kept in an ice bath for 30 min. The red crystals of the compound deposited were filtered, washed with ice-cold water, and dried in vacuum over phosphorus pentoxide (147).

{4}  $\text{RCSHCHCOC}_2\text{F}_5$  (R = phenyl, 2-thienyl, 2-naphthyl).

Dry  $\text{H}_2\text{S}$  was passed for 30 minutes through a solution of  $\beta$ -diketone (5 g) in 250 mL absolute alcohol cooled in an ethanol/dry ice bath. This was followed by the passage of dry HCl for 15 minutes. The mixture was then allowed to stand at room temperature for about 20 hours; the reaction vessel was fitted with a  $\text{CaCl}_2$  drying tube to prevent the access of moisture. Once again, the mixture was cooled to  $-70^\circ\text{C}$ , the passage of gases repeated and the solution allowed to stand at room temperature for 20 h. The resulting red solution was poured into ice-water (400 mL) and kept at  $0^\circ\text{C}$  for 30 min. The product was extracted with 75 mL of petroleum ether and dried over anhydrous sodium sulfate. Removal of the solvent gave the ligand as a red oil (100).

{5}  $\text{RCSHCHCOC}_3\text{F}_7$  (R = phenyl, 2-thienyl, 2-naphthyl).

These ligands were prepared by the HCl-catalyzed action of dry  $\text{H}_2\text{S}$  gas on an alcoholic solution of the  $\beta$ -diketones as described in part {5} above (100).

### 3. Metal Chelate Synthesis

The metal chelates prepared from commercially-purchased ligands are designated with an asterisk (\*). All other complexes were synthesized either by Dr. Manoranjan Das or in our laboratory from ligands prepared by Das.

(a) Chelates of  $\beta$ -diketones

(i) Al(III)  $\beta$ -diketonates

- {1}  $\text{Al}(\text{RCOCHCOCHF}_2)_3^*$  (R = phenyl, 2-thienyl).

Aluminum(III) chloride hexahydrate (0.16 mmole) in water (5 mL) was added to a solution of the ligand (0.48 mmole) in absolute alcohol (3 mL). The mixture was warmed on a steam bath and a sufficient quantity of urea was added to raise the pH to about 4 (as determined by pH indicator sticks). A precipitate formed in the reaction vessel after 15 minutes of heating. The solution was cooled in an ice bath for one hour. The pale orange product was filtered under suction and dried for 2 hours (100 °C oven). The general synthetic method of Fernelius and Bryant was adopted (40).

- {2}  $\text{Al}(\text{RCOCHCOCF}_3)_3^*$  (R = 5-methyl-2-thienyl).

The preparation was similar to that described in {1}. The product was a pale yellow solid.

- {3}  $\text{Al}(\text{RCOCHCOCF}_3)_3$  (R = phenyl, 4-methylphenyl, 4-fluorophenyl, 2-thienyl).

These complexes were synthesized by M.Das based on the general synthetic methods of Fernelius and Bryant (40). Pale pink solids were obtained.

(ii) Ga(III)  $\beta$ -diketonates

- {1} Ga(RCOCHCOCHF<sub>2</sub>)<sub>3</sub> (R = phenyl, 2-thienyl).

Gallium(III) oxide (1.33 mmole) was dissolved in hot aqua regia and then evaporated to dryness. A solution of the ligand (8 mmole) in absolute ethanol (50 mL) was added, resulting in an almost clear solution on warming. The solution was filtered and concentrated ammonia was added to raise the pH to about 5. After storage in a refrigerator for 24 hours, the precipitate was filtered and washed with ice-cold absolute ethanol, giving a pale pink solid (141).

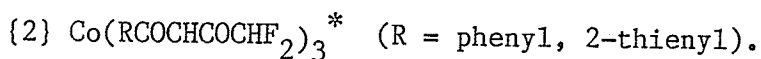
- {2} Ga(RCOCHCOCF<sub>3</sub>)<sub>3</sub> (R = phenyl, 4-methylphenyl, 4-fluorophenyl, 2-thienyl, 2-naphthyl).

The preparation was similar to that described in {1}. Pale pink solids were obtained.

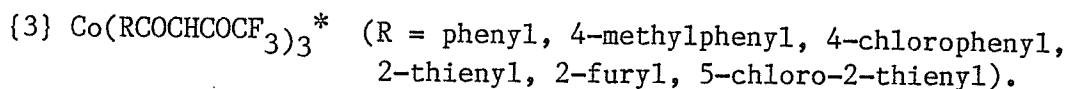
(iii) Co(III)  $\beta$ -diketonates

- {1} Preparation of Co(III) intermediate, Na<sub>3</sub>[Co(CO<sub>3</sub>)<sub>3</sub>].3H<sub>2</sub>O.

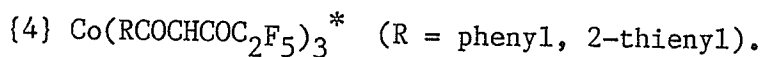
A 50 mL aqueous solution of cobalt(II) nitrate hexahydrate (0.10 mole) and 30% hydrogen peroxide (10 mL) was added dropwise with stirring to an ice-cold slurry of sodium bicarbonate (0.50 mole) in water (50 mL). The mixture was stirred in an ice bath for one hour. The olive-green product was filtered under suction, washed with 30 mL of cold water and then washed with cold absolute ethanol and allowed to dry in air. The synthetic procedure of Bauer and Drinkard was followed (42).



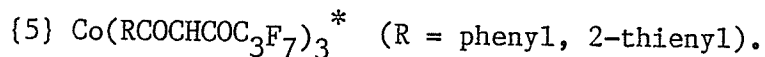
Sodium tris-carbonatocobaltate(III) trihydrate (prepared as described in {1} above; 0.3 mmole) and 6M  $\text{HNO}_3$  (0.15 mL) were added to a solution of the ligand (0.9 mmole) in 1.5 mL of aqueous alcohol (40% ethanol). A reflux apparatus was assembled (Excelo micro-organic kit) and the mixture refluxed for 30 min. The resulting green precipitate was filtered under suction, washed with cold water and air dried. A purity determination was made by TLC and further purification, if warranted, carried out by column chromatography (30% methylene chloride/petroleum ether on silica gel). This synthesis was based on a procedure described by Fay and Piper (43).



The preparation was similar to that described in {2}. Green solids were obtained.



The preparation was similar to that described in {2}. The products were dark green solids.



The preparation was similar to that described in {2}. Dark green, oily liquids were obtained.

(iv) Ni(II)  $\beta$ -diketonates

- {1} Ni(RCOCHCOCHF<sub>2</sub>)<sub>2</sub>\* (R = phenyl).

Nickel(II) acetate tetrahydrate (0.22 mmole) in water (5 mL) was added to a solution of the ligand (0.44 mmole) in absolute ethanol (3 mL). A cloudy, green precipitate formed on mixing. The solution was heated gently on a steam bath for 15 minutes and then cooled in an ice bath for one hour. The precipitate was filtered under suction, washed with cold water, and dried in an oven (100 °C) for 3 hours to give the desired product. The general synthetic method of Fernelius and Bryant was adopted for this synthesis (40).

- {2} Ni(RCOCHCOCHF<sub>2</sub>)<sub>2</sub> (R = 2-thienyl).

Nickel(II) acetate tetrahydrate (4 mmole) in hot ethanol (80 mL) was added to a solution of the ligand (8 mmole) in warm ethanol (30 mL). A pale green solid was deposited upon cooling in an ice bath. After filtering and washing with cold ethanol, the dried product was heated for one hour (110 °C) to give the desired compound (99).

- {3} Ni(RCOCHCOCF<sub>3</sub>)<sub>2</sub>\* (R = phenyl, 5-methyl-2-thienyl).

The preparation was similar to that described in part {1} above. Emerald green (R = phenyl) and pale green solids were obtained.

- {4} Ni(RCOCHCOCF<sub>3</sub>)<sub>2</sub>\* (R = 2-thienyl).

Nickel(II) sulfate hexahydrate (0.2 mmole) in water (5 mL) was added to a solution of the ligand (0.4 mmole) in absolute ethanol (3 mL). The mixture was warmed on a steam bath and urea was added

to raise the pH to about 4. After 15 minutes of heating, a precipitate formed. The solution was cooled in an ice bath for one hour. The precipitate was filtered under suction and dried in an oven (100 °C) for 2 hours to give the desired pale green product. The general synthetic method of Fernelius and Bryant was followed (40).

{5}  $\text{Ni}(\text{RCOCHCOC}_2\text{F}_5)_2$  (R = phenyl, 2-thienyl).

The preparation was similar to that described in {2}. Pale green solids were obtained.

{6}  $\text{Ni}(\text{RCOCHCOC}_3\text{F}_7)_2$  (R = phenyl, 2-thienyl).

The preparation was similar to that described in {2}. Pale green solids were obtained.

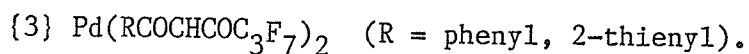
(v) Pd(II)  $\beta$ -diketonates

{1}  $\text{Pd}(\text{RCOCHCOCF}_3)_2$  (R = phenyl, 2-thienyl).

A filtered solution of potassium tetrachloropalladate(II) (4.9 mmole) in 50 mL of water was added to a solution of the ligand (9.8 mmole) in ethanol (50 mL). The mixture was digested for 15 min on a steam bath and then cooled in an ice-bath. The resulting yellow-green precipitate was filtered, washed with water and then with ice-cold absolute alcohol (81).

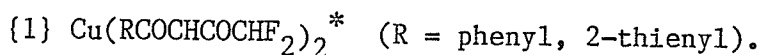
{2}  $\text{Pd}(\text{RCOCHCOC}_2\text{F}_5)_2$  (R = phenyl, 2-thienyl).

These complexes were prepared as described in {1}. For R = phenyl, the product was dried at 110 °C for one hour. Yellow solids were obtained.

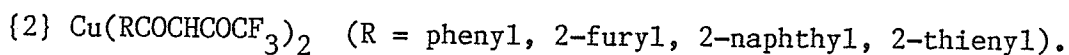


These complexes were prepared as described in {1}. For R = phenyl, the product was dried at 110 °C for one hour. Yellow solids were obtained.

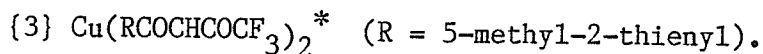
(vi) Cu(II)  $\beta$ -diketonates



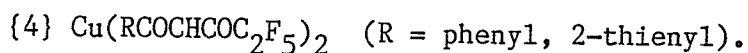
Copper(II) acetate monohydrate (0.2 mmole) in water (5 mL) was added to a solution of the ligand (0.4 mmole) in absolute ethanol (3 mL). The mixture was heated gently on a steam bath for 15 minutes and then cooled in an ice bath for 1 hour. The resulting precipitate was filtered under suction, washed with cold water and dried for 3 hours (100 °C oven). Blue-green (R = phenyl) and olive-green solids were obtained. The general synthetic method of Fernelius and Bryant was adopted (40).



These chelates were synthesized by Reichert and Westmore (125) using the general synthetic method of Fernelius and Bryant (40). Dark green (R = 2'-thienyl) and olive-green solids were obtained.



The preparation was similar to that described in {1}. An olive-green solid was obtained.



These complexes were synthesized by M. Das based on the general synthetic method of Fernelius and Bryant (40). Olive-green solids were obtained.



{5}  $\text{Cu}(\text{RCOCHCOC}_3\text{F}_7)_2$  (R = phenyl, 2-thienyl).

The preparation was similar to that described in {4}. Olive-green solids were obtained.

(vii) Zn(II)  $\beta$ -diketonates

{1}  $\text{Zn}(\text{RCOCHCOCHF}_2)_2^*$  (R = phenyl, 2-thienyl).

Zinc(II) acetate dihydrate (0.2 mmole) in water (5 mL) was added to a solution of the ligand (0.4 mmole) in absolute ethanol (3 mL). The mixture was heated gently on a steam bath for 15 minutes and then cooled in an ice bath for one hour. The resulting precipitate was filtered under suction, washed with ice cold water, and dried for 3 hours (100 °C oven). White (R = phenyl) and yellow-white solids were obtained. The general synthetic method of Fernelius and Bryant was followed (40).

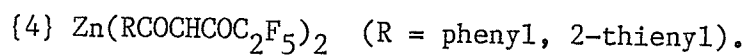
{2}  $\text{Zn}(\text{RCOCHCOCF}_3)_2^*$  (R = phenyl).

The preparation was similar to that described in {1}. A white crystalline solid was obtained.

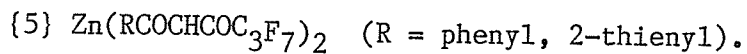
{3}  $\text{Zn}(\text{RCOCHCOCF}_3)_2^*$  (R = 2-thienyl, 5-methyl-2-thienyl).

Zinc(II) sulfate heptahydrate (0.2 mmole) in water (5 mL) was added to a solution of the ligand (0.4 mmol) in absolute ethanol (3 mL). The mixture was warmed on a steam bath and a sufficient quantity of urea added to raise the pH to about 4 (as determined by pH indicator sticks). A precipitate formed in the reaction vessel after 15 minutes of heating. The solution was cooled in an ice bath for one hour and then filtered under suction. The white

product was dried (100 °C oven) for 2 hours. The general synthetic procedure of Fernelius and Bryant was followed (40).



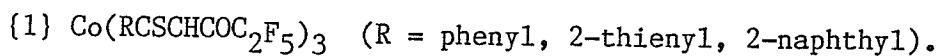
These complexes were synthesized by M. Das based on the methods of Fernelius and Bryant (40). The products were white solids.



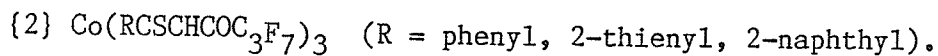
The complexes were prepared by methods similar to that described in {4}. White solids were obtained.

(b) Chelates of Monothio- $\beta$ -diketones

(i) Co(III) Monothio- $\beta$ -diketonates

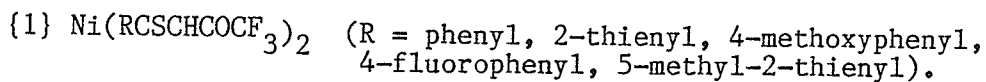


Cobalt(II) acetate tetrahydrate (4 mmole) in absolute ethanol (150 mL) was added to a solution of the ligand (12 mmole) in ethanol (50 mL). The brown solution was filtered and air was passed through the solution for 4 hours. The brown deposit was then filtered and washed with ethanol. For R = phenyl, no solid was formed after the passage of air. The solution was evaporated to 75 mL and cooled. To this solution, 5 mL of water were added and the mixture was kept overnight in a refrigerator. The resulting solid was then filtered and washed with cold ethanol (100).

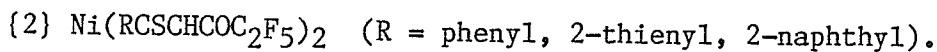


These complexes were prepared as described in {1}. The products were dark brown solids (100).

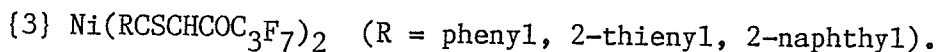
(ii) Ni(II) Monothio- $\beta$ -diketonates



Nickel(II) acetate tetrahydrate (4 mmole) in hot ethanol (70 mL) was added to a solution of the ligand (8 mmole) in ethanol (30 mL). The resulting brown precipitate was filtered and recrystallized from a 1:1 acetone/light petroleum (b.p. 40-60 °C) mixture. The products were dark brown solids. (97,101,143).

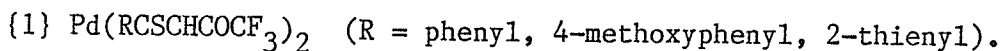


These complexes were prepared as described in {1}. Dark brown solids were obtained (100).

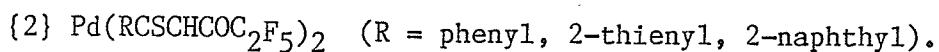


These complexes were prepared as described in {1}. The products were dark brown solids (100).

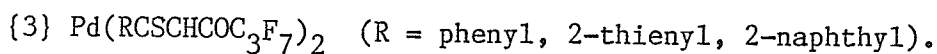
(iii) Pd(II) Monothio- $\beta$ -diketonates



Potassium tetrachloropalladate(II) (4.9 mmole) in water (50 mL) was added to a solution of the ligand (9.8 mmole) in acetone (50 mL). The resulting reddish-orange or brown precipitate was filtered off and recrystallized from acetone (97,144).

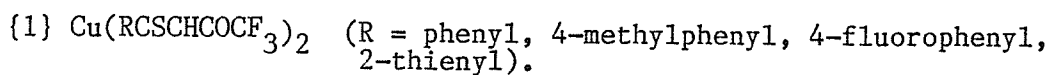


The preparation was similar to that described in {1}. Reddish-orange solids were obtained (100).

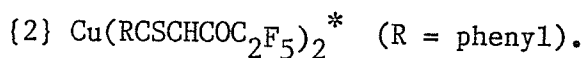


These complexes were prepared as described in {1}. Reddish-orange solids were obtained (100).

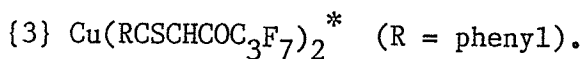
(iv) Cu(II) Monothio- $\beta$ -diketonates



Copper(II) acetate monohydrate (5 mmole) in hot absolute ethanol (100 mL) was added to a solution of the ligand (10 mmole) in ethanol (50 mL). The mixture was cooled and the brown precipitate filtered off. The product was recrystallized from a 1:1 acetone/light petroleum mixture (96,170-172).



This complex was prepared as described in {1}. A green-brown solid was obtained.



This complex was prepared as described in {1}. The product was a dark brown solid.

(v) Zn(II) Monothio- $\beta$ -diketonates

- {1}  $\text{Zn}(\text{RCSCHCOCF}_3)_2$  (R = phenyl, 2-thienyl, 4-methoxyphenyl, 4-fluorophenyl).

Zinc(II) acetate dihydrate (2.3 mmole) in hot absolute ethanol (70 mL) was added to a solution of the ligand (4.6 mmole) in warm ethanol (30 mL). The addition of water to the cooled mixture precipitated the yellow-brown complex, which was then recrystallized from light petroleum (97,143,171,172).

- {2}  $\text{Zn}(\text{RCSCHCOCF}_3)_2$  (R = 5-methyl-2-thienyl).

This complex was prepared as described in {1}, except the product was recrystallized from a 4:1 petroleum ether/benzene mixture to give an orange solid (101).